Final Progress Report

Investigating Principles of Workroom Exposure

Sponsored by
National Institute for Occupational Safety and Health
Grant Number 1 R01 OH07626

September 1, 2001 – August 31, 2005

Charles E. Feigley, Ph.D., Principal Investigator[1]
Jamil Khan, Ph.D., Co-Principal Investigator[2]
James A. Hussey, Ph.D., Co-Investigator[3]
Emily Lee, Ph.D.[1]

March 26, 2008

University of South Carolina
Columbia, SC 29205

[1]Department of Environmental Health Sciences
921 Assembly Street, Room 401
cfeigley@sc.edu
[2]Department of Mechanical Engineering
[3]Department of Epidemiology and Biostatistics

TABLE OF CONTENTS

	Page
Acknowledgements	1
Abstract	2
Highlights and Significant Findings	5
Translation of Findings	8
Outcome/Relevance/Impact	9
Scientific Report	10
1. Introduction	10
2. Background	11
2.1. Exposure assessment in occupational Epidemiology	11
2.2. Exposure Assessment in Industrial Hygiene	11
2.3. Conceptual Model of Workroom Exposures to Airborne Contaminants	12
2.4. Simple Deterministic Models	15
2.4.1. Completely Mixed (CM) Models	15
2.4.2. Uniform Diffusivity (UD) Models	17
2.5. Previous Related Research at Our Laboratory	18
2.5.1. Performance of Deterministic Workplace Exposure Assessment Models – Feigley (2000a)	18
2.5.2. Improving the Use of Mixing Factors for Dilution Ventilation Design – Feigley (2000b)	19
2.5.3. Comparison of Mathematical Models for Exposure Assessment with Computational Fluid Dynamic Simulation – Bennett (2000)	21
2.5.4. Comparison of Emission Models with Computational Fluid Dynamics: Simulation and a Proposed Improved Model – (Bennett 2003)	22
3. Goals and Specific Aims	25

4. Experimental Set-Up and Approach 26
4.1. Experimental Room 26
4.2. Preliminary Experiments 31
4.2.1. Required Monitoring Time 31
4.2.2. Required Spatial Coverage 37
4.2.3. Effects of Temperature Differences 37
5. Specific Aim 1 – Effects of Worker on Concentration and Air Flow 39
5.1. Methods 39
5.2. Results 41
5.3. Discussion 45
5.4. Conclusions 46
6. Specific Aim 2 – Effects of Worker on Worker Exposure 48
6.1. Introduction 48
6.2. Methods 48
6.3. Results and Discussion 50
6.3.1. Effects of Worker's Location 50
6.3.2. Effects of Worker's Orientation 51
6.3.3. Effects of Worker's Movement 54
6.4. Conclusions 55
7. Specific Aim 3 – Develop Deterministic Models 56
7.1. Refinement of Simple Models 56
7.1.1. The Two-Zone Model 56
7.2. Zonal Models 64
7.3. Computational Fluid Dynamics (CFD) 65
8. Specific Aim 4 – Evaluate the Use of Models in Workrooms 66
8.1. Silver Ink and Carbon Dipping in Tantalum Capacitor Manufacturing 66
9. References 88
Publications and Presentations Resulting from Grant 95
Inclusion of Gender and Minority Study Subjects 97
Inclusion of Children 97
Materials Available to Other Researchers 97

ACKNOWLEDGEMENTS

The investigators of this project would like to thank the National Institute for Occupational Safety and Health for their support under grant number 1 R01 OH07626. Many students and researchers made important contributions to this project. First and foremost, we wish to thank Dr. Eungyoung "Emily" Lee, without whose careful, persistent, insightful, and cheerful efforts as a graduate research assistant, and then as a post-doctoral fellow, this project would not have been possible. Particular thanks go out to Dr. Murali Venkatraman, whose skills in programming Matlab and in computational fluid dynamics were essential to our work on zonal models and in CFD analysis. Mr. Nicholas Schnaufer assisted with the field work in a capacitor manufacturing facility, documentation, and analysis, and Mr. Thanh Do performed further analysis of these data and CFD modeling of contaminant transport in the capacitor workroom. Deborah Salzberg, Research Associate, often pitched in with essential support on this project. Other contributors include Malik Ahmed, Lalita Das, J.J. Jenkins, Dr. Kishore Lakshman, Sanjida Tamanna, and Parveen Yadav.

This project is dedicated to workers exposed to hidden hazards in the air they breathe.

ABSTRACT

The ability to estimate worker exposure is essential for evaluating workplace hazards and protecting workers. In research, however, exposure assessment is often the weakest element in examining the relationship between contaminant exposure and occupational disease; thus, the development and improvement of exposure estimation models and methods is extremely important. Here experimental and mathematical methods were used to explore important determinants of exposure to airborne contaminants, particularly worker presence and activity. This research addresses the inherent challenge presented by the variation of concentration with workroom location. The effects of five factors – air flow rate, temperature, air inlet type, worker location, and worker activity – on contaminant distribution and worker exposure were investigated. Mathematical models for exposure estimation were evaluated including simple deterministic models, zonal models, and computational fluid dynamics (CFD). CFD simulations were used to investigate the effects of physical factors and the performance of simple deterministic models, and CFD estimates were compared with measured contaminant concentrations in a manufacturing work area.

Methods. The study was conducted in an experimental room with mixing ventilation and a tracer gas was injected at a constant rate. Concentration was monitored at 144 points with a photoionization detector attached to an automated sampling system. The research was designed to use three constant dilution air flow rates, 5.5, 3.3, and 0.88 m^3/min; but use of the lowest air flow rate was not feasible due to excessive monitoring time requirements. The number of sampling points required to characterize concentration distribution within the experimental room was determined by comparing concentration isopleths from subsets of data containing from 100 to 150 points. No substantial differences in isopleth shape or magnitude were observed over this range. Hence, a 3-dimensional network of 144 points was utilized. Two air inlets types were studied: a wall jet (WJ) with its center 2.12 m above the floor and a vaned diffuser in the center of the ceiling (CD), just above the tracer gas source.

To simulate temperature variability within a workroom, one wall of the experimental room was heated or cooled to represent a building's external wall. A heated mannequin was used to investigate the impact of a stationary worker's presence, and a human participant was used to simulate a moving worker. The contaminant concentration outside the facepiece of an air-supplied respirator was measured at various locations and orientations, and for various activities.

Results. Prior to studying the impact of a worker's presence on concentration fields, it was necessary to assess the effects of physical factors. Experiments were performed at two air flow rates (5.5 and 3.3 m^3/min) and six thermal conditions: isothermal, three summer conditions and two winter conditions. For comparing rooms with different sizes and flow rates but similar physical configurations, the dimensionless room Reynolds number (Re) corresponding to the two flow rates was used. The Re corresponding to the two air flow rates used here are 2,100 and 1,200. The variability of contaminant concentration at the higher flow rate was not affected by thermal conditions; but, at the lower flow rate, winter conditions produced greater variability (coefficient of variability, CV = 0.72 and 1.10) than isothermal and

summer conditions (CV = 0.29 to 0.34). Tests simulating winter conditions suggested that the resulting stable temperature structure inhibited the dilution of the tracer and enhanced its segregation in the lower portion of the room, especially for the lower flow rate.

A worker was located at four different positions near the source, and experiments were performed to study the effect of the worker's presence on contaminant dispersion throughout the experimental room for two air flow rates and two air inlet types. Only small differences in the overall room mean concentrations were observed when the worker was absent versus when the worker was present. However, nine out of ten experimental factor combinations showed that the pollutant dispersion patterns in an occupied room depended upon the location of the worker. For these experiments, the ceiling diffuser inlet was found to be more efficient than the wall jet in diluting contaminant, resulting in a mean reduction of 11% reduction in the overall room contaminant concentration, calculated by averaging the contaminant at all sampling points for each experiment. Very high concentrations were limited to a small volume immediately above the source when the ceiling diffuser was used, and the rest of the room was virtually well mixed. Also, the concentration at one fixed monitoring location was generally higher (on average 8% and 44% higher for flow rates 5.5 and 3.3 m^3/min, respectively) when the worker was stationary or absent than when the worker moved along a fixed path.

The effects of location and orientation of a stationary worker on the worker's exposure were assessed. For three of four flow rate-location combinations, a stationary worker near the tracer gas source (breathing zone 0.40 m horizontally from the source) was exposed to higher concentrations than the concentrations observed at that location when no worker was present. Average exposures were higher when the worker was facing the source. This finding under mixing ventilation was similar to the effect of worker orientation reported from wind tunnel experiments or at hood faces, but smaller in magnitude. Also, the tracer concentration encountered by a worker moving along a fixed path and the concentration along that path when no worker was present differed by less than 5%.

The effects of inlet, exhaust and source locations and of room dimensions on the flow field and contaminant distribution were studied by CFD simulation. Results were used to explore the optimal values for the size of the near-field zone and the air exchange rate between the zones for a simple two-zone mathematical model. The analysis showed that the optimum near-field zone size varied with room configuration and was in the range of 8.5% to 20% of the room volume for the conditions of these simulations. Coarse-grid CFD (CFD with a very small number of cells) and a new multi-zone model were also tested. Noting that accuracy depended upon numerous physical factors and their interactions, we focused on zonal models which recently had been adapted for use within single enclosed spaces.

Zonal models, like CFD, divide a room into separate zones, and simultaneously solve a set of linear equations for conservation of mass and energy for all zones. Unlike CFD, zonal models do not incorporate the equations for conservation of momentum, but compensate by adding empirical terms to describe the penetration of air jets entering a room. Empirical jet equations have been validated for a limited number of room configurations and physical factors. In this research, the zonal models tested gave inaccurate results and were judged to

be inappropriate for describing the details of transport within rooms; instead, other approaches such as CFD need to be used.

To test CFD in an actual workplace, a capacitor manufacturing facility was surveyed extensively and the concentration of isoamyl acetate (IAA) was simulated using CFD. After careful analysis to determine the source boundary conditions for IAA emission, CFD concentration estimates agreed very well with observations at the six locations in the source near-field: a two-tailed, paired t-test found no significant difference between the CFD concentration estimates and the measured values ($p = 0.92$). Thus, we concluded that a very standard CFD model yielded accurate simulations of dispersions, provided that adequate efforts were made to define realistic boundary conditions. Additional research is needed to develop methods for easily and accurately obtaining boundary conditions for enclosed spaces.

HIGHLIGHTS/SIGNIFICANT FINDINGS

The findings of this research can be used to select methods for estimating worker exposure and to understand the effect of workroom factors on exposure.

- Worker location, orientation, and activity were shown to have significant effects on the worker's breathing zone concentration. The ratios of breathing zone concentrations for two supply inlet types and two room Reynolds numbers are given below for various combinations of experimental factors.

Ratios	Supply Inlet	Room Reynolds Number[B]	Mean Conc Ratios (Std. Dev.)
Near-field/Far-field[A]	wall jet inlet	1,220	1.33
		2,100	1.60
	ceiling diffuser	1,220	1.40
		2,100	1.40
Facing toward source/Facing away from source	wall jet	1,220	1.15 (0.16)
		2,100	1.19 (0.16)
	ceiling diffuser	1,220	1.21 (0.23)
		2,100	1.28 (0.37)
Moving worker/Stationary worker	wall jet	1,220	1.14
		2,100	1.25
	ceiling diffuser	1,220	1.34
		2,100	1.51
Moving worker/Concentration along path without worker present	both inlets	both Re #s	<1.05

[A] Worker in the near field was 0.4 m from the source; worker in the far field was between 0.85 and 1.2 m from the source.

[B] Described in Section 4.1 and in Awbi(1991).

Such ratios could be used to develop correction factors for simple mathematical models. However, additional research is needed to make such factors applicable to specific models and to extend them to a wider range of room configurations and physical settings.

- Deterministic mathematical models of exposure assessment must be selected within the context of their intended use, inherent limitations, and data requirements. Simple models, such as the one-zone and two-zone completely-mixed models, are based upon simplifying assumptions that are only approximately correct in most cases. Nevertheless, they are valuable because they are easily applied and may be used to rule out the need for more sophisticated approaches. Continued efforts to test and improve their accuracy, precision, and range of usefulness are needed.

  The next level of complexity for models that simulate transport of contaminants within an enclosed space includes multi-zone mixed models, zonal models, and coarse-grid CFD. The implementation of these models, as tested in our research, appear to over-reach their capabilities. They attempt to estimate contaminant concentrations throughout a space without using a fully-detailed representation of the complex, recursive, physical transport processes that give rise to contaminant distributions. For this, CFD seems to be only choice.

  In this research, CFD was used successfully to simulate capacitor production facilities. This was accomplished with a standard formulation of the CFD model (e.g., treatments of turbulence, walls, and isothermal conditions). However, special emphasis was placed on defining realistic boundary conditions for the supply air inlets, pedestal fans, and contaminant source. This careful definition of the problem was found to be essential before computational analysis was attempted. Currently, CFD is finding greater acceptance in occupational hygiene research, but the software and the methods for defining boundary conditions will require further development before more use by hygiene practitioners can be expected.

- Tests simulating winter conditions suggested that the resulting stable temperature structure inhibited the dilution of the tracer and enhanced its segregation in the lower portion of the room, especially for the lower flow rate (3.3 m^3/min). Therefore, failing to explicitly address thermal effects in exposure modeling may impact the accuracy and precision of contaminant estimates when used for rooms that are non-isothermal and not well mixed. These findings also have implications for air monitoring. Dispersion patterns for different thermal conditions were found to be substantially different, even when the mean concentrations were nearly the same. For example, at Re= 1220 the concentration was 15 times greater at an Ar=4900 for the winter condition than at an Ar=4900 for the summer condition Thus, consideration of seasonal effects is necessary when room temperature (including air and wall temperatures) or airflow rates change significantly with time of year, even if emission rates do not change.

  In addition to model applications, these observations have relevance to workroom air monitoring for exposure measurement. Data from a single season should not be assumed to be representative of longer periods if temperature gradients vary with time of year.

- The monitoring time required to determine the concentration at particular workroom locations within desired precision limits varied greatly: over three orders of magnitude difference between shortest and longest required monitoring time. One of the most interesting findings has been that tracer concentrations were not statistically stationary

at some locations for the lowest flow rate investigated (0.88 m^3/min), even after six hours of monitoring. This has significant implications for generating experimental data for validation of mathematical models, CFD simulation methods, and innovative instrumental methods at low air flow conditions. Under such low flow conditions, thermal convection likely dominates mechanical convection, resulting in unstable air flow patterns.

TRANSLATION OF FINDINGS

- Improved exposure models should, to the extent possible, address the factors investigated here for estimating worker exposure in the breathing zone. Correction factors may be developed for adjusting the results from simple models or estimating one worker's exposure from the measured exposure of another worker.
- Occupational hygiene professionals should not assume that monitoring data from a single season is representative of the entire year. When performing exposure assessments, consideration should be given to collecting data from both warm and cool weather periods, since greatly differing dispersion patterns were found here under different seasonal conditions.
- A supply air diffuser in the ceiling with vanes that direct air across the ceiling seemed to be generally more efficient for reducing worker exposure than a supply air jet in one of the walls.
- As a result of the impact of worker location, orientation and movement on breathing zone concentrations, the experiments here clearly demonstrate the importance of basing exposure estimates on personal sampling rather than on area sampling.
- Results were distributed to occupational hygiene practitioners and engineers through seven peer-reviewed articles and 17 papers with refereed abstracts presented at national or international professional meetings. One additional paper has been accepted for presentation at the American Industrial Hygiene Conference in June, 2008.
- Dr. Jimmy Perkins has incorporated some of the results, including some figures, from this research into his chapter entitled "Dilution Ventilation for Contaminant Control" in *Modern Industrial Hygiene* (Chapter 7, Volume 3, 2008) now in press. This will broaden distribution of our findings and enhance their accessibility to practitioners.

OUTCOMES/RELEVANCE/IMPACT

This research was possibly the first experimental effort to study systematically the impact of physical and worker-related factors that determine the distribution of airborne contaminants throughout a workroom, and thereby determine worker exposure. The long-term goal was to develop more reliable methods for assessing inhalational exposure of workers in enclosed spaces. In addition to the experimental work, mathematical models for exposure assessment were evaluated and enhanced, and applied in a manufacturing facility.

This project was unique in several respects. The effects of a worker's presence on his or her own exposure have been studied previously in strongly directional air flows such as in wind tunnels, near exhaust hoods, and in displacement ventilation. Here, the degree to which a worker's location, orientation, and activity influenced exposure was measured in a room with dilution (mixing) ventilation. These results suggest ways of improving the average accuracy of simple mathematical models for estimating exposure.

Limitations of more complex models were encountered. Most surprising was that the zonal models tested were not capable of simulating the details of airflow and contaminant distribution patterns inside an enclosed space. Unlike zonal models, computational fluid dynamics (CFD) is a method of representing and combining the effects of all the important determinants of flow, including the patterns associated with air jets entering enclosed spaces. CFD had been used reliably to simulate phenomena related to fluid flow, but application to the circulating (recursive) airflow patterns in enclosed spaces has proven to be challenging. This project demonstrated that some of the most common assumptions of CFD modeling can give results which agree very well with observed contaminant concentration profiles an actual, complex manufacturing work area, provided that the boundary conditions of the contaminant source, supply air jets, and fans are realistically portrayed in the model formulation.

SCIENTIFIC REPORT

1. Introduction

Assessing workers' exposure to chemical hazards is an essential aspect of occupational hygiene, but it is often the weakest component of research in occupational health. Exposure assessment is necessary in order to establish occupational exposure limits, to determine compliance with those limits, to aid in the selection of personal protective equipment, and to improve the design specifications of engineering controls. Also, current methods for determining worker exposure must be validated and improved to understand fully the myriad diseases and conditions which appear to be linked with occupational and environmental exposures to chemicals and other agents.

The bulk of research in exposure assessment has been on exposure monitoring methods such as air sampling and biological monitoring methods. However, little work has been done to explore the physical determinants of occupational exposures.

2. Background

2.1. Exposure assessment in Occupational Epidemiology

Exposure assessment is crucially important for occupational epidemiology research. Checkoway (1986) presented a hierarchy of approaches for exposure classification in occupational epidemiology, but recognized that the investigator's choice of approach is often constrained by data and methods availability. Most of the methods used for categorizing workers by their exposure, such as sorting by job title, length of service, or professional judgment, have not been validated against measured exposures. Stewart and Dosemeci (1994) presented a bibliography including 22 papers dealing with the validity of such indirect methods. Of these validations, only 3 compared the indirect approaches with measured exposure or dose, while 17 compared one indirect approach with another.

Tielemans (1998) demonstrated the need for finding better exposure assessment methods for categorizing workers in occupational epidemiology. Statistical analyses of exposure-effect relationships were shown to be very adversely affected when the between-group variance of concentration is small compared with the within-group variance. Grouping by job title generally results in only moderate between-group contrasts (Kromhout, 1996). Tielemans (1998) concluded that grouping schemes should be based on the factors that actually affect exposures, not assigned *a priori* by job title. However, research on the physical factors that determine occupational exposure has been superficial to date.

Rappaport (1991), upon analyzing data from 31 worker groups from 9 industrial processes, demonstrated the importance of developing better methods for worker grouping. He found that uniform intragroup exposure was very rare. Also, the intragroup variation was very high for a substantial proportion of groups studied: 25% of the 110 groups studied had a range of concentration ratios which included both the 95^{th} and 5^{th} percentiles. Refinement of group selection criteria could yield greater power for associating exposure and health outcomes.

2.2. Exposure Assessment in Industrial Hygiene

In addition to their use in occupational epidemiology, groups of like exposure are useful for other purposes. Identification of homogeneous exposure groups (HEGs) of workers was recommended. In recognition that contaminant exposure of any particular worker group is seldom truly homogeneous in the strict statistical sense, this term has been supplanted by the designation of ‘similarly exposed groups’ or SEGs (Mulhausen, 1998). These groups are used in establishing air monitoring strategies, assigning personal protective equipment, and setting up medical monitoring programs.

Exposure assessment was originally focused on determining compliance with occupational exposure limits (OELs), usually comparing the maximum worker exposure with the appropriate OEL. However, the applications of exposure assessment have expanded to include: assessing worker risk over a range of exposures, assessing the risk to other stakeholders (i.e., community groups or customers), designing exposure controls, and determining the need for additional exposure characterization work. Given these other

applications, exposure assessment often requires determination of the statistical distribution of exposure and the uncertainty associated with exposure estimates in addition to estimation of maximum exposure (Mulhausen, 1998; Rappaport, 2008).

Exposure estimates are ideally based on exposure measurements for all employees potentially exposed to toxic substances, with replicate measurements for individual workers. However, this is seldom feasible for even a moderate number of workers. Thus, various other methods have been developed including: expert systems such the EASE model (Cherrie, 2005; Creely, 2004; Johnston, 2005); stochastic models, for instance Bayesian methods (Ramachandran, 2001 & 2003); and deterministic models ranging from simple box models through zonal models to computational fluid dynamics (Jayjock, 2003; AIHA Exposure Assessment Committee, 2000). This research focuses on deterministic approaches for estimating exposure to airborne contaminants in a single workroom. Developing a better understanding of the factors that determine worker exposure can provide a basis for more reliable and feasible approaches for assessing exposure. Efforts in this direction can provide a foundation for improving deterministic models, and for appreciating the uncertainties in their estimates.

The accuracy and precision of required of deterministic models, or any other method, depends upon the intended end use of the estimate. Crude models known to overestimate exposure for most environments are sometimes used to rule in or rule out the need for more accurate determinations. Greater accuracy is required in occupational epidemiology research where estimates should be as unbiased as possible and random errors should be minimized.

2.3. Conceptual Model of Workroom Exposures to Airborne Contaminants

Roach (1991) discussed the components of occupational exposure variability found in monitoring results from industry surveys. He noted that the exposure of an individual worker often varies greatly with time. The variation from one worker to another performing the same job is also quite large. He lists the following causes of variation: "local sources of heavy contamination, process changes over time, individual work practices, and large scale air turbulence."

Here two possible sources were recognized to be responsible for variation of worker's exposure: changes in the concentration field (i.e. the concentration throughout a workroom) with time, and changes in the worker's position within the concentration field. Making this distinction led to a conceptual model that allows exposure to be viewed as the interaction of workroom characteristics, air flow patterns, source factors, and workers' activities.

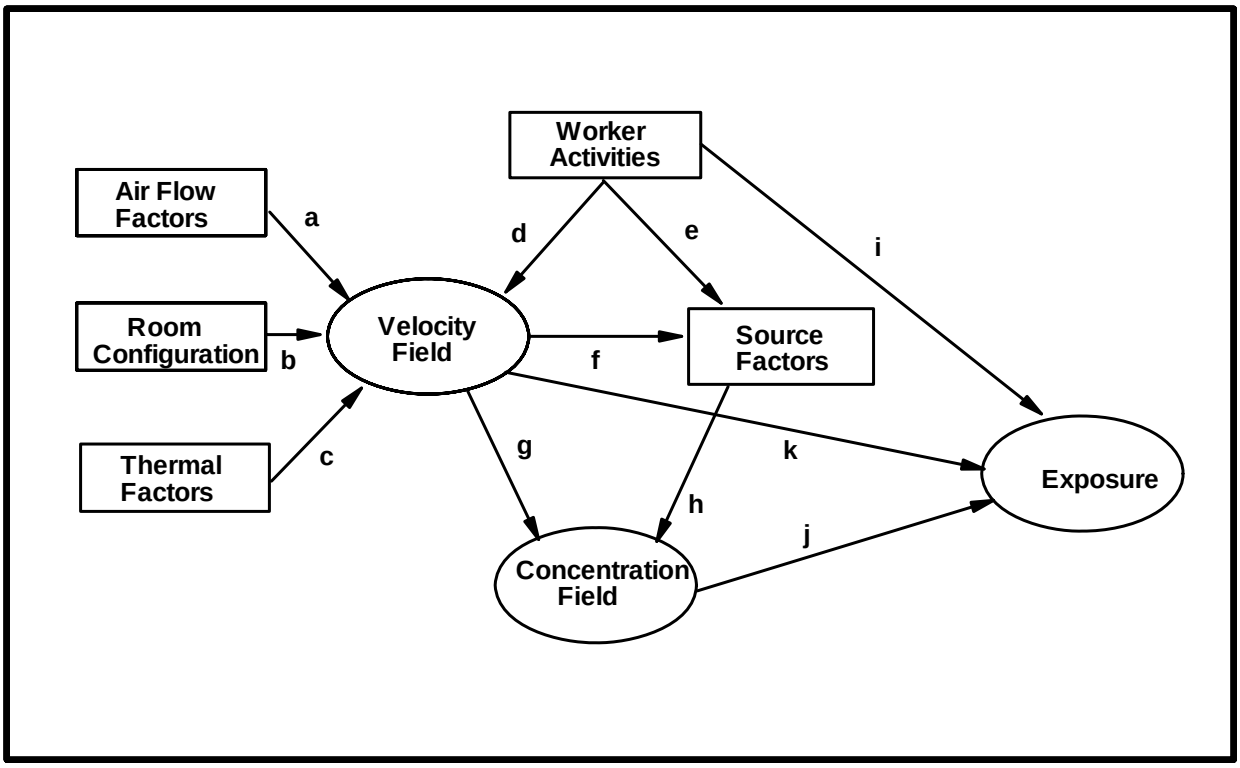

Figure 2.1. Conceptual Model of Airborne Contaminant Exposure in a Workroom

The conceptual model in Figure 2.1, developed for this project, graphically shows the interactions that determine exposure to airborne workroom contaminants. Room configuration includes room size, locations of air inlets and outlets, furniture, and source locations. Air flow factors include air flow rates, air diffusers, and inlet velocity. Thermal factors refer to temperature differences between walls and room air, temperature differences between incoming and room air, heat sources within a room, and heat transfer properties of interior surfaces. Worker activities encompass factors such as body movement and path through the workroom over time, work practices and the use of personal protective equipment. This includes intentional and unintentional actions that impact source emissions. Source factors include contaminant identity, concentration, density, temperature, emission rate, and velocity. The air velocity and contaminant concentration fields are the values of velocity and contaminant concentration throughout a workroom.

The interactions of air flow factors, room configuration and thermal factors (a, b and c in Figure 2.1) determine the velocity field within the workroom. The interaction of the velocity field with the contaminants emitted from the source (g and h, Figure 2.1) produces the contaminant concentration field. The effects of air flow, room configuration, and thermal factors have been studied, primarily by engineers interested in heating and cooling applications (Awbi, 1991). Experiments and numerical simulations (i.e. computational fluid dynamics) have been used to study these effects. A review of the use of computational fluid dynamics (CFD) to predict the velocity and concentration fields in rooms was presented by Emmerich (1997). In general, CFD has been used to simulate effects a, b, c, g and h, and can be extended to incorporate effects d, e, and f in very simple cases. Although important

progress has been made in CFD, considerable uncertainty still exists regarding CFD estimates of velocity and concentration fields for a particular room, principally because little work has been done to validate the use of CFD under work room conditions.

In some circumstances, the velocity field can affect source characteristics (f, Figure 2.1). The emission rates from many sources depend on mass transfer between the source and the room air. This is most often the case when the source is an evaporating liquid. The rate of vaporization is determined not only by the vapor pressure of the contaminant, but also by the mass transfer resistance of the air boundary layer near the liquid surface. This has been described for open surface tanks (Bishop, 1982), for surface coatings by (Riley,1968; Feigley,1981), and for pools of volatile materials (Hanna, 1987; Hummel,1996; Keil and Nicas, 2003; Lennert, 1997; Neilsen, 1995; AIHA, 2000).

The effect of the presence and activity of workers on the velocity field and on the exposure has been explored for limited sets of conditions. For instance, considerable attention has focused on the effect of a worker's presence on the velocity field in the vicinity of an exhaust opening (Dunnett, 1994) and the impact of this on the worker's exposure (much of Flynn's research, for example, Flynn, 1990; and Kim and Flynn, 1991).

Worker activity may change the source characteristics also (e, Figure 2.1). For instance, workers walking past the face of a laboratory hood may increase emissions from the hood. It appears that the effect of a worker's presence and activities away from an exhaust inlet on workroom contaminant distribution had not been studied. Also, active workers may increase the degree of mixing in the room (d, Figure 2.1). They may alter their own exposure and that of other workers (i, Figure 2.1).

When workroom air is quiescent, exhaled air may impact exposure. Contaminants which are absorbed in the respiratory system may be present in exhaled air at levels which are lower than those in room air. Exhaled air then may dilute contaminants in breathing zone air, reducing exposure. In addition, thermal air movement resulting from temperature differences between the worker and the room air influence exposures. This effect is intentional in the application of displacement ventilation: clean air is introduced at low velocity near the floor and emissions from heated sources are allowed to rise to the upper portions of the room where they are captured in exhaust air flow. This control method has received some study recently, for instance Emmerich and McDowell (2005).

Some aspects of the interaction of worker activity and concentration field (i and j, Figure 2.1) have been studied extensively. This is especially true of the aspiration, inhalation, and deposition of aerosols in the respiratory system. This continues to be an area of active research. For instance, Hoffman (1996) reviewed modeling of particle deposition in the human lung and Aitken (1999) carried out experimental measurements of aerosol aspiration efficiencies in environments with low air velocities.

The independent variables in the conceptual model above are those that impact exposure averaged over some time period, say several minutes. On such a time scale, their effect on exposure may be view as predominantly deterministic. However, it must be recognized that

exposure at any point in a workroom usually has a stochastic component as well. Even if the independent variables are constant, random variations in exposure will occur as a result of air turbulence. Turbulence is the momentary, random fluctuation of velocity caused by spatial gradients in velocity and/or density. Air turbulence has both long-term and very short-term effects on exposure. The short-term effects are evident when monitoring concentration with a continuous instrument with a short averaging time.

2.4. Simple Deterministic Models

For many years, monitoring has been used for estimating exposure to airborne contaminants. Now, mathematical models increasingly are employed as an adjunct to monitoring. Models, such as the familiar dilution ventilation rate equations, are used instead of monitoring for estimating exposures during process design or in retrospective epidemiologic studies. In addition, these models are used extensively for controlling worker exposure to airborne contaminants, for example to specify dilution air flow rates required to protect workers, and to estimate contaminant emission rates. These models are important because they can make predictions in a wide variety of scenarios, they can be used for rapid screening, and they can reduce the need for monitoring. However, the most widely used models are based on simplistic assumptions regarding air flow and contaminant transport, and the errors resulting from these assumptions have not been systematically evaluated. Validation is essential because these models ignore the principal determinant of airborne contaminant distribution -- convective air flow patterns.

2.4.1. Completely Mixed (CM) Models assume that the contaminant concentration in a room, or portions of a room, may be treated as uniform. This assumption permits the development of formulas for a variety of circumstances from a pollutant mass balance equation (which sets contaminant accumulation in a defined space over a given time period equal to the inputs minus the losses of contaminant over that period). The concentration in a completely mixed room at steady-state with clean dilution air is given by:

$$C = G/Q \qquad \text{Eq. 2.1}$$

where G = contaminant emission rate, and Q = dilution air flow rate.

However, no room with both localized sources and a flow of clean air into the room has perfectly uniform concentration. Thus, it is important to determine under what circumstances non-uniform concentration can lead to significant errors in estimating C. Early efforts to account for spatial variation of concentration employed mixing factors (Lidwell and Lovelock, 1946) or safety factors that incorporated the effect of incomplete mixing (Brief, 1960). A recent study of hydrocarbon exposure among commercial painters in the Netherlands showed that the single zone model did not adequately describe exposure (Burstyn and Kromhut, 2002). The effect of source strength was greater than expected and general ventilation did not provide a protective effect. This is likely to be due to spatial variability of hydrocarbon concentration, anticipated to be much higher near the source.

One approach to deal with spatial concentration variation is to break up the workroom into two or more zones, each of which is considered to be well-mixed (Hemeon, 1963; Heinsohn, 1991; Nicas, 1996). Adjacent zones exchange air and contaminant.

Two examples of two-zone models (CM-2) are illustrated in Figure 2.2. At steady-state with clean dilution air flow, the CM models of the two zones are as follows:

$$\text{Far Field}: \quad C_{F,SS} = \frac{G}{Q} \qquad \text{Eq. 2.2}$$

$$\text{Near Field}: \quad C_{N,SS} = \frac{G}{Q} + \frac{G}{\beta} \qquad \text{Eq. 2.3}$$

where $C_{F,SS}$ = the far field concentration,
$C_{N,SS}$ = the near field concentration,
Q = the flow rate of clean dilution air into the far field zone,
β = the flow rate of air exchange between the two zones, and
G = the contaminant emission rate.

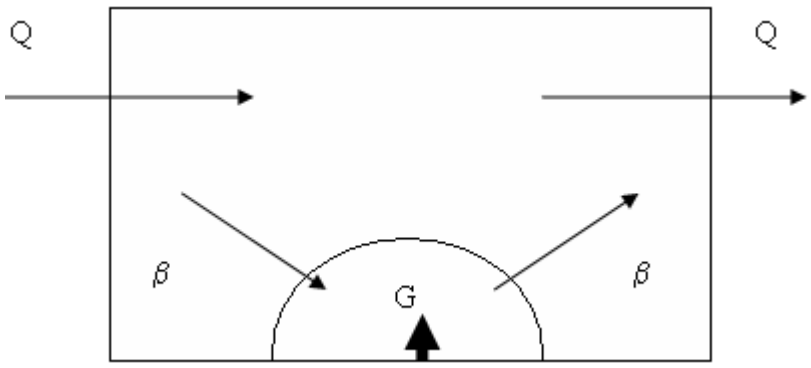

Figure 2.2. Two-Zone Model.

Various approaches may be used to estimate β. For restricted air flow to the near field such that β<Q, the concentration in the near field is higher than in the far field. In a room with vigorous mixing and/or low dilution air flow rate such that β>>Q, the CM-2 model predicts that the concentrations in the two zones are essentially equal. Thus, when β>>Q, a single zone model is more appropriate.

Although the multi-zone model improves upon the single zone model when β<Q, there are numerous problems in applying this model to real rooms. The National Research Council (1991) concluded that the development of more sophisticated models was not justified because of the uncertainty in flow patterns and the difficulty of specifying source and sink characteristics. Models with a large number of zones were proposed by Sinden (1978) for contaminant exchange among rooms in a building, and applied later by Park and Garrison (1990). However these models are generally not practical for prediction unless extensive

measurement of convective and diffusive transfer rates can be made. In most cases, it would be easier to measure the concentrations directly in each compartment. Like the 1-zone model, zones containing contaminant sources are not completely mixed. In fact, the steepest concentration gradient occurs in the near field zone. Thus, estimation of concentration within some of the zones is subject to the same problems as the single zone model. Also, there is currently no guidance available for establishing the number of zones, the individual zone size, and the zone configuration. Obviously, the concentration within each zone should be as uniform as possible. However, no research has been done to explore how these zones should be configured and the limitations of the multi-zone approaches.

2.4.2. Uniform Diffusivity (UD) Models are generally applied close to a contaminant source (in the "near field"), where significant concentration gradients exist. Pollutant transport away from the source is assumed to be due to turbulent diffusion, the intermingling and mixing of parcels of air, sometimes termed eddies, resulting in a net movement of contaminant from high to low concentration regions. Under this assumption, the ratio of the turbulent diffusion rate to the concentration gradient is a constant called the eddy diffusivity. Application of these models, while taking concentration variations into account, presupposes that contaminant transport is the same in all directions from the source and that the concentration decreases monotonically with distance from the source. This assumption is seldom met in real workrooms because mechanical ventilation and natural convection usually establish airflow patterns that are principally responsible for contaminant distribution. Consistent patterns produce a flow around contaminant sources with a constant mean direction. Under such conditions, contaminant concentrations are expected to be higher downstream than upstream. Thus, room conditions often do not comply with the assumptions inherent in this model. Nevertheless, the accuracy of this approach has not been evaluated.

A typical formulation of this model for a source on the floor of a room with isotropic diffusion from a point source at the center of a hemisphere is given in Eq. 2.4. (Keil,1997). It was derived by analogy with heat transfer from Carslaw and Jaeger (1959):

$$C = \frac{G}{2\pi Dr}\left[1 - erf\left(\frac{r}{\sqrt{4Dt}}\right)\right] \qquad \text{Eq. 2.4}$$

where D = the turbulent diffusivity,
r = distance from the source,
t = time after emission begins,
erf = error function.

When using Eq. 2.4, selecting the effective turbulent eddy diffusivity between the source and another location in a workroom is little more than guesswork. For steady-state conditions, one way to work around this deficiency has been to measure concentrations at two different distances from the source. Applying Eq. 2.4 to both points yields two equations that are solved simultaneously for G and D (Conroy, 1995). D values have been reported from three to 690 m^2/hr (Franke, 1989; Wadden, 1989; Wadden, 1991; Scheff, 1992; Conroy, 1995; Keil, 1997a). Jayjock (2003) reports D values from 3 to 690 m^2/hr with a typical value of 12 m^2/hr. The method's assumptions include: (1) contaminant transport is by turbulent

diffusion only; (2) pollutant transport is independent of direction from the source; (3) G and D are constant with respect to time; (4) the observed time-averaged concentrations are the result of emissions during the sampling period; (5) the contaminant is emitted from a single point source. For the first and second assumptions to be true, there must be no persistent convective flow patterns within the region near the source. Paradoxically, the turbulence necessary for turbulent diffusion in rooms is created and maintained principally from either forced or natural convection. (The only other process generating turbulence is mechanical stirring caused by the motion of people or objects within the room.) Because most rooms have some convective flows, which significantly affect contaminant distribution even at low air speeds, few conform to the first two assumptions of this method. Thus, the approach is fundamentally invalid for many applications. It is not clear under what circumstances this method may be used as an approximation.

In the studies referenced above, the concentration at one location was sometimes lower than the concentration at a location further removed from the source. Using such a pair of observations results in negative estimates for D. Conroy (1995) rejected G estimates if the estimated D was considered physically unrealistic, i.e. $D<0$ or $D>100$ m^2/min. These estimates of G and D are assuredly invalid, but estimates of G and D for $0 \leq D \leq 100$ m^2/min also might be invalid. There is no way of determining how far from the source and under what conditions UD models are applicable, if at all.

2.5. Previous Related Research at Our Laboratory

Prior to receiving NIOSH funding for "Investigating Principles of Workroom Exposure," our research group was funded by a cooperative agreement from the Association of Schools of Public Health to evaluate models for airborne workroom contaminants (ASPH Project Number S646-17/17). A number of results were derived from those earlier efforts, and those investigations gave rise to the subsequent NIOSH investigation. The preliminary results are briefly described below. They are divided into three sections which correspond to three publications (Bennett, 2003; Feigley, 2002a; Feigley 2002b).

2.5.1. Performance of Deterministic Workplace Exposure Assessment Models – Feigley (2002a)

Contaminant concentration estimates from simple models were compared with concentration fields obtained by computational fluid dynamic (CFD) simulations for various room and source configurations under steady-state conditions (Feigley, 2002a). Airflows and contaminant distributions in a 10X3X7-m room with a single contaminant source on a 1-m high pedestal were simulated using CFD for steady, isothermal conditions. For a high wall jet inlet, simulations were performed for nine room air exhaust locations and eight source locations. For a ceiling diffuser inlet the impact of two exhaust locations and eight source locations were investigated. Because CFD treats determinants of contaminant transport explicitly and CFD simulation of air flow patterns in another experimental room agreed well with experimental results (Bennett, 2000), CFD was used as the standard for comparison.

Parameters of the one- and two-zone completely mixed models (CM-1 and CM-2) and the uniform turbulent diffusivity model (UD) were determined from CFD simulation results. Concentration estimates from these were compared with CFD results in the breathing zone

(BZ) plane (1.5 m above the floor), for the source ‘‘near field,’’ the source ‘‘far field,’’ and the entire BZ.

Table 2.1. Summary Statistics of Percentage Difference of Model from CFD Concentration Estimates over All Simulations

	Near Field		Far Field	
Model	Mean	SD	Mean	SD
CM-1	-21.9	26.8	-4.8	29.5
CM-2	32.3	111	-2.3	31.4
UD	126	103	-36.3	28.4

For the conditions and configurations studied, the CM-1 model generally had the best performance for applications such as occupational epidemiology, where the objectives include finding the most accurate estimates possible and characterizing errors associated with these estimates. However, CM-1 tended to underestimate the near field concentration; thus, CM-2 was judged to be better in the near field when underestimation is undesirable, such as when determining compliance with occupational exposure limits in order to protect workers from overexposure to contaminants. The agreement of CM-2 estimates with CFD results in the near field was more variable than that of the CM-1. Nevertheless, for the conditions studied here, CM-2 appears to be more appropriate than CM-1 for near-field worker protection and compliance determination because it provided a margin of safety.

The UD model performed poorly on average in both near and far fields. The mathematical relationship between concentration and distance from the source did not agree well with CFD-simulated contaminant distribution patterns. In addition, the difficulty in accurately estimating the turbulent diffusivity presents a significant impediment to UD model use for exposure estimation.

2.5.2. Improving the Use of Mixing Factors for Dilution Ventilation Design – Feigley, 2002b

In specifying dilution ventilation flow rate, a safety factor, K, is often used to provide a margin of safety and to compensate for uncertainties and health impact severity. An equation for calculating dilution airflow rate requirements for controlling exposure to airborne contaminants in a room often is derived by assuming that the room is well mixed. Solving the contaminant mass balance for steady-state conditions and clean dilution air, and adding a safety factor, K, yields the familiar equation (ACGIH, 2004):

$$Q = K\frac{G}{C} \qquad \text{Eq. 2.5}$$

where Q = dilution airflow rate,
C = target contaminant concentration, such as an occupational exposure limit,
G = contaminant emission rate, and
K = multipurpose safety factor.

The safety factor is used to account for a variety of uncertainties and concerns, including deviations from the assumption of complete mixing, the severity of contaminant health effects, and the number of workers exposed. In rooms with an active contaminant source and clean dilution air flow, very high contaminant concentrations are found immediately downwind of the source (also in the wake of persons standing upwind of the source) and very low concentrations are found in the inlet air stream. Thus, such rooms are often not well mixed, at least in a strict sense.

In current practice, the selection of K is very subjective. Here, the component of K which accounts for imperfect mixing, K_m, was studied to develop more effective and efficient design procedures (Feigley, 2002b). Air flow and contaminant distribution in a 10X3X7-m room with a single contaminant source on a 1-m high table were simulated for steady, isothermal conditions using computational fluid dynamics. A series of 10 simulations explored factorial combinations of air exchange rates (1, 2, 4, 8, 16 ACH) and inlet types (a high wall jet and a ceiling diffuser). Nine additional simulations explored exhaust opening location effects and 13 other simulations investigated source location effects. K_m was calculated at each of 25,600 grid locations within the room by linear regression of emission rate/flow rate (G/Q) on concentration (C). The linear relationship between C and G/Q at each of the points was nearly perfect ($R^2 \geq 0.97$). For the simulations with varying dilution flow rate, K_m ranged from 0.19 to 2.86 for the wall jet and from 0.94 to 4.34 for the ceiling diffuser. Holding G/Q at 100 ppm and varying source and exhaust locations produced room average concentrations from 55.7 to 173 ppm.

These simulations suggest that air monitoring data often can be used to calculate dilution flow rate requirements, unlike orthodox design approaches. They also shed light on both improvements and limitations of dilution ventilation design. When changes to an existing dilution ventilation system are motivated by measured overexposure of room occupants to a contaminant and the existing dilution flow rate can be determined, this study suggests that the ratio of the current concentration exposure to the concentration exposure limit can provide a more accurate means of accounting for incomplete room mixing than the familiar "K-factor" approach (Eq. 1). Proper application of this method requires that the inlet air velocity at individual points across the inlet face vary proportionally to the flow rate. Thus, elbows close to air inlets should be equipped with turning vanes or system modifications to promote uniform inlet velocity. Also, if an occupant's exposure varies significantly, the exposure measurements must characterize the full range of exposure to be useful for determining the dilution flow rate required for control.

When the purpose of dilution ventilation is to reduce concentration throughout a room rather than at a specific location, use of the 99th percentile of K_m as a design parameter to account for mixing may be feasible; but other control measures should be considered if K_m exceeds 2 to 3. K_m may be reduced by enhancing room mixing with fans or by altering air inlet configuration. However, mixing should not be increased if the altered room air currents could transport contaminant to an occupant's breathing zone or interfere with other control methods that depend on segregation of incoming air and contaminant. These other approaches, including local exhaust, air islands, push-pull systems, and displacement flow, when properly designed and maintained, are frequently more effective than dilution ventilation.

2.5.3. Comparison of Mathematical Models for Exposure Assessment with Computational Fluid Dynamic Simulation – Bennett (2000)

In occupational settings, mathematical models increasingly are employed as adjuncts to monitoring, for instance, during process design or in retrospective epidemiological studies. Models can make predictions in a wide variety of scenarios, can be used for rapid screening, and may reduce the need for monitoring in exposure assessment. However, models make simplifying assumptions regarding air flow and contaminant transport. The errors resulting from these assumptions have not been systematically evaluated. Here we compare exposure estimates from the single-zone completely mixed (CM-1), two-zone completely mixed (CM-2), and uniform diffusivity (UD) models with workroom concentration fields predicted by computational fluid dynamics (CFD). The room air flow, concentration fields, and the breathing zone concentration of a stationary worker were computed using Fluent V4.3 for factorial combinations of three source locations, three dilution air flow rates and two emission rate profiles, constant and time-varying. These numerical experiments were used to generate plausible concentration fields, not to simulate exactly the processes in a real workroom. Thus, "error" is defined here as difference between model and CFD predictions.

Prior to the CFD simulation, grid independence was confirmed. Also, the CFD approach used was subjected to an external validation exercise using the data described by Hawkins (1995) and Hosni (1996). Examining a plane at standing breathing zone height, the maximum difference between CFD and observed air speeds was 30%, and the differences were negligible large portions of the plane.

For both constant and time-varying emission sources, exposure estimates depended on receptor and source location. For the constant source case, ventilation rate was shown to be inconsequential to CM-1 model error. CM-1, CM-2, and UD models differed in their agreement with CFD. UD was closest to CFD for estimating concentration in the simulated breathing zone (BZ) near the source, although large errors resulted when the model was applied to the plane of possible breathing zones. CM-1 performed better for this plane but underestimated the near-source BZ exposure. For the near-source BZ location, CM-2 replicated CFD predictions more closely thanCM-1 did, but less closely than UD did. Error in CM-1model estimation of short-term average exposure to a time-varying source was highly dependent on ventilation rate. Error decreased as ventilation rate increased.

2.5.4. Comparison of Emission Models with Computational Fluid Dynamics: Simulation and a Proposed Improved Model – Bennett 2003

Understanding source behavior is important in controlling exposure to airborne contaminants. Industrial hygienists are often asked to infer emission information from room concentration data. This is not easily done, but models that make simplifying assumptions regarding contaminant transport are frequently used. The errors resulting from these assumptions are not yet well understood. Bennett (2003) compared emission estimates from the single-zone completely mixed (CM-1), two-zone completely mixed (CM-2), and uniform diffusivity (UD) models with the emissions set as boundary conditions in computational fluid dynamic (CFD) simulations of a workplace and developed a more accurate model for application to time-varying sources. This approach – evaluating other methods for estimating one of CFD boundary condition based upon a CFD simulation results – is called an "inverse" problem because it proceeds from the CFD solution to the boundary condition. The room airflow and concentration fields were computed using Fluent 4. These numerical experiments were factorial combinations of three source locations, five receptor locations, three dilution airflow rates, and two generation rate profiles, constant and time-varying.

Once the concentration field, $C(x,y,z,t)$, was obtained through CFD simulation, concentration information was available for thousands of locations in the room volume. Particular attention was paid to the monitoring locations where data was collected in the study conducted by Stewart, (1992) and to the exhaust duct as shown in Figure 2.3. These represent the

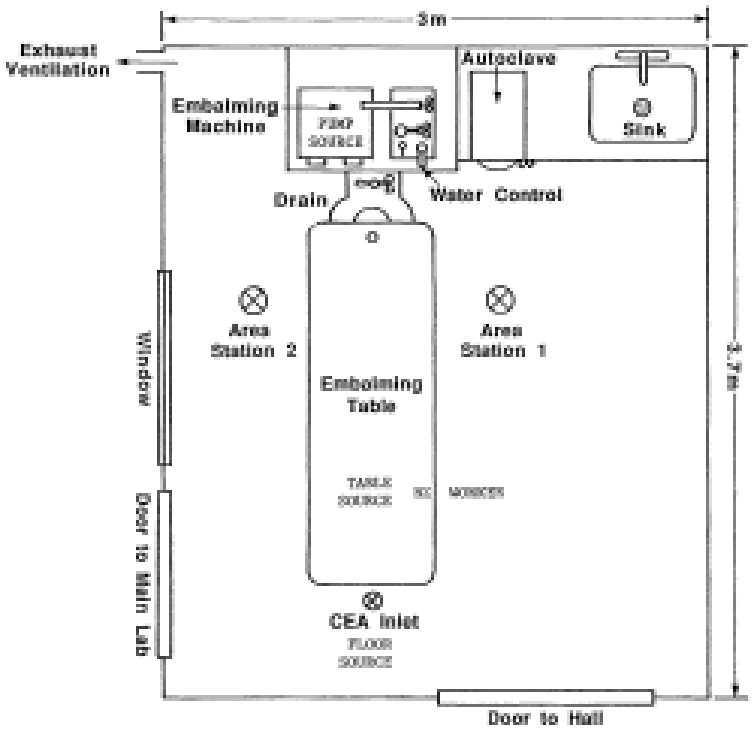

Figure 2.3. Plan view of workroom showing monitoring and source locations.

locations most likely to be chosen by an industrial hygienist for making actual concentration measurements. In evaluating the CM-1 model, formaldehyde concentration measure with a continuous instrument at a fixed monitoring location was used. For the CM-2 model, the breathing zone (BZ) concentration was used as the near-field concentration, and the exhaust concentration as the far-field. The UD model employed the BZ concentration. For the time-dependent case, the model emission estimates were compared with the emission used for CFD simulation, with respect to total mass and shape. Table 2.2 summarizes the study design. These comparisons were done at three ventilation rates to investigate the effects of this variable on the accuracy of emission estimates.

TABLE 2.2. Experimental Design

Variable	Model			
	CM-1	CM-2	CM-L	UD
Source Location	floor, pump, table	Table	floor, pump, table	floor, pump, table
Source Type	constant time-varying	Constant time-varying	time-varying	constant time-varying
Receptor Location	A1,A2,BZ,CEA,EX	BZ	A1,A2,BZ,CEA,EX	A1,A2,BZ, CEA,EX
Ventilation Rate (m^3/min)	0.522, 2.44, 6.23	0.522, 2.44, 6.23	0.522, 2.44, 6.23	0.522, 2.44, 6.23

The aim was to compute plausible concentration fields, not to simulate exactly the processes in a real workroom. Thus, error is defined here as the difference between model and CFD predictions. For the steady-state case, the UD model had the lowest error. When the source near-field contained the breathing zone receptor, the CM-2 model was applied. Then, in order of decreasing agreement with CFD were UD, CM-2, and CM-1. Averaging over all source and receptor locations (CM-2 applied for only one), in decreasing order of agreement with CFD were UD, CM-1, and CM-2. Both the source and receptor locations had large effects on emission estimates using the CM-1 model and some effect using the UD model.

A location-specific mixing factor (location factor) derived from steady-state concentration gradients was used to build a more accurate time-dependent emission model, CM-L. This model is based upon a spherical control volume centered at the source with a radius equal to the distance from the source to the “receptor”. Here the receptor is considered to be the continuous monitoring instrument. Assuming uniform concentration within the control volume, $C(t) = C_i(t)$, where i designates any location within the volume. The time-varying emission rate, G(t), could then be calculated as:

$$G(t) = V_i \frac{dC_i}{dt} \qquad \text{Eq. 2.6}$$

where V_i is control volume and the derivative of C_i was determined from the continuously monitored concentration. Total mass emitted from a time-varying source was modeled most accurately by CM-L, followed by CM-1 and CM-2. The algorithm for calculating G from the UD model for time-varying emission rate was not stable. Thus, UD was not applicable to this case.

Recommendations include:

(1) CM-1, CM-2, and UD should not be used to derive a generation rate from near-field concentration measurements when the airflow near a source has a well-defined direction, with the exception that CM-1 may be used upwind or with a location factor for the steady-state case.
(2) CFD models using coarse grids and RANS turbulence models can provide good information on airflows where the forced convection from air inlets dominates, compared with the disorganized flows mentioned previously. Thus, for the situations where CM-1, CM-2, and UD are weak, CFD is an effective tool for understanding the behavior of these models.
(3) Conversely, the application of CFD to flows highly influenced by worker movement, breathing, and natural convection due to heat sources is difficult in terms of setting boundary conditions, finding sufficient computing resources, and obtaining convergence.
(4) For time-varying generation rate: CM-2 can be used effectively when the generation rate is being derived from near-field concentrations, keeping in mind recommendation (1). UD seems to not be stable. CM-1 is simple and robust but is less accurate than CML. CM-L is versatile because, unlike the other three models, it does not rely on the assumption of a particular room concentration structure.

3. GOALS AND SPECIFIC AIMS

The long-term goal of this research was to develop more reliable exposure assessment methods by investigating how physical factors in a workroom govern worker exposure and its spatial variation. The specific aims were:

(1) To determine the effects of worker presence and activities on the workroom concentration and velocity fields;
(2) To determine the effects of worker presence and activities on worker personal exposure;
(3) To develop a deterministic model for exposure assessment that accounts for the fundamental physical determinants of workroom exposure;
(4) To evaluate the use of this model in several workrooms.

4. Experimental Set-up and Approach

An experimental room was designed and constructed. Prior to experiments on the interaction of workers and the workroom environment, preliminary tests were carried out to characterize the room and measurement systems and to determine the required number of sampling locations and required monitoring times at each location. Before the impact of the worker could be determined, a thorough study of the room concentration and velocity fields without a worker present was necessary to obtain baseline data for comparison. These experiments characterized the tracer gas concentration throughout the room for partial factorial combinations of the physical determinants of the concentration field – supply air flow rates, inlet type/location, and temperature gradients. Finally, the effects of worker location, orientation, and movement were investigated at various combinations of the physical determinants previously explored.

4.1. Experimental Room

A rectangular room of dimensions 2.86m(L) x 2.86m(W) x 2.35m (H), shown in Figure 4.1, was constructed with an interior surface of plywood and insulated with Rmax-plus®. The room included a dilution air inlet, a room air exhaust to the roof for outdoor discharge, and a source pedestal. The interior surface of the plywood was coated with Teflon paint to prevent chemical sorption by the surface. One of the vertical walls had a Lexan® (transparent acrylic) window (1.2m (H) x 1.2m (L)) for viewing the workroom. The 1 m high source pedestal had a small opening in the upper surface with a windscreen through which a tracer gas was discharged to the room at a velocity much lower than the room air velocity near the source. That height was chosen because it is nearly midway between two recommended heights for a standing workplace. The recommended heights are 107 cm for light assembly, writing, and packing tasks and 91 cm for tasks requiring large downward or sideward forces (Eastman Kodak Company, 1983). Dimensions of objects and the coordinate positions of their centers are listed in Table 4.1.

Table 4.1: Dimensions and positions of object centers

		Size	*Position (x, y, z)*
Inlet	*Wall Jet*	0.39 m (L) x 0.24 m (H)	0.81 m, 2.12 m, 2.86 m
	Ceiling Diffuser	0.28 m (L) x 0.28 m (W)	1.43 m, 2.35 m, 1.43 m
Outlet		D = 0.1 m	2.71 m, 0.18 m, 2.86 m
Source pedestal		0.1 m (D) x 1.0 m (H)	1.43 m, 1.0 m, 1.43 m

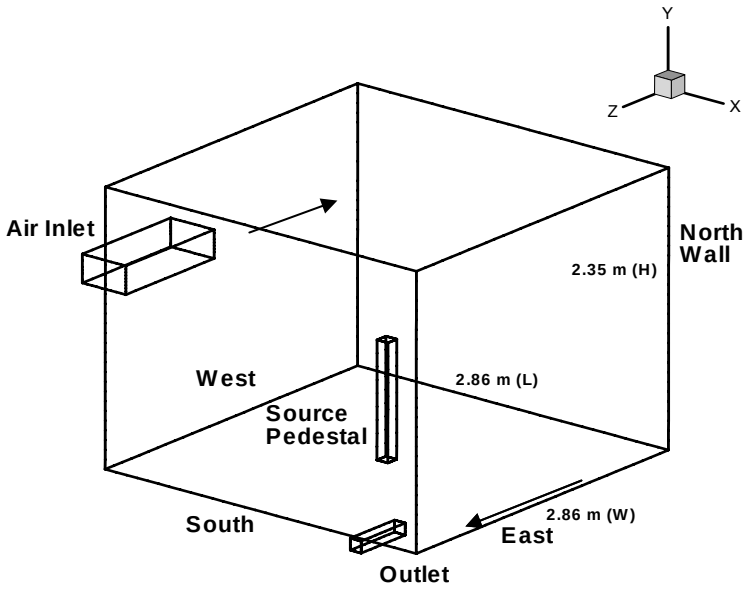

(a) Room with wall jet air inlet

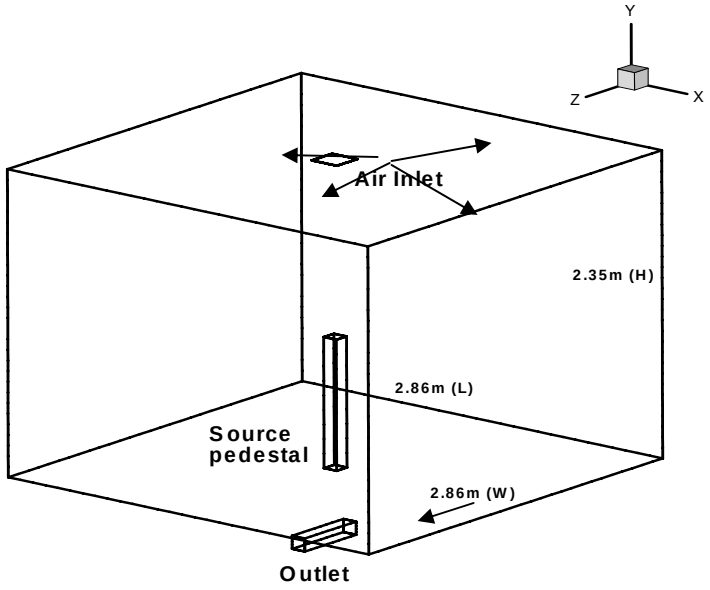

(b) Room with Ceiling Diffuser Air Inlet

Figure 4.1: The Experimental Workroom

The north wall shown in Figure 4.1(a) was chosen to represent a building's external wall for simulating summer and winter conditions. This wall was designed to be controlled to a higher or lower temperature than air in the experimental room.

The experimental room for simulating contaminant transport and exposure in workrooms was placed within a thermostatically controlled laboratory room. To simulate work rooms somewhat larger than the space available, the experimental parameters were set based on similarity criteria. In geometrically similar spaces (for example, a 1 × 2 × 3 meter space is similar to a 2 × 4 × 6 meter space), airflow patterns are similar when the ratios of all the forces that affect fluid motion are equal (Awbi, 1991). When all three of a room's physical dimensions are increased proportionally for isothermal conditions, the airflow patterns within the room will also change proportionally if the Reynolds number (Re) is kept constant. Re is the ratio of inertial forces ($u\rho$) to viscous forces (μ/x), where u=air velocity, x=a characteristic linear dimension of the space, ρ = gas density, and μ = gas viscosity. That is,

$$Re = ux\rho/\mu = 2Q/(\nu(W+H)) \qquad \text{Eq. 4.1}$$

The second form of Re is obtained by substituting: the hydraulic diameter, 2WH/(W+H), for x; the kinematic viscosity, ν, for μ/ρ; and the flow rate, Q, divided by WH, for u.

For constant temperature and pressure, both gas density and viscosity are constant. Re may be held constant by keeping the product of u and x constant. Thus, if the physical dimensions of a room are increased by a scaling factor of S, in order to keep Re constant, the dilution airflow rate must also be increased by a factor of S. For this example, the volume of the room changes by a factor of S^3. Therefore, the air change rate (Q/V) is decreased by a factor of S^{-2}.

The experimental room (Figure 4.1) was 2.86 m (L) × 2.86 m (W) × 2.35 m (H), with a volume of 19 m^3, which is equivalent to larger workrooms with respect to air flow patterns. For instance, the velocity pattern for experimental conditions of Q = 3.3 m^3/min or 10.3 air changes per hour (ACH) is similar to a room six times larger in all dimensions at Q = 19.8 m^3/min. Such a room has a volume of 4152 m^3 and a normalized flow rate of 0.29 ACH. Similarity criteria are discussed in greater detail in an appendix to Lee (2007).

Room air was supplied by either a wall jet (WJ) air inlet or a ceiling diffuser (CD) air inlet with a common exhaust outlet. The jet from the wall inlet is near the ceiling and parallel to it. The CD jet also was directed along the ceiling by several turning vanes in the diffuser. Both jets, though expanding somewhat with distance from the inlets, maintained some attachment to the ceiling by the Coanda effect. The measured air speeds in the occupied zone did not exceed the recommended comfort limit of 18 m/min.(Awbi, 1991; Baldwin and Maynard, 1998) The dimensions and positions of object centers are listed in Table 4.1.

A centrifugal fan located outside the building exhausted room air through the outlet of the experimental room at known flow rates of 5.5 m^3/min and 3.3 m^3/min, drawing clean air into the room. The room was tested for leakage by comparing airflow rates at the inlet and the exhaust. In addition, velocities in the exhaust duct were measured before and after

experiments to ensure a constant airflow rate by obtaining velocity along two perpendicular six-point traverses across a 4-inch diameter exhaust duct with a thermoanemometer (model 8350 VelociCalc; TSI Inc., St. Paul, Minn.).

A photoionization analyzer (PID 101; Process Analyzers, Walpole, Mass.) was used to measure BZ concentration. For quality assurance, the PI analyzer was calibrated before and after each experiment using a known concentration of propylene (100 ppm) in a Tedlar bag. The analyzer was connected to a data logger (StowAway Volt; Onset Computer Corp., Pocasset, Mass.) to record readings every other second.

Pure propylene (99.5%) was used as a tracer to represent a gaseous contaminant. It was bled from a compressed gas tank at constant pressure through a calibrated rotameter and continuously injected at 200 cm^3/min for the 5.5 m^3/min airflow and at 150 cm^3/min for the 3.3 m^3/min airflow. Different tracer emission rates were applied to keep tracer concentrations within the optimal range for measurement with the PI analyzer. Also, pure propylene was selected as the tracer gas because it is easily measured using the PI analyzer, is relatively non-reactive at the level of oxidizers commonly found in indoor and outdoor air and is nontoxic at the concentrations observed.

To promote a uniform distribution of tracer across the opening, tracer was discharged through a fine screen in the opening on top of the source pedestal. The room was allowed to equilibrate for 2 hours at constant air and tracer gas flow rates to achieve steady-state conditions before monitoring began. Three replicate sets of measurements were taken on different days for each combination of experimental variables: two inlet types and two airflow rates.

Automated Sampling System. Figure 4.2 is a schematic drawing of the automatic sample collection and monitoring system (a) viewed from one side of the room, and (b) showing the sampling locations as viewed from above the room. Two steel shafts were mounted on opposing (east and west) walls at 2.2 m above the floor. Each shaft was equipped with eight diecast metal V-groove pulley wheels spaced 0.38 m apart. Braided steel wire was connected to turnbuckles and fed through opposing pulleys forming eight individual continuous loops, called "sampling belts." Tygon® tubes (3 individual tubes per sample belt) were fed through a central opening in the east wall and hung below each of the sample belts using O-rings. The three Tygon® tubes for each sample belt were then cut at heights of 0.4 m, 1.2 m, and 2.0 m above the room floor. The terminal ends of the tubes functioned as 24 individual sampling positions which could be moved across the room from west to east. A stepper motor (DM4050, Microkinetics Corporation, Kennesaw, GA) driven by an MN100 motion controller was mounted on the east wall. A rubber belt connected the stepper motor and the east shaft. The sampling tubes were connected to solenoid valves located outside the room and controlled by the Labview™ software (National Instruments).

The automated system was tested and found to be capable of reproducibly positioning the sampling tubes across the width of the experimental room.

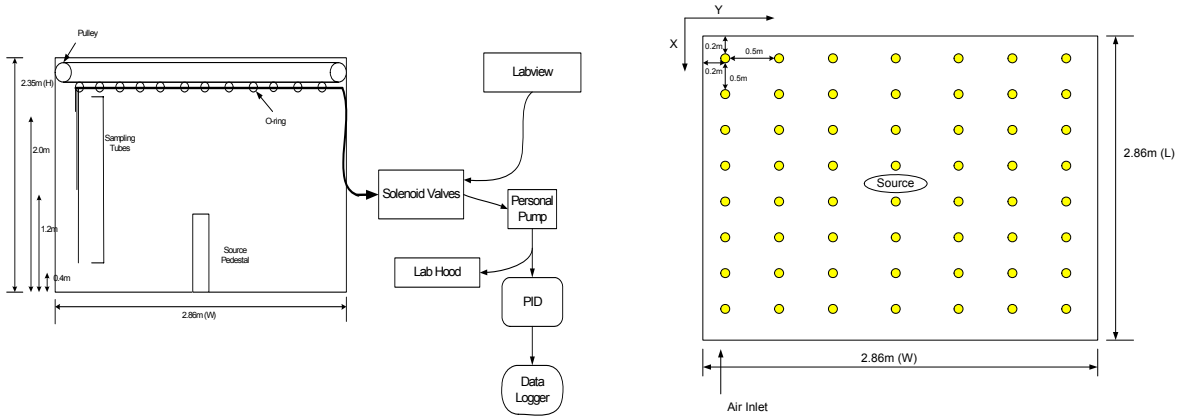

Figure 4.2: (a) The elevation view of automatic sample collection and schematic of monitoring and data acquisition system; (b) The plan view of sampling points.

Wall Heating and Cooling System. The north wall was selected to represent an exterior wall that could be either hotter or colder than the air in the room. All the other workroom walls were insulated plywood, which has a thermal conductivity of below 0.12 W/(m-K^o). Similarly, Lexan® has a low thermal conductivity (0.14 W/(m-K^o)). The thermal conductivity of the insulation material (Styrofoam) is 0.029 W/(m-K^o). The temperature controlled wall was made of 1.5-mm thick aluminum sheets with ten rows of copper tubes (ID=1.25 cm) attached to the outer side (Figure 4.3). The external surface of this wall was insulated with 2.5-cm thick rigid Styrofoam insulation. The copper tubes were connected to a water heater/chiller (Model 3013, Fisher Scientific International Inc.) capable of servicing a heating load of 800 W, a cooling load of 660W at +20 °C (200W at –20 °C), and circulating water through the copper tubes at about 15 L/min. Fifteen k-type thermocouples connected to a computerized data acquisition system running Labview® were uniformly attached to the surface of the "exterior" wall. Four extra thermocouples were added: two at the water inlet and outlet of the copper tubes to measure the enthalpy change across the tubing network and two in the air inlet and outlet ducts to measure the enthalpy change of air passing through the room.

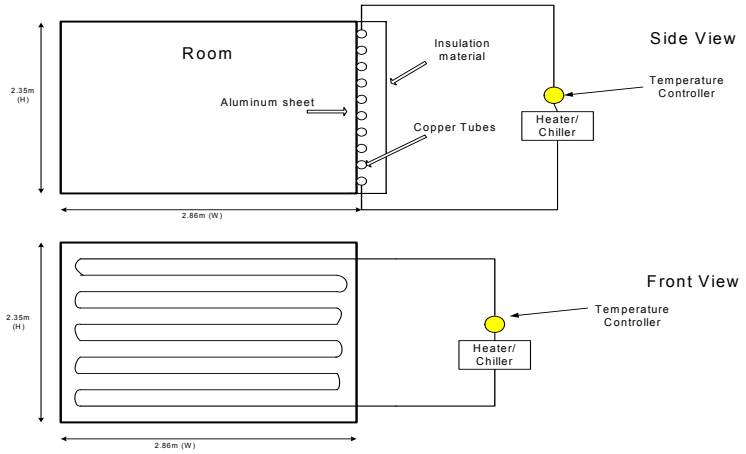

Figure 4.3: The schematic of the heating and cooling system

After modification of the room, leak tests were repeated under static conditions (no air flow). A bolus of tracer gas was added to the room air, the air was mixed using two fans, and the tracer concentration was monitored to determine the rate of tracer loss. The loss rate was barely measurable.

Measuring Personal Exposure. A human participant in the room, wearing a full facepiece air supply respirator (Neoterik Health Technologies, Inc., MD, USA), represented a stationary worker and a moving worker. For the stationary worker experiments, various worker orientations (i.e., rotation to different directions, 0^{o}, 90^{o}, 180^{o}, and 270^{o}) and the locations were tested. Twelve sampling points were selected including 4 points near the source pedestal. In order to minimize bias and random error for the moving worker experiments, the path to be taken by the worker was kept consistent from run to run by putting tape markings on the floor and establishing times for the worker to reach each point. As shown in Figure 5.2, two paths were employed, a forward path beginning at sampling point 1 and ending at sampling point 12, and the reverse path which began at sampling point 12 and ended at sampling point 1. The worker walked along each path for three minutes. Eight sampling points far from the source were used (sampling points 1-8) and four sampling points near the source were used (sampling points 9-12). A continuous sample was drawn through a length of 1/16" Tygon® tubing positioned in front of the respirator, between the mouth and the nose, to measure breathing zone exposure. Preliminary tests did not show any influence of the relatively clean air coming out the bottom of the facepiece respirator on the tracer gas concentration in the breathing zone. Personal exposure was measured over the entire time period, and monitoring of one randomly-selected area sampling point (location (x, y, z): 1.34m, 1.2m, 0.45m) was also conducted to see if the worker's movement disturbed the contaminant concentrations at a fixed point. The outlet concentration of all combinations was checked before and after each experiment.

4.2. Preliminary experiments Preliminary experiments were performed to determine the monitoring time required at each point and the number of measurement points needed to give a detailed representation of the room.

4.2.1. Required Monitoring Time. Here we used the standard deviation ratio (SDR) method to determine the minimum monitoring time required to estimate the mean concentration within a specified precision limit. Tracer gas concentrations at nine sampling locations in an experimental room were measured to estimate population parameters. At flow rates of 0.9, 3.3, and 5.5 m^3/min, contaminant concentrations were measured using a photoionization analyzer.

4.2.1.1. Methods. One method for determining the appropriate sampling time, called standard deviation ratio (SDR) method, was presented by Luoma and Batterman (2000). This approach calculated the required number of sequential samples, and hence the required sampling time. This approach is based upon two parameter estimates: the standard deviation and the autocorrelation. These two parameters are then used to calculate the

standard deviation of the mean, also called the standard error, for correlated measurements. The formula for this calculation is given by Equation 4.2.

$$\sigma_{1,n} = \frac{\sigma}{n}\left[n + 2\sum_{i=1}^{n-1} i\rho^{n-i} \right]^{1/2} \qquad \text{Eq. 4.2}$$

where ρ is the autocorrelation coefficient between pairs of measurements separated by one unit of time, σ is the standard deviation of the population of all measurements, and $\sigma_{1,n}$ is the standard deviation of a sample of size n.

For a first-order autoregressive process, SDR ($\sigma_{1,n}/\sigma$) and ρ are required to find the proper sample size, where the SDR is found by simply taking the ratio of the correlated standard error and the standard deviation. We expanded the SDR method to construct confidence intervals around the mean concentration such that the interval length falls within a desired precision. In this case, a third parameter, the population mean, must also be estimated.

In the current study, concentration data at nine locations in an experimental room have been collected to estimate the standard deviation of the population and the autocorrelation coefficients.

The measure of precision (*d*) used is one-half the width of the confidence interval for μ_c, the true mean concentration (i.e., the distance between the upper/lower confidence limit and the observed mean concentration). For a normally distributed random variable, the confidence interval for the mean is given as:

$$\bar{x} \pm (Z_{1-\alpha/2})\left(\frac{\sigma}{\sqrt{n}}\right), \qquad \text{Eq. 4.3}$$

where $\bar{x}$ = sample mean concentration , $\frac{\sigma}{\sqrt{n}}$ = standard deviation of the sample mean (standard error), and $Z_{1-\alpha/2}$ is the z-value from the standard normal distribution that relates to the $(\alpha/2)$ percentage. Note that for small sample sizes (generally considered at n<30), the t-distribution with n-1 degrees of freedom should be used instead of the standard normal distribution. Thus, we can define a desired half width of the confidence interval as:

$$d = (Z_{1-\alpha/2})(\sigma_d) \qquad \text{Eq. 4.4}$$

where σ_d = standard error corresponding to desired precision, *d*, and α is such that the interval is a (1-α)100% confidence interval.

If a 95% confidence interval is desired, then $Z_{1-\alpha/2} = Z_{.975} = 1.96$. If the confidence limits are desired to be within 10% of the true mean of measured concentration, then $d = 0.1\,\mu_c$. Then $(\sigma_n)_d$ is calculated by rearranging Equation 4.4:

$$(\sigma_n)_d = \frac{d}{(Z_{1-\alpha/2})} = \frac{0.1\mu_c}{1.96} = \frac{\mu_c}{19.6} \qquad \text{Eq. 4.5}$$

Since the true concentration of the population, μ_c, requires an infinite number of measurements, in practice, this can be replaced with the sample mean, $\overline{X}$, which represents a set of measurements which were collected long enough to represent a true mean concentration. Thus, Equation 4.5 can be rearranged as:

$$(\sigma_n)_d = \frac{d}{(Z_{1-\alpha/2})} = \frac{0.1\overline{X}}{1.96} \qquad \text{Eq. 4.6}$$

The desired standard deviation ratio, SDR_d, can be calculated as:

$$SDR_d = \frac{\sigma_d}{\sigma} \quad , \qquad \text{Eq. 4.7}$$

where σ can be estimated by *s* (standard deviation of $\overline{X}$), the sample standard deviation of concentration estimated from concentration measurements. Using the value of SDR_d and the value of ρ based on concentration measurements, the necessary sampling size was determined from Figure 5, an expanded version of a graph presented by Luoma and Batterman (2000). They presented a graph of SDR versus sample size with separate lines for values of the autocorrelation coefficient (ρ) from 0 to 0.95. The required monitoring time was then calculated as follows:

Required monitoring time = n_{req} x $Time_{(x2-x1)}$ Eq. 4.8

where n_{req} = the required sample size estimated from the SDR approach
$Time_{(x2-x1)}$ = the time interval between concentration measurements.

Tracer concentrations were monitored at nine locations (Figure 4.6) for 20 minutes each.

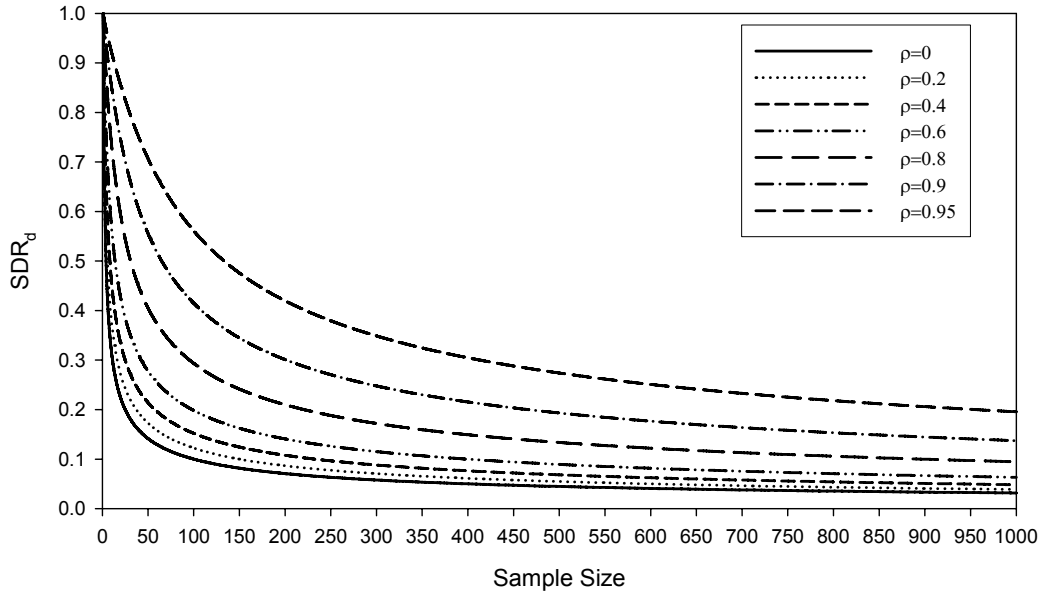

Figure 4.5. Predicted variability of the SDR_d (σ_d/σ) for various sample sizes (n = 1 to 1000) and autocorrelation coefficients (ρ).

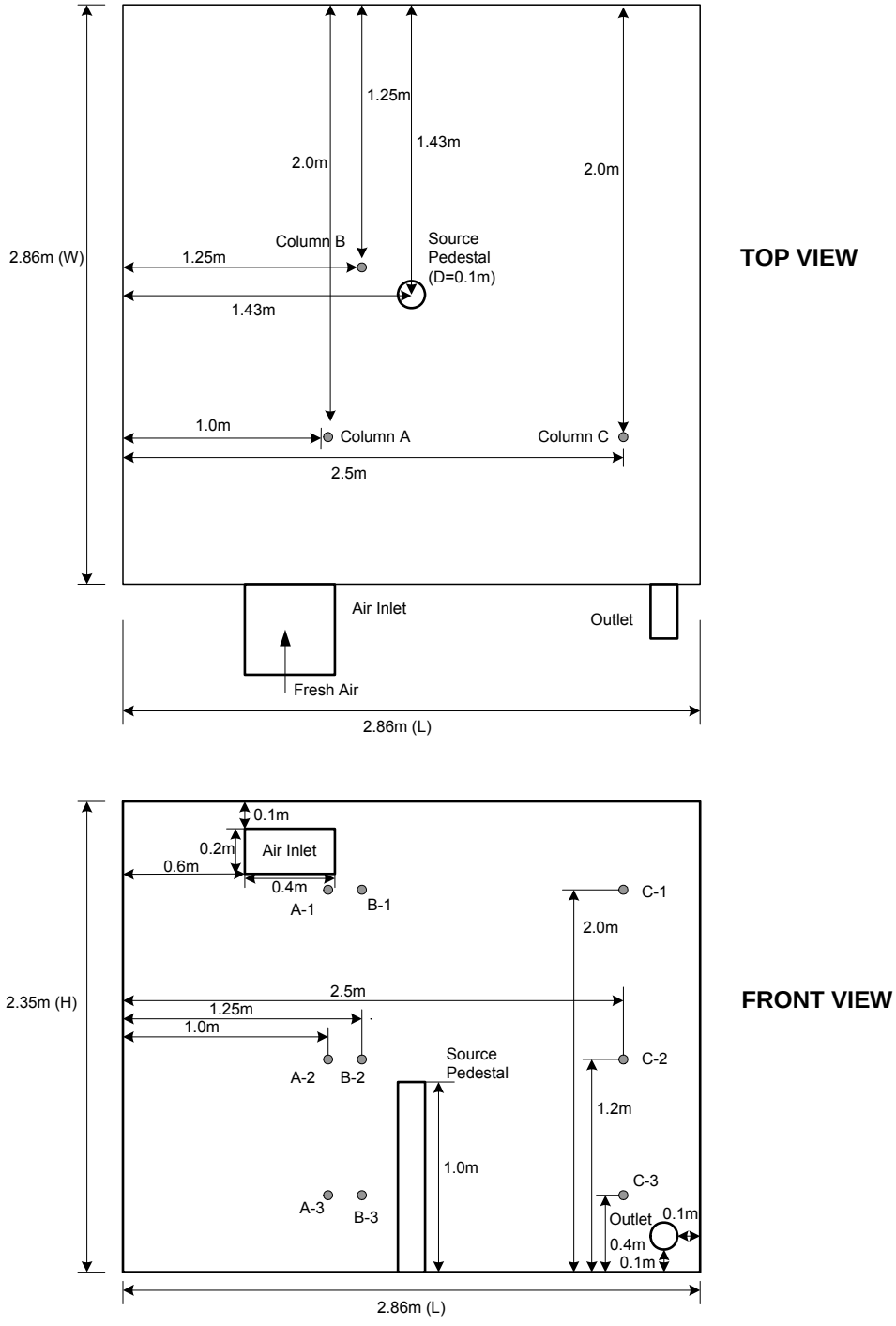

Figure 4.6. Sampling locations: viewed from above (upper figure) and viewed from side (lower figure)

4.2.1.2. Results. The autocorrelation coefficient (ρ) was calculated from a total of 600 measurements. At most sampling points, the estimated ρ was greater than 0.6, except for one sampling point (A-3 at 3.3 m^3/min) in Table 3. After obtaining autocorrelation coefficients, the required monitoring time using the SDR approach was estimated and is summarized in Table 4.2. For each condition, three desired precisions, 20% (d = 0.2), 10% (d = 0.1), and 5% (d = 0.05), were employed. It was observed that the required monitoring time at a constant flow rate varied by more than 3 orders of magnitude among the 9 sampling points. For 3.3 m^3/min, the longest monitoring time requirement was observed at the point B-2, while for 5.5 m^3/min, the longest requirement was observed at point A-1. For 3.3 m^3/min at point B-2, more than 6 hours were required to obtain representative concentration estimates for $100d/\mu_c$ with a 5% precision and more than 1.5 hours were required with 10% precision. On the other hand, at some sampling points (A-3, C-1, C-2, C-3) marked by a double asterisks (**), only one reading (2 seconds) was necessary. This happened because the variability required to achieve the desired precision was greater than the variability of the measured concentrations ($SDR_d > 1$). For those sampling points requiring only one concentration measurement, it is advisable to use some minimum monitoring time, such as 1-min, or 2-min.

Table 4.2. Autocorrelation coefficients (ρ) and required monitoring time (sec)

Sampling Points	3.3 m^3/min					5.5 m^3/min			
	ρ[a]	Required monitoring time (sec)				ρ	Required monitoring time (sec)		
		20%[b]	10%[b]	5%[b]			20%	10%	5%
A-1	0.70	6	52	226		0.89	432	1782	7180
A-2	0.74	32	150	624		0.86	366	1506	6068
A-3	0.45	4	26	110		0.93	2**	138	658
B-1	0.82	40	200	830		0.84	124	536	2178
B-2	0.92	1408	5710	22960		0.83	424	1730	6954
B-3	0.87	448	1838	7398		0.84	6	94	412
C-1	0.72	22	116	484		0.71	2**	2**	26
C-2	0.84	70	322	1320		0.62	2**	2**	4
C-3	0.78	16	106	446		0.87	2**	2**	72

[a]Autocorrelation coefficients at lag 1.

[b]Desired precision, $100d/\mu_c$.

** = SDR_d is greater than 1; therefore, minimum sampling time, such as 1-min or 2-min is recommended.

An interesting preliminary finding was that, at the lowest flow rate (0.9 m^3/min), statistically stationary concentrations were not reached after 20 minutes at 6 of the 9 monitoring points. Additional measurements were made at sampling point C-1 for 5 hours, but concentration generally increased over this time period with some short-term variation superimposed; the highest 20-min average instrument reading was about 6.8 times greater than the lowest 20-min average reading. This result indicates an unpredictable air flow movement inside the room due to dominant air motion by thermal convection rather than by forced convention. This result has been discussed in greater detail elsewhere (Lee, 2006a). Because stationary concentrations were not obtained over extended monitoring periods, the lowest flow rate explored was judged to be impractical for subsequent study. It appeared that extremely long

monitoring times would have been required to obtain validation data. This unpredictable phenomenon limited the experimental flow rates to those that generated stationary concentrations in the room.

4.2.1.3. Conclusions. At the lowest air flow rate studied (Q = 0.9 m^3/min), statistically stationary concentrations were not reached, even after 5 hours of monitoring at one sampling point. At a randomly selected sampling point, the ratio of instrument readings between the highest 20-min and the lowest 20-min was approximately 6.8. Thus, adequate monitoring times for this condition could not be estimated. These air flow conditions are not extreme and thus similar circumstances may be encountered elsewhere. The implication for developing monitoring strategies is that accurate characterization of mean long-term concentrations in rooms with low air flow rates may require extremely long monitoring times, even when emission rate and air flow rate are relatively constant.

This preliminary experiment also showed that monitoring time requirements vary substantially with location within a room and depend on air flow rates, which cause variation in air flow patterns and, thus, in concentration. For the two higher flow rates studied, the required monitoring times varied by more than 3 orders of magnitude among the 9 sampling points. Locations near the air inlet and outlet openings showed the least variation and required relatively short monitoring times, whereas large random variations were observed near the source, requiring longer monitoring times.

4.2.2. Required Spatial Coverage. Contaminant concentration was measured at various locations in the experimental room to get a detailed concentration profile. Samples were taken through permanent individual tubes for each of the 89 measurement locations. Data collection was initially done manually, which required opening and closing individual valves for each of the locations. To reduce the number of tubes in the room and to minimize the amount of labor involved in data collection, we designed and implemented an automated sampling and data collection system. In this design, 21-tubes (7 traverses at 3 heights) were mounted on a pulley system and were positioned by a stepper motor. Fewer tubes allowed easier movement in the room, which proved to be an advantage for later experiments.

The 3-D sampling matrix in the workroom was explored using experimental measurements and CFD simulation. Subsets of concentration data containing from100 to 150 points were used to generate concentration isopleth plots using TecPlot. No substantial differences in isopleth shape or magnitude were observed over this range of points. Thus, a 3-dimensional network of 144 points was utilized for the characterization of the concentration fields in the unoccupied room.

4.2.3. Effects of Temperature Differences. Prior to studying the impact of worker's presence on concentration fields, it was necessary to assess the effects of physical factors. The effect of temperature differences within a room on spatial contaminant distribution was evaluated and reported by Lee (2006a). Tracer gas (99.5% propylene) concentrations were monitored automatically at 144 sampling points with a photoionization detector. Experiments were preformed at two flow rates (5.5 and 3.3 m^3/min, equivalent to room Reynolds Number,

Re of 12,200 and 7,300) and six thermal conditions: isothermal, three summer conditions (Archimedes number (Ar) = 2500, 4900, and 7400) and two winter conditions (Ar = 2500 and 4900). The room Re as defined by Awbi (1991) is a dimensionless number used to characterize the room air flow regime. For 5.5 m^3/min and all thermal conditions, the coefficient of variation (CV) ranged from 0.34 to 0.45 and the normalized average concentrations were similar. For 3.3 m^3/min, winter conditions produced greater spatial variability of concentration (CV = 0.72 and 1.10) than isothermal or summer conditions (CV range = 0.29–0.34). Tests simulating winter conditions suggest that the resulting stable temperature structure inhibited the dilution of the tracer and enhanced its segregation in the lower portion of the room, especially for the lower flow rate (3.3 m^3/min). Therefore, not explicitly addressing thermal effect in exposure modeling may impact the estimated accuracy and precision when used for rooms that are non-isothermal and not well mixed. These findings also have implications for air monitoring. Dispersion patterns for different thermal conditions were found to be substantially different, even when the mean concentrations were nearly the same. Thus, monitoring data from a single season should not be taken as representative of the entire year, when summer and winter conditions create temperature gradients in a room.

5. SPECIFIC AIM 1 – EFFECTS OF WORKER ON CONCENTRATION

Under some circumstances, the location, orientation and activity of a worker can affect contaminant concentrations throughout a workroom. We have reported the findings of our research on the effects of the presence of a stationary worker on the concentration field in the experimental room under isothermal conditions (Lee, 2005). This appears to have been the first experimental study of these effects performed in a room with mixing ventilation. Previous studies where performed either in a wind tunnel (Hyun, 2001; Welling, 2000), or in a room with displacement ventilation (Bjorn, 2002; Mattsson, 1994; Mattsson, 1996; Mattsson, 1997; Xing, 2000). The impact of worker presence is expected to be different for different air flow regimes. In addition, most previous studies did not sample throughout the workroom. In a separate paper, we reported on the impact of worker motion in the experimental room on the concentration at a single location for mixing ventilation (Lee, 2007).

5.1. Methods

The effect of an worker's presence on contaminant dispersion and other physical factors were studied in the experimental room including a 1-m high source pedestal located in the center of the room, a dilution air inlet (either wall jet (WJ) air inlet or ceiling diffuser (CD) air inlet), and an outlet, as shown in Figure 4.1. Factorial combinations of two flow rates (3.3 and 5.5 m^3/min), two air inlet types (WJ air inlet and CD air inlet), and four worker locations, as shown in Figure 5.1 for the WJ and one worker location (north of the source) for the CD, were employed and compared with those when the worker was absent. Here for the CD inlet, the only worker location examined was north of the source. From the preliminary

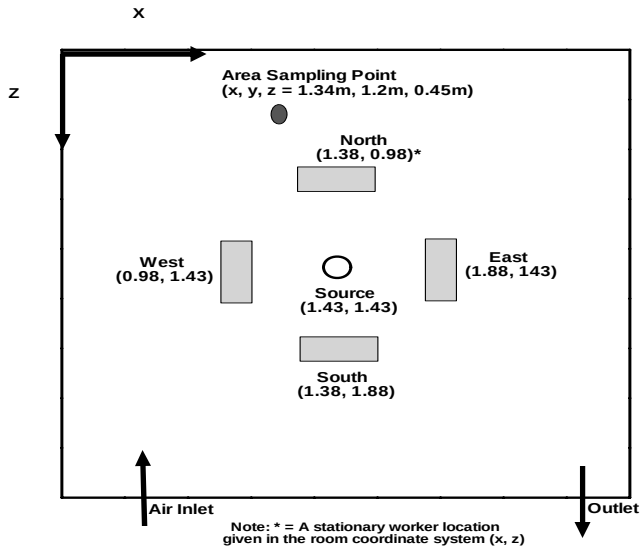

Note: The grey boxes indicate locations of the heated mannequin given in the room coordinate system (x, z)

Figure 5.1. Locations of the heated mannequin (120 W) and area sampling point in the room.

experimental results, a worker in the north had a considerable effect on the contaminant distribution, and the CD produced a symmetrical flow pattern about the source when the source was located at the center of the room. A mannequin was used to represent an worker, and it was wrapped with resistance-heating wire to produce a heat load of 120W, because thermal heat loss from the body has been shown to affect the airflow field near the body (Johnson, 1996).

Under steady-state conditions, tracer gas (99.5% propylene) concentrations were monitored automatically at 144 sampling points with a photoionization detector. The room was divided into three planes, 0.4m, 1.2m, and 2.0m above the room floor, and each plane had 48 sampling points. Two different tracer emission rates, 2.0×10^{-4} m^3/min for the 5.5 m^3/min and 1.5×10^{-4} m^3/min for the 3.3 m^3/min, were employed.

To explore uniformity of concentrations within the room (i.e., mixing effectiveness), the coefficient of variation (CV) the standard deviation (SD) divided by the mean concentration – was calculated and compared among the cases investigated. Graphical comparison using the Kriging interpolation method was performed for a qualitative comparison. For a quantitative comparison, a statistical analysis, randomized complete block design (RCBD) test, was performed to test if the measured concentration in the room was the same with no workers as the measured concentration corresponding to the same sampling point when the worker was in the four different positions. Here sampling positions in the room and the worker locations were employed as a blocking variable and treatments, respectively. A total of four comparisons were conducted, and for the WJ inlet, the Tukey test was performed for individual comparison. A significance level of a=0.05 was used.

A separate set of experiments (Lee, 2007) was performed to see if a worker's activity disturbed the average contaminant concentration at a randomly selected sampling point (location (x, y, z): 1.34 m, 1.20 m, 0.45 m) shown in Figure 5.1. The worker walked along the path from point 1 to point 12 in numerical order, shown in Figure 5.2, and then reversed direction. For both air inlets and both flow rates, area monitoring results with a moving worker in the room were compared with area monitoring results at the same point with a stationary worker present. Figure 5.1 shows locations of the mannequin in the room and the fixed area sampling point. (Impact of worker's presence and motion on the worker's exposure is discussed in the Section 6.)

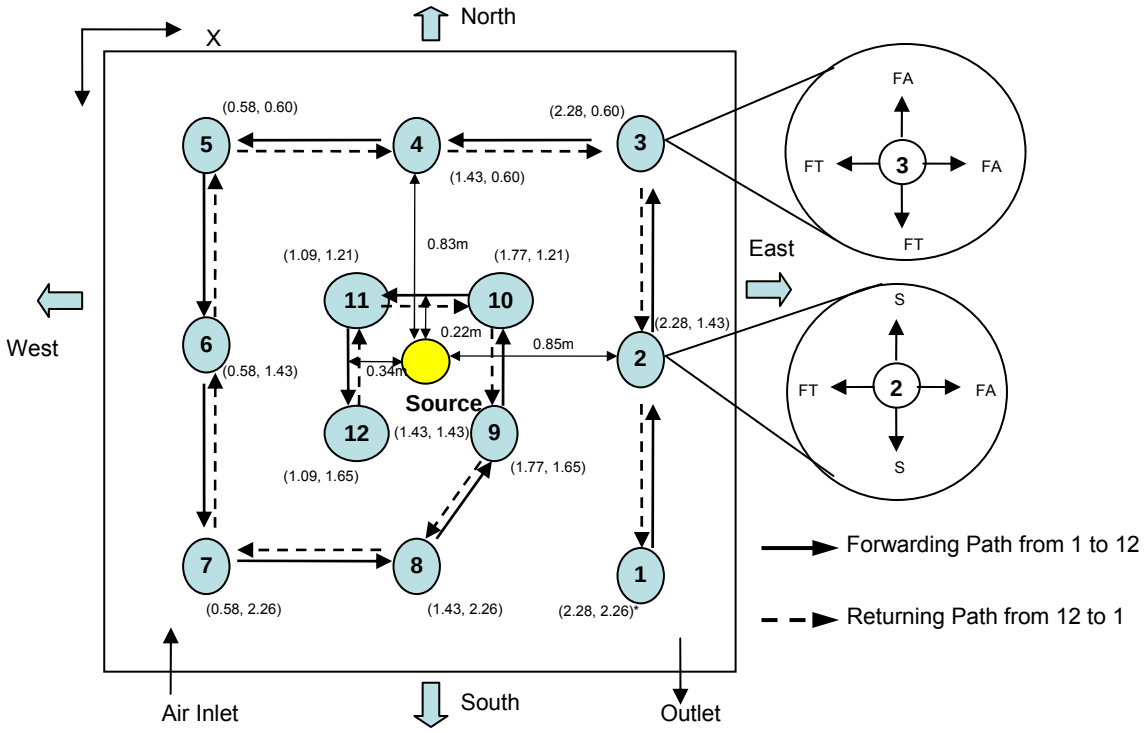

Figure 5.2. Numbered sampling points for a stationary worker and the path of a moving worker (a human being was used in the experiment), Note: * = Sampling location given in the room coordinate system (X, Z), Worker orientation: FT = facing toward the source, FA = facing away from the source, and S = sideways to the source.

5.2. Results

Qualitative comparison. For both inlet types, only slight differences were observed from the comparison of overall mean concentrations when the worker was absent versus when the worker was present in each location. The overall mean concentration for all monitoring locations ranged from 39.8 to 41.4 ppm for the WJ/5.5 m^3/min, from 48.8 to 52.7 ppm for the WJ/3.3 m^3/min, from 32.7 to 37.3 ppm for the CD/5.5 m^3/min, and from 41.9 to 46.9 ppm for the CD/3.3 m^3/min.

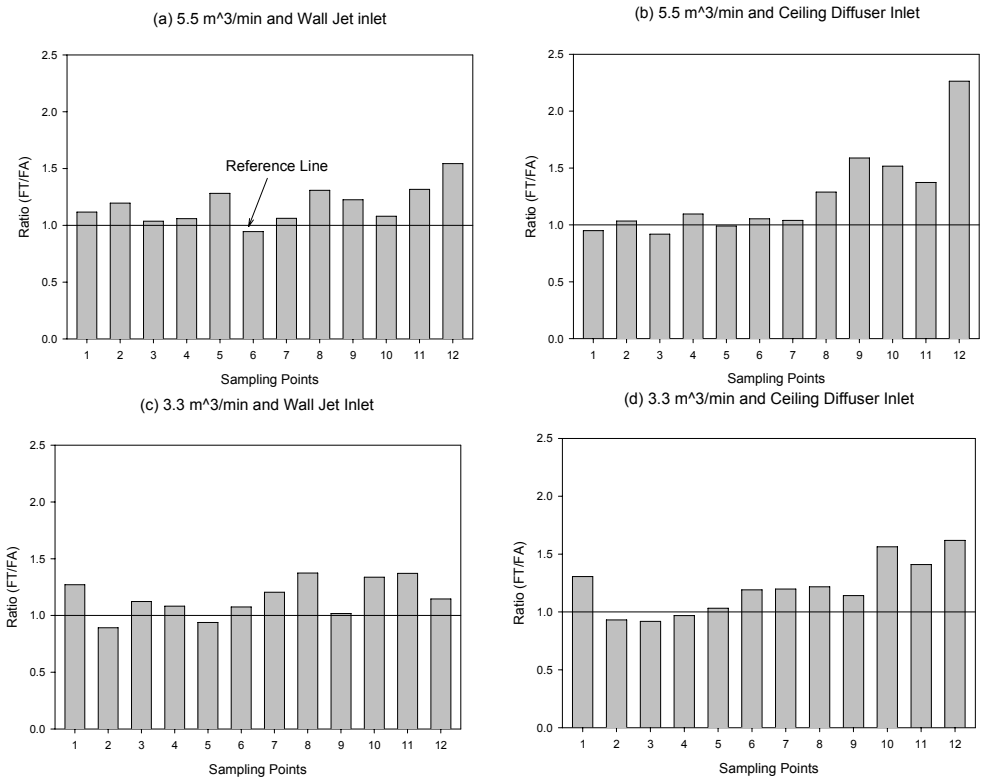

FIGURE 5.3. Ratio of breathing zone concentration for facing toward the source (FT) and facing away (FA) from the source.

As shown in Figure 5.3, for the WJ air inlet, relatively more variation of contaminant concentrations was observed in overall CVs for 5.5 m^3/min than those for 3.3 m^3/min. For all four worker locations, the effect of worker's presence was to increase overall CVs at 5.5 m^3/min and to decrease overall CVs at 3.3 m^3/min. For the CD air inlet, the overall mixing effectiveness when the worker was located north of the source for 5.5 m^3/min was the same as when the worker was absent. When the worker was north of the source at 3.3 m^3/min, the overall CV (0.23) was lower than the CV when the worker was absent (0.31). Hence, at the lower flow rate, the contaminant and clean dilution air were less segregated (i.e., better mixed) than when the worker was present. Presumably, thermal convection from the heated mannequin promoted better mixing of room air.

The Figure 5.4 shows the distribution of the contaminant concentration in the middle plane for the WJ/5.5 m^3/min. Lighter shades of gray indicate lower concentration. The worker's presence in all four locations generated higher concentrations above the source pedestal due to the reduced convection and dilution of the tracer as compared to the same area when the worker was absent. Also, when the worker was absent, two higher concentration areas, one area just above the source and one to the north of the source, were observed; whereas only one higher concentration area, which was above the source, was observed when the worker was present either south or north of the source. For the WJ/3.3 m^3/min, the worker's presence in each of the four locations also affected the dispersion pattern of contaminant concentrations in the middle plane.

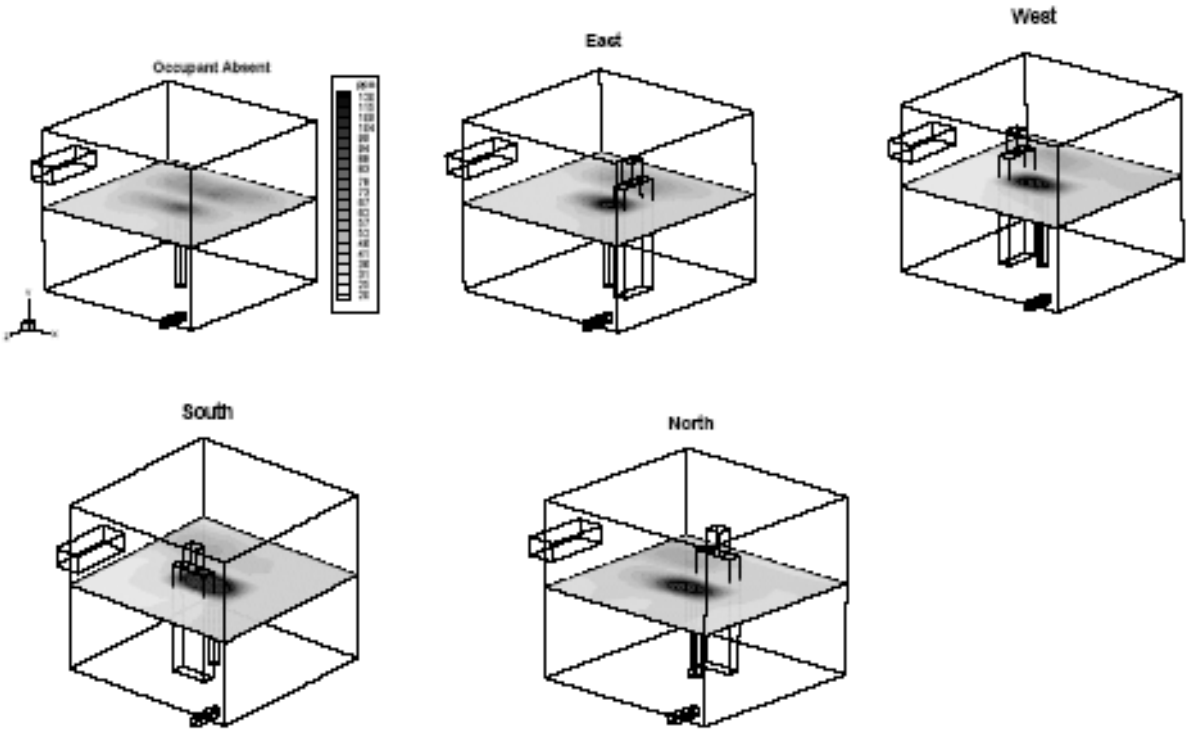

Figure 5.4. Distribution of the contaminant concentration in the middle plane (5.5 m^3/min, Y=1.2m)

For the CD/5.5 m^3/min, lower concentrations were observed in the bottom plane than in the top plane, unlike the dispersion pattern of the WJ air inlet. This would appear to be caused by the ceiling diffuser, because the air coming in from the CD blew along the ceiling in all horizontal directions, down the walls and back along the floor towards the center of the room. As the air flowing back toward the center of the room along the floor reached to the source pedestal and turned upward, the combined effect of air convection and turbulent diffusion from the source pedestal resulted in vertical movement of the tracer and generated higher concentrations in the top and middle planes. Also, the contaminant dispersion pattern in the middle plane was very similar to the pattern when the worker was absent, unlike the CD/3.3 m^3/min experiments in which the worker's presence affected dispersion pattern in the middle plane.

An interesting result was observed in the comparison of contaminant distribution with and without the worker present to the north of the source at the 3.3 m^3/min flow rate and for both inlet types. As shown in Figure 5.5, with no worker present, the highest concentration area among all three planes was observed in the middle plane, but when the worker was placed to the north, the highest concentration area was observed in the bottom plane, not in the middle plane.

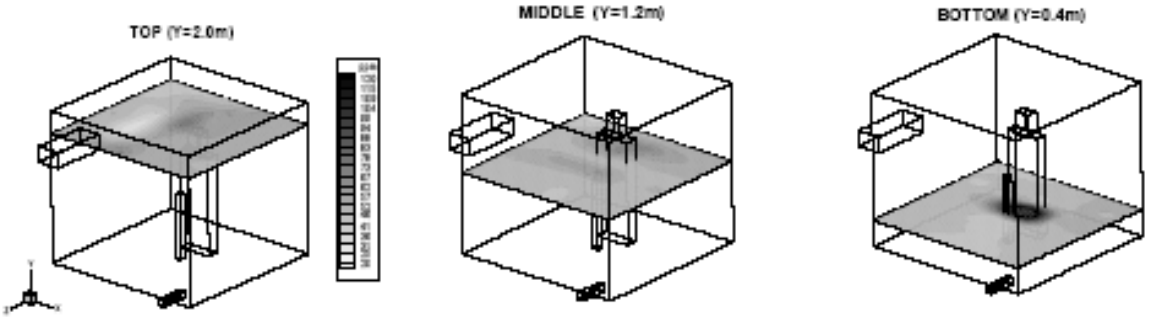

Figure 5.5. Distribution of the contaminant concentration
(3.3 m^3/min, Worker location: North)

Quantitative comparison. As shown in the Table 5.1, overall, a statistically significant difference (overall p-value: 0.0731) was not detected for the WJ/5.5 m^3/min flow rate, and no significant differences were detected from RCBD tests on room mean concentrations for all individual comparisons investigated. On the other hand, an overall significant difference in contaminant concentration (overall p-value: <0.0001) was detected for the WJ/3.3 m^3/min flow rate. Using Tukey's method, no significant differences were found between mean concentrations for the worker present north and east of the source and among mean concentrations for the worker absent and present to the south and the west of the source. For the CD inlet, the RCBD test detected a strongly significant difference between concentration means for the worker present and absent at 5.5 m^3/min (overall p-value: <0.0001), and no significant difference was detected for the 3.3 m^3/min (overall p-value: 0.5011).

Comparison of area concentrations for varying conditions of a worker's activity. Table 5.2 reports TWA concentrations at the fixed point ((x, y, z) = 1.3 m, 1.2 m, 0.5 m) for varying conditions of a worker's activity and locations. For both flow rates, when the worker was walking along the path, the area monitoring result was generally lower than or almost equal to results for other conditions. The shortest distance from the worker's path to the area sampling point was 15 cm. The worker's movement probably disrupted the room airflow and generated more mixing of room air, causing lower concentration at the sampling point. That is, presumably, when the worker was absent or standing still, incomplete mixing of room air generated locally lower or dead-air-space at the sampling point and thus promoting higher concentrations at that specific point.

Overall, statistically significant results were detected from comparisons of area concentrations for varying conditions of a worker's activity; overall p-values for both flow rates were less than 0.0001 (< 0.05). Individual comparison was performed by using Scheffe's method to determine where the differences were; as shown in Table 5.2, no statistical significance was detected from the comparison of Worker West (WW) vs. No Worker (NW), NW vs. Worker East (WE), and Worker South (WS) vs. Worker North (WN) vs. Moving Worker (MW) for the 5.5m^3/min; and the comparison of WS vs. MW, NW vs. WN, and WE vs. WW for the 3.3 m^3/min.

Table 5.1. *Overall p-value and individual comparison of mean room concentrations from RCBD test for the WJ and CD inlet*

Inlet Type	Flow Rate m^3/min	Overall p-value [A] (F-test statistics)	Tukey Grouping[B]	Individual Comparison Condition (Worker Location)	Average Conc.[C] (ppm)
WJ	5.5	0.0731 (2.15)	A	East	41.36
			A	South	40.75
			A	North	39.98
			A	Absent	39.18
			A	West	38.74
	3.3	< 0.0001 (7.31)	A	North	52.73
			A	East	52.56
			B	Absent	49.55
			B	South	49.15
			B	West	48.77
CD	5.5	< 0.0001 (23.20)	N/A	Absent	36.10
				North	34.55
	3.3	0.5011 (0.45)	N/A	Absent	45.39
				North	44.67

[A]Statistical test result by RCBD test

[B]Same characters indicate non-significant difference

[C]Room mean concentration over 144 monitoring locations

5.3. Discussion

The worker's presence influenced the contaminant dispersion pattern in the occupied portion of the room for the WJ inlet at both flow rates and for the CD inlet at 3.3 m^3/min. Interestingly, for the CD inlet and 5.5 m^3/min, the worker present north of the source did not affect the contaminant dispersion pattern in the occupied zone compared to the pattern when the worker was absent. For the 5.5 m^3/min flow rate and the WJ inlet, concentrations were higher near the source pedestal for all worker locations than those when no worker was present. Perhaps, the worker partially blocked airflow near the source pedestal, reducing convection and dilution of the tracer. For the 3.3 m^3/min and the WJ inlet, when the worker was located to the west and north, the combined thermal effect of the worker and air turbulence in front of the worker caused better mixing of room air that resulted in low concentrations around the worker. Unlike the experiments at 5.5 m^3/min and both inlet types, when the worker was located to the north, a higher concentration area was observed in the bottom plane for the 3.3 m^3/min flow rate, but not in the middle plane. Perhaps, the warm air rising around the heated body was replenished by adjacent downdrafts of cooler air conveying contaminant toward the floor.

Although no statistical differences were detected in the comparison of overall and individual mean concentrations, one should be cautious with this interpretation because graphical comparisons showed that the distributions of contaminant concentrations were very different.

Table 5.2. Mean room concentrations for varying conditions of worker's activity at a randomly selected sampling point (location ((x, y, z) = 1.3 m, 1.2 m, 0.5 m) (WJ inlet)

5.5 m^3/min flowrate				3.3 m^3/min flowrate			
Condition[A]	Conc[B] (ppm)	Individual Comparison [C]		Condition[A]	Conc[B] (ppm)	Individual Comparison [C]	
WS	40.8	A		WS	54.7	A	
WN	41.7	A		MW	50.6	A	
MW	45.1	A		NW	68.6		B
WW	51.5		B	WN	69.8		B
NW	52.6	C	B	WE	83.2	C	
WE	56.0	C		WW	89.2	C	
F-Test statistics (p-value) [D]: 54.5 (< 0.0001)				F-Test statistics (p-value) [D]: 107.2 (< 0.0001)			

[A] Conditions of worker's activity: MW = moving worker, NW = No worker or mannequin present, WE, WW, WS, and WN = heated mannequin present east, west, south, and north of the source, respectively.
[B] TWA concentration at the fixed sampling point for each condition.
[C] Same letters indicate the difference of concentrations was not significant.
[D] From ANOVA test.

5.4. Conclusions

Nine out of ten comparisons showed that the pollutant dispersion patterns in an occupied, ventilated room depend upon the location of the worker and the worker's interaction with the velocity field. For the CD inlet and the 5.5 m^3/min flow rate only, the dispersion pattern of contaminant concentrations when the worker was present north of the source was similar to the pattern when the worker was absent.

This investigation showed that the worker's presence near the source affected concentration in an area near the source, but the distribution pattern in the remaining area was very similar to the pattern when the worker was absent. Further research investigating effects of worker presence on exposure of other workers with varying distances would be valuable.

Also, under the same room configuration studied here, the ceiling diffuser inlet in the center of the ceiling was more efficient than a wall jet. High contaminant concentrations were only found in a limited area above the source; the rest of the room was virtually well mixed and uniform.

In addition, the concentration at a fixed monitoring location was generally higher (on average 8% and 44% higher for flow rates 5.5 and 3.3 m^3/min respectively) when the worker was

stationary or absent than when the worker moved along a fixed path. Presumably, the worker's movement generated a better dilution of room air, at least near the sampling point; however, without further study, this conclusion must be limited to the conditions studied here, since the area concentration was monitored at only one location.

6. SPECIFIC AIM 2 - EFFECTS OF WORKER ON WORKER EXPOSURE

Experiments were performed to assess the effect of a worker's location, orientation and activity on the worker's exposure to the tracer gas. This research was reported in Lee (2007).

6.1. Introduction

A worker's exposure to airborne contaminants is a function of physical factors that affect contaminant transport within the workroom. For example, personal exposure to an airborne contaminant depends directly upon the distribution pattern of the contaminant within the workroom. The distribution of contaminant concentrations, in turn, depends upon the room air velocity field, as well as the effects of source factors, such as contaminant composition, density, and generation rate. Some other factors that affect velocity and concentration fields include: the type of supply air diffusers; the temperature differences between walls and room air; the room configuration; and the worker's location, orientation, and activities. These factors have an impact on the worker's exposure, but experimental investigation of the effects of all these factors and their interactions is very challenging.

Most previous studies of the effects of worker factors (such as location, orientation, and activity) on exposure were performed in wind tunnels using displacement ventilation, which differs substantially from dilution-ventilated rooms. Thus, research on these worker factors in dilution ventilation is needed. Also, previous studies of a moving worker restricted the worker's movement to a single dimension, back-and-forth in the middle of room, not walking around a room. Therefore, the primary objective of a portion of the study was to investigate the effect of worker's location, orientation, and activity on breathing zone concentration (BZC) of a gaseous contaminant in a room with dilution ventilation.

6.2. Methods

Pure propylene (99.5%) was used as a tracer to represent a gaseous contaminant. It was bled from a compressed gas tank at constant pressure through a calibrated rotameter and continuously injected at 200 cm^3/min for the 5.5 m^3/min airflow and at150 cm^3/min for the 3.3 m^3/min airflow. Different tracer emission rates were applied to keep tracer concentrations within the optimal range for measurement with the PI analyzer. Also, pure propylene was selected as the tracer gas because it is easily measured using the PI analyzer, is relatively non-reactive at the level of oxidizers commonly found in indoor and outdoor air, and is non-toxic at the concentrations observed. To promote a uniform distribution of tracer across the opening, tracer was discharged through a fine screen in the opening on top of the source pedestal. The room was allowed to equilibrate for 2 hours at constant air and tracer gas flow rates to achieve steady-state conditions before monitoring began. Three replicate sets of measurements were taken on different days for each combination of experimental variables: two inlet types and two air flow rates.

A person in the room, wearing a full facepiece, air-supplied respirator (Neoterik Health Technologies, Inc., MD, USA), represented a stationary worker and a moving worker. Procedures involving a human subject were reviewed and approved by the University of South Carolina Institutional Review Board (IRB) before measuring BZCs.

After achieving steady-state conditions, the worker entered the room and the entrance was sealed with tape. An additional waiting period of 20-25 minutes was used to reach steady-state conditions.

For the stationary worker experiments, BZCs of the standing worker were measured at 12 sampling locations and four worker orientations (i.e., east, west, south, and north) at each location (Figure 5.2). These experiments were performed: 1) to determine the ratio of BZCs in the near-field of the source to those in the far-field; and 2) to investigate the effect of the worker's orientation on BZC.

A total of 12 sampling locations were selected to compare average concentrations near to and far from the source for each condition investigated. The far-field was taken to be sampling points 1 – 8, and the near-field was taken to be sampling points 9 – 12. In previous studies, defining near-field and far-field has been somewhat arbitrary. Near-field has been defined as a volume of 8 m^3 surrounding a worker (Cherrie, 1999a; Semple 2001), a 1-m distance from a worker (Cherrie, 1996; Cherrie, 1999b), and a 1-m radius hemisphere with the source at its center (Lee, 2005). Far-field is generally defined as the rest of the area or volume outside the near-field. In this study, the near- and far-field distance was smaller than those in previous studies because of a smaller room size. For example, room volumes in previous studies were in the range of 38 m^3 – 3008 m^3 (Semple, 2001) and 210 m^3 (Lee, 2005), which are 2 – 158 times bigger than the room size used in the present study.

Worker orientations at each sampling point were categorized in three groups: facing toward the source (FT), facing away from the source (FA), and sideways to the source (S) (i.e., one shoulder was toward the source). Two orientations, to the south and north at sampling points 2 and 6, respectively, and to the east and west at sampling points 4 and 8, respectively, comprise the sideways orientation groups (see Figure 5.2). At each orientation for each sampling point, BZCs were monitored for one minute. After each change of orientation, one minute was allowed to flush out the sampling tube. The estimated average residence time in the sampling tube was less than 10 seconds.

For the moving worker experiments, the worker walked continuously along the path defined by the 12 numbered sampling points, shown in Figure 5.2, for 3 minutes. After the worker walked along the path from point 1 to point 12 (solid line in Figure 5.2), the worker returned back from point 12 to point 1 (dotted line in Figure 5.2). Consistent paths were employed through the numbered points to allow comparison of BZCs for a moving worker with that of stationary workers. The pace of worker movement was also monitored and kept consistent for all experiments. For each condition, a continuous sample was drawn through a length of 1/16" tubing (Tygon®) with the open end positioned in front of the respirator, between mouth and nose (height (H): 1.6m), to obtain BZCs. Preliminary tests showed no influence of relatively clean air coming out from the bottom of the respirator on the tracer gas

concentration in the breathing zone. Three replicates of experiments on different days were performed. However, because of anomalies in the data from one experiment at 5.5 m^3min^{-1} (WJ condition), the results of only two experiments were reported for this condition. Three replicate experimental results were reported for other conditions.

Absolute percent error occurring from the replicates was calculated for the effect of worker's orientation. The following equation was used: Abs % error = $|C_i - C_{avg}| \times 100/C_{avg}$, where C_i = time weighted average (TWA)-BZC at sampling point *i* and C_{avg} = average TWA-BZC of three replicates at sampling point *i*.

Statistical tests were performed for quantitative comparisons using the statistical software package SAS v 9.1 (SAS Institute Corporation, Cary, NC). Paired t-tests were performed for the effect of worker's orientations with respect to the source. The hypothesis was that there was no significant difference between BZCs when the worker was facing toward and facing away from the source (H_o: $BZC_{FTi} = BZC_{FAi}$, where BZC_{FT} = TWA-BZC as the worker faced toward the source, BZC_{FA} = TWA-BZC as the worker faced away from the source, and i= number of sampling location).

For the effect of worker's activity, one-way analysis of variance (ANOVA) was conducted to determine if there was any significant difference between the overall BZC of the stationary worker and the BZC for the worker walking along the path (Ho: $BZC_{SW} = BZC_{MW}$, where BZC_{SW} = average BZC when the worker was stationary at 12 locations (Figure 5.2), and BZC_{MW} = average BZC when the worker was walking along the path).

Area concentrations for varying conditions of worker's activity were analyzed by a one-way ANOVA test to determine if any significant differences existed among average area concentrations for all conditions investigated (H_o: $C_{MW} = C_{NW} = C_{WE} = C_{WW} = C_{WS} = C_{WN}$, where C_{MW} = average area concentration when the worker was walking along the path, C_{NW} = average area concentration when no worker was present, and $C_{WE, WW, WS, and\ WN}$ = average area concentration when the heated mannequin was present east, west, south, and north of the source, respectively). For the individual comparison, multiple comparison procedures, using Scheffe's adjustment, were performed to determine where there were differences. A significance level of $\alpha = 0.05$ was used for all analyses.

6.3. Results and Discussion

6.3.1. Effect of worker's location

As shown in Table 6.1, the overall average concentration near the source (sampling points 9, 10, 11, and 12) was higher than the overall average concentration far from the source, as anticipated. The ratios of overall average concentration between near to and far from the source ranged from 1.33 to 1.60. Better mixing of room air was observed in the far-field, showing lower coefficients of variation (CVs) than the CVs in the near-field. Higher concentration gradients were observed in the near-field.

A similar study was performed by Cherrie (1999a). Cherrie simulated exposure levels using a box model with a source in the near-field by employing factorial combinations of five far-field volumes, five air exchange rates between the far-field and outside the room, and three air exchange rates from the near-field to the far-field. Cherrie reported the results in four categories, factorial combinations of two room sizes (small ($\leq$ 100 m^3) and large ($\geq$ 1000 m^3)), and two ventilation rates (good ($\geq$ 10 ACH) and poor ($\leq$ 1 ACH)). The experimental room described here falls in the small room/good ventilation category ($\leq$ 100 m^3 and $\geq$ 10ACH). The range of near-field to far-field concentration ratios measured in the current study (1.33 – 1.60) was in the lower portion of the range estimated by Cherrie, 1.20 – 5.56.

Table 6.1. Overall average concentration (ppm) and CV near and far from the source

Inlet type/flow rate		Average concentration (ppm)		Coefficient of variation (CV) [C]		Ratio of concentration (Near/Far)
		Near [A]	Far [B]	Near	Far	
Wall Jet	5.5 m^3/min	59.9	37.4	0.22	0.14	1.60
	3.3 m^3/min	69.8	52.5	0.21	0.13	1.33
Ceiling Diffuser	5.5 m^3/min	42.7	30.6	0.36	0.05	1.40
	3.3 m^3/min	56.8	40.7	0.27	0.14	1.40

[A] Overall average concentration of 4 sampling points nearest the source. Horizontal and vertical distance from the center of the source was 34cm and 22cm, respectively (Sampling point from 9 to 12, Figure 8)
[B] Overall average concentration of 8 sampling points farthest from the source. Horizontal and vertical distance from the center of the source was 85cm and 83cm, respectively. (Sampling point from 1 to 8, Figure 8
[C] Coefficient of variation (CV) = standard deviation (SD) / average concentration

6.3.2. Effect of worker's orientation

Table 6.2 shows the average absolute percent error occurring from three replicates of experiments. Overall, average absolute percent errors for WJ conditions showed less variation than those for CD conditions for both flow rates.

Table 6.2. Average absolute percent error (%)

Orientation	Flow rate/Inlet type			
	5.5 m^3min^{-1}/WJ[B]	5.5 m^3min^{-1}/CD	3.3 m^3min^{-1}/WJ	3.3 m^3min^{-1}/CD
East	12.6	7.9-8.7	15.0-25.5	16.9-33.1
West	5.1	8.9-14.6	11.4-14.4	14.7-28.2
South	5.0	10.1-16.7	12.1-18.1	13.3-23.1
North	9.4	7.3-11.7	13.3-19.5	14.4-23.6
Average[A]	8.0	10.7	15.6	20.1

[A] Overall average absolute percent error for all orientations
[B] Only two replicates of experiments were reported due to anomalies in the data from one experiment at this condition.

As shown in Table 6.3 and Table 6.4, BZCs when facing toward the source at each sampling point were higher (FT/FA ratio: 1.15 – 1.25 for 37 out of 48 sampling points) or nearly the

same (FT/FA ratio: 0.89 – 0.99 for 9 out of 48 sampling points) than those when the worker was facing away from the source. For the WJ air inlet, sampling points 11 and 12 for 5.5 m^3/min and sampling points 10 and 11 for 3.3 m^3/min showed the largest differences. These sampling points were located near the source, an area with high concentration gradients. The same pattern was observed for the CD air inlet where large differences were observed at all sampling points near the source.

Interesting results were observed when the worker was oriented with the side of his body toward the source. For both flow rates/WJ condition, BZCs for sideways orientation at sampling points 4 and 6 were higher than FT and FA orientations at those sampling points. Also, for 3.3 m^3min^{-1}/CD condition, BZCs for all sideways orientations were higher than measured BZCs for FT and FA. Explanation of this phenomenon is very complicated because of unpredictable flow directions in the room, unlike unidirectional flow in a wind tunnel.

Previous studies by Hyun and Kleinstreuer (2001) and Welling (2000) came to the same conclusions, but presented very different ratios. Hyun and Kleinstreuer (2001) concluded that when a heated mannequin faced towards the source with a breathing zone height of 1.6 m and air blowing toward the back of the mannequin at a velocity of 0.15 m/s, the steady-state personal dose was about 22 times greater than the dose when the mannequin faced away from the source and into the air flow. Welling (2000) measured the mean concentration of vaporized acetone at a height of 0.94 m and a distance of 0.35 m at nose level with freestream velocity of 0.3 m/sec in a wind tunnel. A worker, represented by a 1.75-m mannequin, was positioned in three different orientations, with air flowing from behind, in front of, and from the side of the mannequin. They found that mean acetone concentrations with freestream flow from behind the mannequin were 126 and 57.5 times greater than the mean acetone concentration with freestream flow from in front. Both studies were conducted in unidirectional turbulent flow in a wind tunnel, and discrepancies between the two studies are probably due to different velocities and source locations. In the current study, the worker's orientation had a smaller, but still significant effect on BZC in the experimental room, which more realistically represented a typical workroom.

Statistical tests also detected that exposures were significantly higher when the worker was facing toward the source than when facing away from the source for all positions analyzed. P-values were 0.0083 for 5.5m^3min^{-1}/WJ, 0.0329 for 5.5m^3min^{-1}/CD, 0.0092 for 3.3m^3min^{-1}/WJ, and 0.0154 for 3.3m^3min^{-1}/CD.

Table 6.3. Breathing zone concentrations and statistical test results (5.5 m^3/min)

Sampling Point	Experimental Condition							
	Wall Jet Air Inlet				Ceiling Diffuser Air Inlet			
	FT	FA	S	FT/FA	FT	FA	S	FT/FA
1	22.7	20.3	-	1.12	34.0	35.8	-	0.95
2	31.0	25.9	31.5	1.20	28.7	27.8	27.8	1.03
3	43.0	41.5	-	1.04	31.1	33.9	-	0.92
4	46.0	43.4	51.1	1.06	28.4	25.9	28.1	1.10
5	49.5	38.6	-	1.28	31.0	31.3	-	0.99
6	26.0	27.5	50.2	0.94	31.0	29.4	29.9	1.05
7	34.4	32.4	-	1.06	30.4	29.2	-	1.04
8	46.8	35.8	42.4	1.31	35.4	27.5	30.0	1.29
9	66.6	54.4	-	1.22	54.7	34.4	-	1.59
10	56.2	52.0	-	1.08	52.0	34.3	-	1.52
11	63.7	48.4	-	1.32	47.5	34.6	-	1.37
12	83.8	54.3	-	1.54	58.5	25.8	-	2.26
Average	47.5	39.6	-	1.20	38.6	30.8	-	1.25
Paired t-test [A] (p-value)		0.0083				0.0329		

[A] Paired t-test was performed to detect any statistical difference between BZCs when facing toward and facing away from the source.

Table 6.4. Breathing zone concentrations and statistical test results (3.3 m^3/min)

Sampling Point	Experimental Condition							
	Wall Jet Air Inlet				Ceiling Diffuser Air Inlet			
	FT	FA	S	FT/FA	FT	FA	S	FT/FA
1	61.8	48.7	-	1.27	45.5	34.9	-	1.31
2	52.3	58.7	57.4	0.89	42.4	45.5	50.8	0.93
3	66.7	59.4	-	1.12	42.5	46.3	-	0.92
4	60.5	55.9	71.4	1.08	34.3	35.5	40.4	0.97
5	32.4	34.5	-	0.94	33.7	32.6	-	1.03
6	50.5	46.9	52.9	1.08	41.5	34.8	50.2	1.19
7	42.1	34.9	-	1.20	43.3	36.1	-	1.20
8	68.5	49.9	55.7	1.37	36.3	29.9	44.2	1.22
9	66.7	65.6	-	1.02	62.7	54.9	-	1.14
10	71.2	53.2	-	1.34	67.1	42.9	-	1.56
11	91.1	66.5	-	1.37	63.9	45.3	-	1.41
12	76.7	66.9	-	1.15	72.7	44.9	-	1.62
Average	61.7	53.4	-	1.15	48.8	40.3	-	1.21
Paired t-test [A] (p-value)		0.0092				0.0154		

[A] Paired t-test was performed to detect any statistical difference between BZCs when facing toward and facing away from the source.

6.3.3. Effect of worker's movement

As shown in Table 6.5, the time weighted average (TWA) exposure for the moving worker was consistently higher, ranging from 1.14 to 1.51 times greater than TWA exposure for the stationary worker standing still at designated stopping points. Statistical tests also showed the same results from those comparisons (p-values for all four conditions: <0.01).

Other experimental results (Cheong, 2003; Brohus, 2006; Awbi, 1991) have indicated that disruption of convective flow along the front of a moving worker has an important effect on exposure. In a room using displacement ventilation with a stationary, heated mannequin, clean air from lower areas of the room was transported up along the surface of the mannequin due to natural convection. However, when the mannequin was moved back and forth, the effectiveness of entrainment of clean air in the mannequin's boundary layer (the thermal convective flow layer generated from the difference between body temperature and room air temperature) decreased, resulting in higher personal exposure for a moving mannequin than for a stationary mannequin, either sitting or standing. In the current study, the same result was observed in a room with dilution ventilation; when the worker walked along the path, the natural convection boundary layer along the front of the worker was disrupted, allowing room air at breathing zone height to penetrate the breathing zone.

Table 6.5. Comparison of TWA breathing zone concentration

Condition	5.5 m^3/min		3.3 m^3/min	
	WJ Inlet	CD Inlet	WJ Inlet	CD Inlet
Stationary worker [A] (ppm)	44.9	34.6	58.2	46.0
Moving worker [B] (ppm)	56.1	52.3	66.1	61.7
Ratio [C]	1.25	1.51	1.14	1.34
F-test statistics (p-value) [D]	14.12 (0.0002)	24.62 (< 0.0001)	7.10 (0.0081)	30.92 (< 0.0001)

[A] The overall average concentration of 12 sampling points for a stationary worker.
[B] The overall average concentration walking path defined by the 12 sampling points for 3 min.
[C] Ratio = TWA exposure of the moving worker/ TWA exposure of the stationary worker
[D] From one-way ANOVA test.

6.4. Conclusions

Breathing zone concentrations of the stationary worker were monitored at various locations and four orientations at each location. In this study, the average BZC was higher in the near-field of the source than in the far-field because of higher concentration gradients in the near field. The experimental results also demonstrated that the worker was likely to have higher exposures when facing toward the source than when facing away from the source. BZC of the worker walking along the path connecting the 12 sampling points within the room was significantly higher than BZC of the worker standing still at these points along the path. This might have happened because motion disrupted the vertical convective flow around the body of the moving worker at low air speeds as observed by other researchers (Cheong, 2003). Also, when the worker walked along the path, the average area concentration at the fixed sampling point was generally lower than when the worker was absent or stationary in the room. Presumably, the worker's movement generated better mixing of room air at that specific location. However, this conclusion applies to a single monitoring location and cannot be assumed to represent concentrations throughout the experimental room.

The outcomes for conditions studied here are: the average ratio of BZC in the near-field versus far-field was 1.43 (ranging from 1.33 to 1.60); of facing toward the source versus facing away from the source was 1.20 (ranging from 0.89 to 2.26); and for the moving worker versus the stationary worker was 1.30 (ranging from 1.13 to 1.51). These ratios indicate that personal exposure is not just a function of one characteristic. Findings from this investigation indicate that a worker's activity in a room should be taken into account when estimating BZC mathematically (Semple, 2001; Keil 1997; Keil 2000; Nicas, 1996) or computationally (Johnson, 1996) in epidemiologic studies. For example, BZC estimation of a worker facing toward a source might be underestimated if the worker's orientation is not considered. One reason for underestimating the true concentration would be that most such models do not explicitly account for other characteristics of the work environment that may affect exposure. Therefore, inclusion of a worker's orientation and activity in exposure assessment models would likely increase accuracy and precision of exposure estimates. However, treatment of those factors investigated here as distinct model parameters is not feasible in most cases, because workers' activities are often irregular and complicated. Instead, these findings may be used to assess uncertainty or adjust exposure estimates from simple models. For example, a model estimate multiplied by the average ratio of worker's movement and standing still promises a more accurate estimate than the model estimate itself. However, differences between an actual workroom and the one studied here must be carefully considered before applying these ratios. One important difference could be the elevation of the source and/or density differences between the emissions and the surrounding room air. In this study, the emission height was about 1.0 m, which is about 0.6 m below the breathing zone. Further studies are needed to investigate the range of these ratios for various workroom conditions not explored in the present study.

7. SPECIFIC AIM 3 -- DEVELOP DETERMINISTIC MODELS

7.1. Refinement of Simple Models

Assessment of workroom exposure is required under a variety of circumstances. Considerations of time and resources may not allow personal sampling. In some cases, retrospective or prospective exposures must be assessed, or a tiered approach is used. Clearly, there is an important role for mathematical models in exposure assessment; and this portion of our research was aimed at improving these models. Our aim was to strike a balance between improving existing models and keeping the application of the new models simple and user friendly.

The room geometries and sources were modeled using Gambit and the Fluent CFD solver software was used. The effect of inlet, exhaust and source locations and of room dimensions on the flow field and contaminant distribution were studied. Correlations were used to improve the two-zone model and to create a new multi-zone model, where each zone was completely mixed. Also, a preliminary investigation of the use of coarse-grid CFD (CFD with a very small number of cells) was performed. The full description of these efforts is given in Tamanna (2004).

The results with the two-zone model may prove to be valuable. This model is frequently employed for tiered exposure assessment, yet few efforts have been made to optimize the manner in which this model is applied. The findings for the two-zone model are summarized below and were presented at the American Industrial Hygiene Conference (Tamana, 2003).

Our efforts in developing both multi-zone and coarse grid models proved problematic. The accuracy of predictions was generally poor for the limited number of cases considered. Thus, we resolved to focus our efforts on zonal models, which have been used to assess the distribution of heat and contaminant species within rooms, as well as throughout multi-room buildings.

7.1.1. The Two-Zone Model

Methods. A 7.8m (L) X 5.4m (W) X 3.0m (H) room was chosen for CFD simulations with an air inlet opening of 0.9m X 0.3m on the side walls or 0.6m X 0.6m in the ceiling, and an exhaust opening of 0.6m X 0.6m. A source table of 0.9m (L) X 0.9m(W) X 1.0m (H) was located on the floor in the middle of the room. Contaminant gas emanated from a 0.3m X 0.3m opening at a low flow rate of 1.40×10^{-5} m^3/s. No other flow obstructions were in the room and no worker was present. A hexahedral structured mesh with 37,284 cells of size 0.15 m X 0.15 m X 0.15 m was modeled in Gambit 2.0, (Fluent Inc, Lebanon, NH).

The steady-state segregated CFD solver, Fluent 6.0, based on the finite difference method, was used to solve the system of governing equations – conservation of mass, conservation of momentum, and species transport equation. Only isothermal cases were studied.

Figures 7.1 (a), (b), and (c) show the room geometries with the locations of the inlet and exhausts. Simulations were performed with the combination of 5 different exhaust locations with one inlet location and 3 different air flow rates. The flow pattern and the concentration distributions were studied using the tracer gas isobutylene as a contaminant (its density is equal to that of air).

The effects of the relative locations of the inlet and exhausts on the contaminant concentration in comparison with the results obtained using the two-zone model were studied.

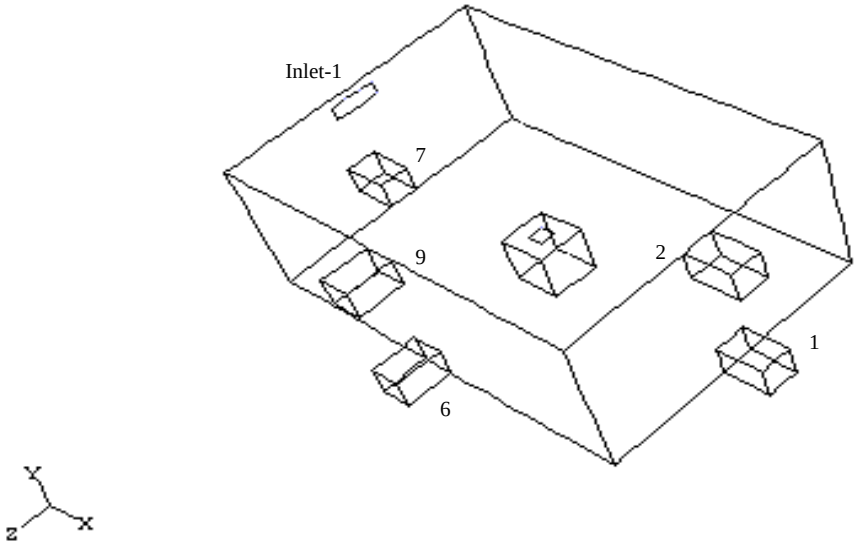

Figure 7.1 (a): Middle room source location, Inlet-1, different exit locations.

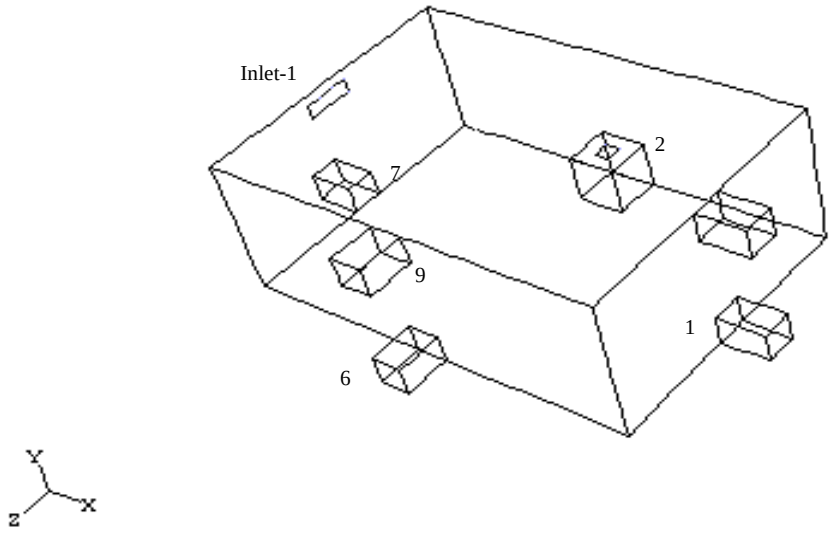

Figure 7.1 (b): Side wall source location, Inlet-1, different exit locations.

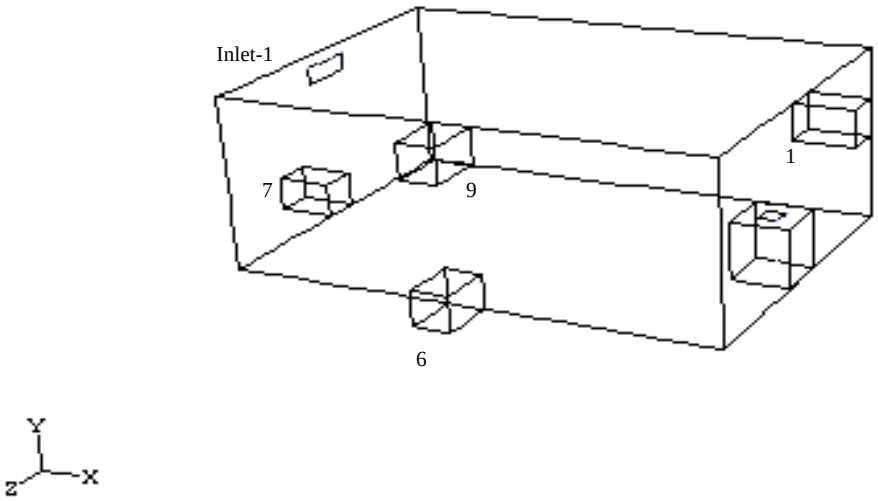

Figure 7.1 (c): Opposite wall source location, Inlet-1, different exit locations.

For all CFD simulation cases, the room domain was discretized to 37,284 cells of size 0.15 m X 0.15 m X 0.15 m. Grid independence was established by changing the grid sizes and

comparing the results. One selective case at 4 ACH for Inlet-1, Exhaust-1 for air and tracer gas (density equal to that of air) was simulated with a finer mesh of 63,757 cells of size 0.125 m X 0.125 m X 0.125 m. The difference between the average concentrations in the entire room, in the breathing zone (1.5 m high), and in the near-source breathing zone were found to be 0.1%, 0.85% and 1.55%, respectively.

Figure 7.2 shows the geometry modeled in Fluent 6.0 in order to obtain the flow rate of air between the two zones. The room was first divided into two zones. A near-field was created surrounding the source in the middle of the room.

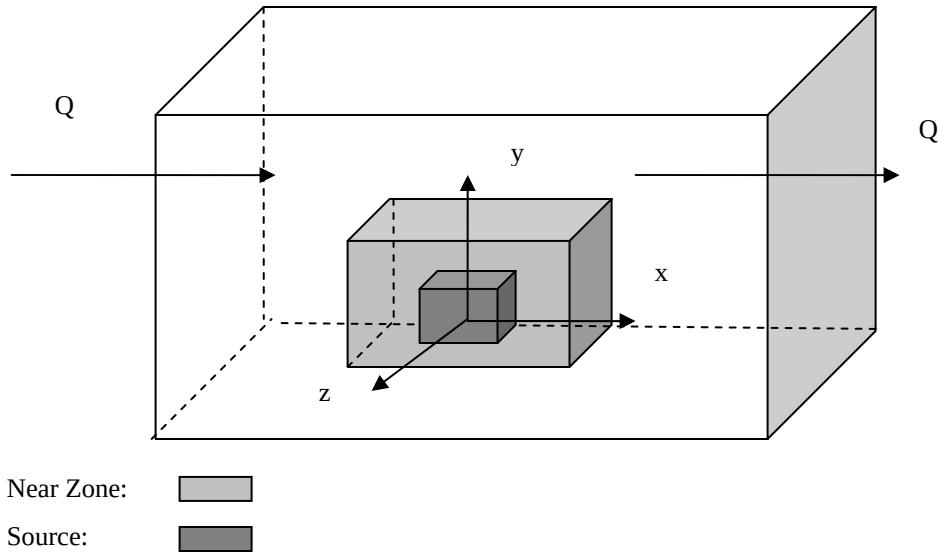

Figure 7.2: Two-zone model analysis for obtaining β value

The area weighted average of velocity was calculated at each face of the near zone volume along with direction. Therefore, at each face, the flow rate was obtained, along with the direction, using the following equation:

In a control volume,

Inflow = Out flow

$$\sum_{i=1}^{n} A_i V_i = \sum_{j=1}^{n} A_j V_j = \beta \qquad \text{Eq. 7.1}$$

where, A = area of a face of the near field
V= area weighted average of velocity
i= number of faces having positive flow directions
j= number of faces having negative flow directions

Optimum near field size. From the two-zone model equations it is clear that the flow rate of air between the zones (β) must be obtained before one can use the two-zone model to

estimate concentration. But, this β value is obtained for a particular size of near field which is arbitrary. Thus, it is necessary to determine the optimum near-field size for a particular room. In order to determine the optimum near field size for the two-zone model, several different near field sizes (volume of near field as percentage of the room volume, ranging from 4.7% to 40%) were created based upon CFD results. The volume flow rate (β) for each near-field size was obtained. Then the concentration in the near field was calculated using the two-zone model equation. Figure 7.3 shows the comparison of the near-field average concentration from CFD and from the two-zone model estimate.

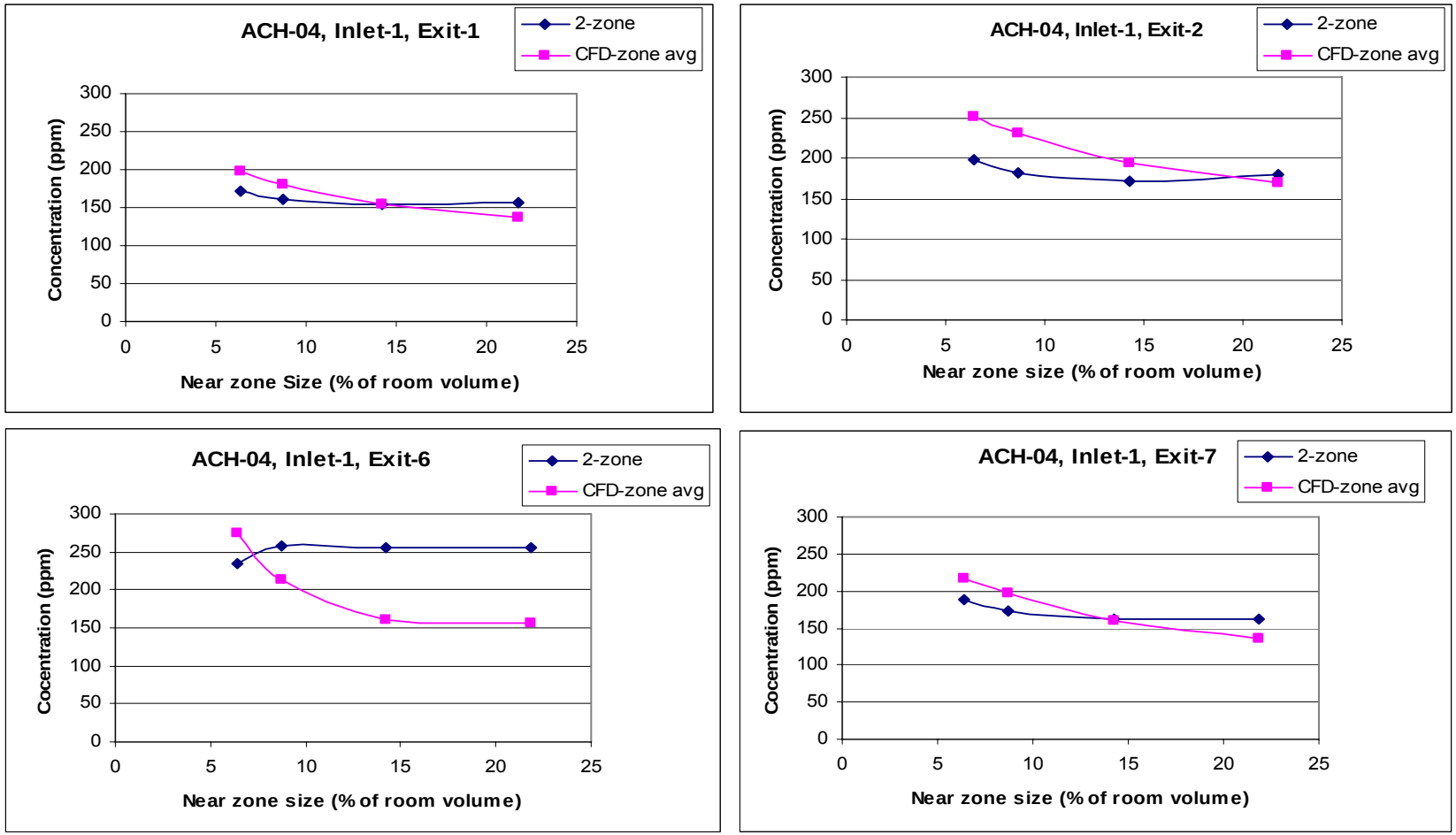

Figure 7.3: Comparison of near field average concentration from CFD and Two-zone model for Inlet-1, Exit location 1, 2, 6 and 7 for ACH – 04.

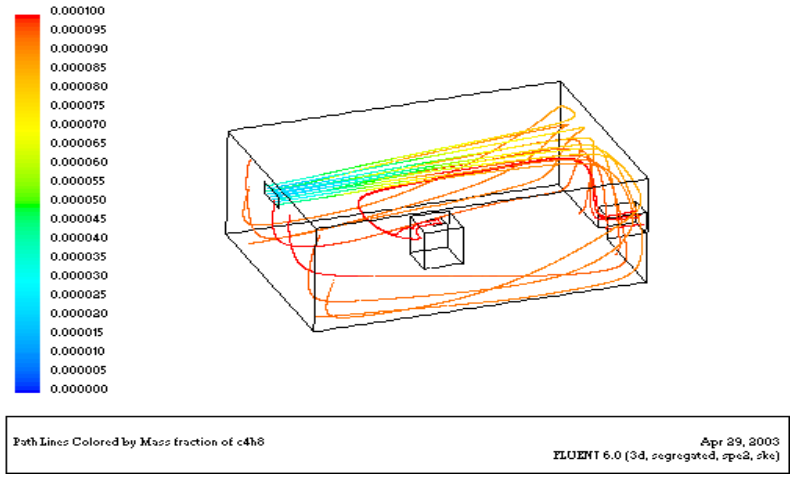

Figure 7.4 (a): Path lines of species with inlet-1, exit-1 location

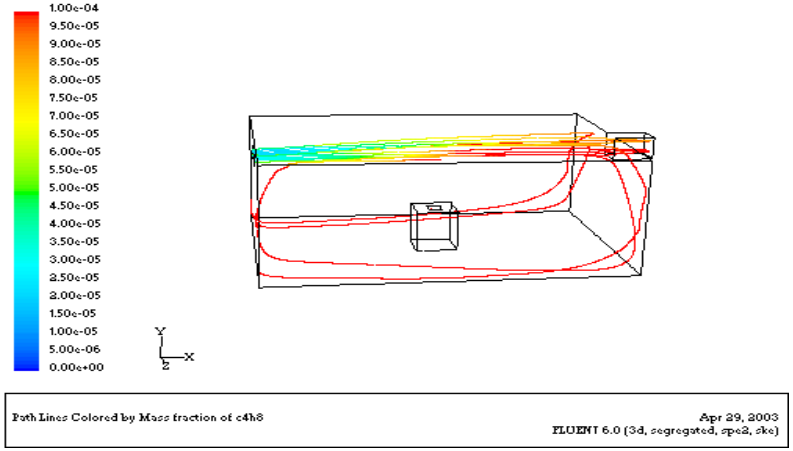

Figure 7.4 (b): Path lines of species with inlet-1, exit-2 location

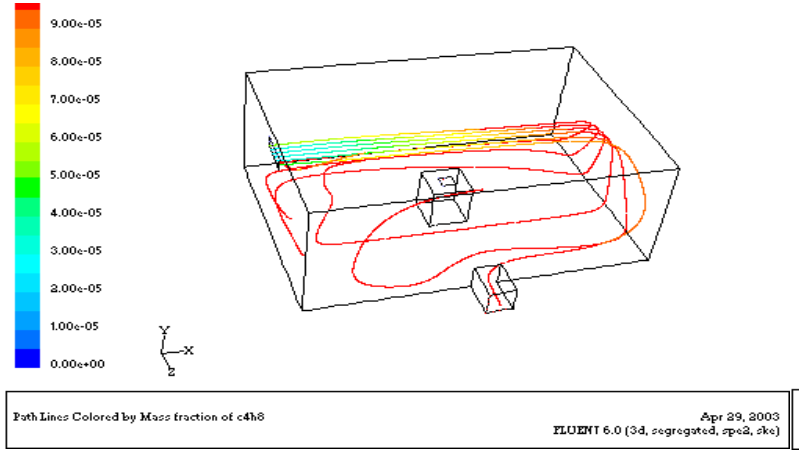

Figure 7.4 (c): Path lines of species with inlet-1, exit-6 location

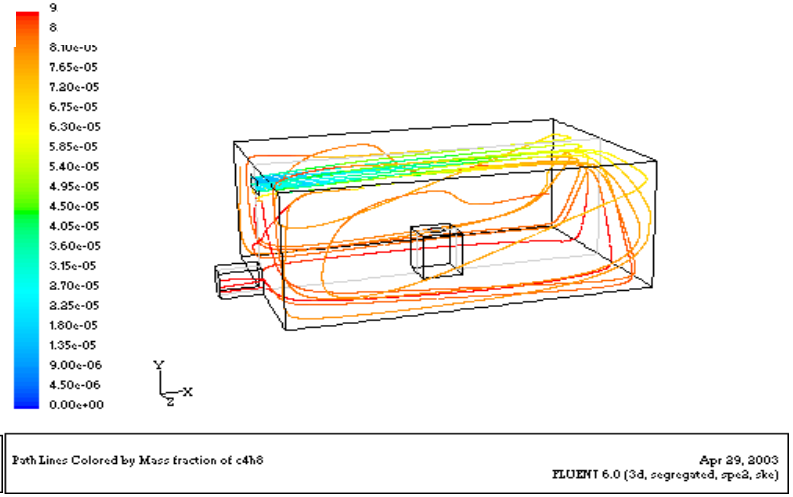

Figure 7.4 (d): Path lines of species with inlet-1, exit-7 location

The comparison of the contaminant concentration in the near-field zone, calculated using the two-zone model and from CFD, shows interesting results.

From Figure 7.4, it is very clear that the relative locations of the inlet and exhausts in the room significantly effect the determination of the best near-field size for the two-zone model. As depicted by the Figures 7.4 (a) – (d), the air flow pattern in the room and the mixing of air and contaminant varies with the relative location of inlet and exits. Therefore, the concentration plots (CFD and two-zone) intersect at different optimum zone sizes for different room configurations.

The mixing of the room can be explained with the Figures 7.4 (a), (b) (c) and (d). Figure 7.4(a) shows that the contaminant is getting entrained with the flow of the dilution air and then leaves the room through the exit, which is at the end wall. So, the contaminant in the near field was diluted quite a bit. On the other hand, in the case with exit-2 (Figure 7.4(b)), there is a short circuiting of dilution air and so mixing of contaminant with dilution air was greatly reduced. These results explain the curves in Figure 7.3 (a) and (b). The volume of the optimum near-field zone for the exit-2 case is larger than the exit-1 case because there was less mixing in the room. The room using exit-6 (Figures 7.3(c) and 7.4(c)) had the lowest optimum near-field zone size because the flow from the inlet jet entrains some contaminant from the source and comes back re-circulating towards the exit. Hence, the concentration gradient near the source is quite steep. Exit-7 results closely resemble those for Exit-1.

Conclusion. Investigation on using a two-zone model for workroom exposure has revealed some important aspects of applicability and usefulness of the model. Calculation of concentration in a workroom containing a contaminant source using a two-zone model involves parameters including the size of the near-field zone and the flow rate between zones. It has been observed that both the near-field zone size and the flow rate between the near- and far-field zones are affected by the room configuration. The optimum near-field zone sizes for the room inlet and exit locations and a single source location was determined using CFD simulations. The analysis showed that the optimum near-field zone was in the range of 8.5% to 20% of the room volume. The relationship between clean air dilution rate and flow rate between zones was found to be linear for different room configurations. The comparison of concentrations obtained from CFD and the two-zone model showed that the two-zone model can be applied to the rectangular room with inlet on the upper part of the shorter wall and exit opposite to the inlet (Inlet-1, Exit-2) and exit at the same wall as that of the inlet (Inlet-1, Exit-7). However, this model performed less satisfactorily for the other cases.

7.2 Zonal Models

After considering working on refinement of the two-zone model, we began developing multi-zone and coarse grid models. These efforts proved problematic. The accuracy of predictions was generally poor for the cases considered. Thus, we resolved to focus our efforts on zonal models, which have been used to assess distribution of heat and contaminant species within rooms, as well as within multi-room buildings.

As pointed out above, the deterministic models in widespread use among occupational hygienists do not account for effects such as the complexity of workroom air flow, thermal convection, and worker activity. Nevertheless, these models have an important place in exposure assessment because they are easily understood and applied. Also, the accuracy achieved is sufficient for some purposes: for instance models yielding conservatively high estimates may be used to rule out the need for extensive and expensive air monitoring. CFD, on the other hand, is technically very sophisticated and is capable, when properly applied, of accounting for nearly all workplace determinants of exposure. However, CFD requires considerable technical sophistication on the part of the user, and much more time and more powerful computational resources than simpler models. It is still uncertain when CFD will be sufficiently refined for use by occupational hygiene practitioners. A third, middle path, includes the more recently explored approaches of zonal models and coarse-mesh CFD. Zonal models, like CFD, divide a space into separate zones, and simultaneously solve the equations for conservation of mass and energy for all zones. For application to a workroom, zonal models generally are easier to set up than CFD and require less time for solution, but have not been extensively validated.

Several zonal approaches had been developed for modeling air flow, and heat and contaminant transport within buildings (Axley, 2001; Ren, 2005; Wurtz, 1999). Early zonal models were developed during the mid-20th century; they considered the entire building as the control volume, or "zone." Then, models linking individual spaces within a building, i.e. multi-zone models, and models dividing single spaces into several sub-zones were derived. The approach described by Axley (2001) appeared to be designed for simulating flow within single rooms. We implemented this approach for a single workroom using Matlab.

Zonal models are based upon mass and energy balance equations describing the transport between adjacent zones. Unlike CFD, zonal models do not have momentum balance equations. Empirical jet equations were added to compensate for the absence of momentum equations, which preserved the linearity of the system of equations to be solved.

After working on our zonal model for a full-year, we were satisfied that our implementation was correct. Nevertheless, the model simulations of our experimental room did not compare well with our observations, nor were they similar to any of our CFD simulations. Without the momentum equations, the zonal solutions flow patterns were laminar in appearance. Addition of empirical jet equations improved the appearance, but contaminant distribution predicted by the zonal model was still quite inaccurate.

At the Vent 2006 conference in Chicago, as we were concluding our efforts with zonal models, a round table discussion was held on "Challenges of Applying Computational Fluid Dynamics to Ventilated Spaces." Dr. Feigley and Dr. Axley were both participants. In his presentation and in subsequent questioning, Dr. Axley made it clear that the principal objective of his application of zonal models in ventilated spaces was to obtain predictions quickly without the need for extensive computational resources and that accuracy for distribution of an airborne contaminant was not a high priority. In his recent paper (Axley, 2007), he states: "multizone modeling is only appropriate for investigating spatially averaged airflow rates; when transport details within rooms are needed, other simulation tools, such as computational fluid dynamics, are required." Thus, we must conclude that zonal models are not a valid approach for estimating exposure to airborne contaminants at specific locations within workrooms.

7.3 Computational Fluid Dynamics (CFD)

CFD has been complementary to experimentation in this research. In addition to serving as the modeling tool of choice in the simulation of an actual workroom under Aim 4, CFD has allowed us to better understand the transport processes that produced the observed 3-D distribution of contaminants in our experimental room. One of the applications was to simulate, by validated methods, contaminant transport in 162 room combinations of inlet and outlet locations and types, and contaminant densities. The room geometries with and without a worker present were generated by using Gambit 3.5 (Fluent Inc., Lebanon, NH). The experimental results were compared with CFD simulations for the same boundary conditions and found to match very well. These results were published in *Building and Environment* (Khan, 2006). Other simulations included: unsteady-state simulation of a hot wall and a cold wall to determine the time required to achieve constant wall temperature, and simulations exploring the effect of furniture and different heat sources in a workroom on pollutant exposure.

8. SPECIFIC AIM 4 -- EVALUATE THE USE OF MODELS IN WORKROOMS

8.1. Silver Ink and Carbon Dipping in Tantalum Capacitor Manufacturing

Location. The sampling survey conducted in the study took place at an electronic component manufacturing facility. This particular facility is a very large manufacturer of solid tantalum and multilayer ceramic capacitors. The process for the manufacture of tantalum capacitors was evaluated. Specifically, this study was concerned with the "silver ink" station where capacitors were dipped into a solution of silver in isoamyl acetate (IAA) and then set aside to dry. Previous personal sampling conducted by the site industrial hygienist yielded 4.8 ppm over 305 min and 2.5ppm over 410 minutes, which were well below the IAA exposure limits. The Occupational Safety and Health Administration's 2005 permissible exposure limit (OSHA-PEL) and the American Conference of Governmental Industrial Hygienists 2004 Threshold Limit Value© (ACGIH-TLV) both equal 100 ppm as an 8-hour time weighted average (TWA).

A typical capacitor run on the dipping stations was approximately 30 minutes. This involved dipping a capacitor rack into the solution inside a laboratory hood, and then moving it to a staging cart that was centrally located in the workroom, followed by moving the capacitor rack into a vented drying hood. IAA evaporated from capacitors while on the staging cart. A typical run involved 18 capacitor racks.

Workroom Data. Care was taken to map and delineate all physical characteristics of the room. The room was 63' L x 29'11"W x 14' H with several large pieces of equipment including six drying ovens that were 3'3" W x 5'6" H x 7' L. Total volume of the room was 26,386 ft^3 which was reduced to 25,636 ft^3 after subtracting the volume of the ovens. The presence of other equipment had an insignificant effect on total room volume.

Air velocity measurements were taken using a thermoanemometer (CompuFlow 8585, Alnor, Shoreview, MN). The workspace had its own dedicated single pass air supply system so that temperature, humidity and airflow were controlled. Since the system operation was constant during the sampling period, it was determined that only one set of air flow measurements was necessary. There were eight supply vents measuring approximately 1' x 2', and each vent had 16 horizontal and 31 vertical vanes. The vents were paired and located on opposite sides of the air supply duct, discharging air perpendicular to the duct, approximately 167 inches above the floor.

Detailed analysis of air flow within the workroom was presented in Do (2006). Each supply vent was divided into a grid of 12 sections of equal area and measurements were taken at the center of each section. The volumetric air flow rate at each grid was calculated by

multiplying the average velocity times the total area of the vent. The flow rate ranged from 0.330 to 0.473 m^3/s, yielding a total dilution air flow rate of 3.23 m^3/s.

The exhaust systems included four lab hoods (two of which belong to the silver dipping area), twelve drying hoods throughout the room (five of which belong to the silver dipping station), and a floor level exhaust at the end of the exhaust. Outside the room, but attached to the same exhaust system, there was a silver ink quality assurance (QA) lab hood and a reclamation cabinet in which sponges that had been used in the silver ink dipping process were stored. The elements of the exhaust system were numbered from 1 to 16. The flow rates of each of the six ovens attached to the exhaust systems were not directly measured, but each was set at a regulated rate of 50 cfm. Measures of air flow rates from supply inlets and exhaust vents employed the methodology described by the ACGIH ventilation manual (ACGIH, 2004). A plot plan of the entire workspace with locations for the supply and exhaust ventilation is found in Figure 8.1. The air flow rate in the exhaust duct was measured by dividing the duct into seven equal-area zones and measuring the velocity in each. The exhaust flow rate was found to be 2.93 m^3/s. Comparing the supply flow with the exhaust, approximately 0.30 m^3/s of air leaves the room through openings to adjacent spaces or by infiltration to ambient air.

The four ovens and two exhaust hoods are all connected to a large main exhaust duct that serves as a plenum. Because the main exhaust duct is so much larger than the six individual branch ducts, the suction where each branch enters the main duct may be assumed to be the same for each branch. Six equations were derived by setting the static pressure drop for each branch duct as a function of branch flow rate equal to the static pressure main duct. The loss coefficients for exhaust vent entry and branches were obtained from ACGIH (2004). A seventh equation was obtained by setting the sum of the branch flow rates equal to the measured flow in the main exhaust duct. The six unknown flow rates and the main exhaust duct static pressure were obtained by nonlinear solution of these seven equations using Mathcad® software.

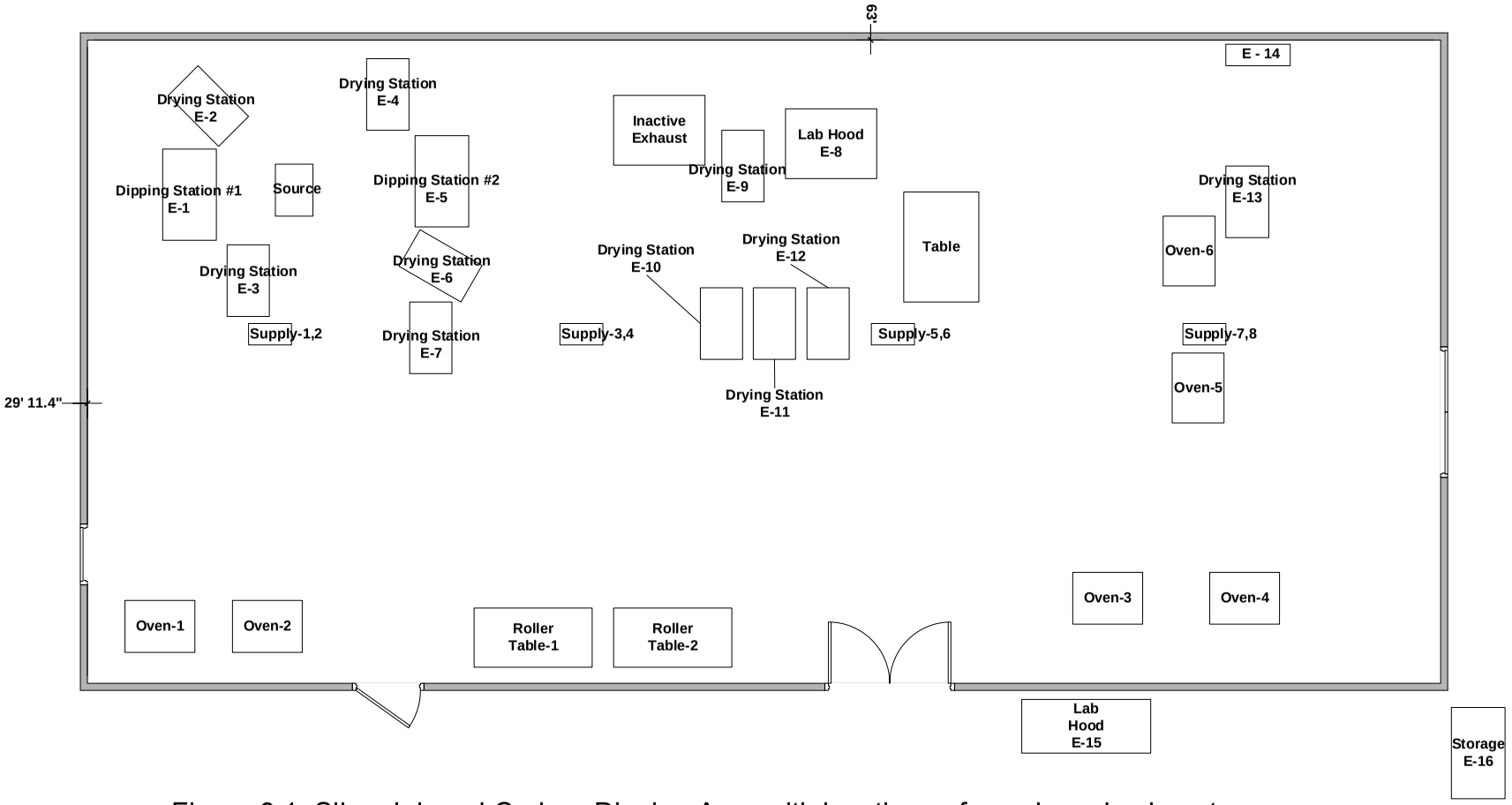

Figure 8.1 Silver Ink and Carbon Dipping Area with locations of supply and exhaust sources.

Further analysis focused on the "silver ink" station on the right side of the workroom as shown in Figure 8.1. A detail of this area is shown in Figure 8.2. Temperature, humidity, and CO_2 readings were taken throughout the sampling periods with two indoor air quality instruments (IAQ Calc, TSI Inc., St. Paul MN). One was placed inside the work room and the other was placed outside of the building, near the supply intake, to determine background conditions.

Sixteen volatile organic compound (VOC) diffusive samplers (Chemdisk, Assay Technologies, Pleasanton, CA) were spread throughout the work area with an additional two samplers placed on workers. Eight 50/100 charcoal tube area samples were collected using low flow personal air pumps (224-PCXR8 and Pocket Pump 210 Series, SKC Inc., Eighty Four, PA), seven in the work area and one in the exhaust stack on the roof. A diagram of the workspace including locations of diffusive samplers (D), charcoal tubes (C), and the temperature/humidity reading locations (IAQ) is found in Figure 8.2. Figure 8.3 is a close-up drawing of the source area showing the sampler locations.

The set of samples described above were collected for three days during the day shift. Diffusive samples were collected over an entire shift and the charcoal tubes were used as full-shift sequential samples. The number of charcoal tube samples collected during a shift depended upon the production rate. The Chemdisk diffusive samplers were analyzed by Assay Technologies (Pleasanton, CA) and the charcoal tubes from the active sampling were analyzed by the consolidated industrial hygiene laboratory at U. S. Navy Environmental and Preventive Medicine Unit #2 (Norfolk, VA).

CFD Simulation. The silver ink portion of the workroom was modeled using CFD software from Fluent, Inc. (Lebanon, NH). A tetrahedral mesh with 120,584 cells was generated using Gambi 2.0; it was determined that this was an appropriate number of cells given the complexity of equipment within the space that was to be simulated. The mesh represents an extremely complex system of coupled difference equations, which were then solved by finite difference numerical methods using CFD Fluent 6.1.22. The equations describe the conservation of mass, momentum, and the contaminant isoamyl nitrate. The room environment was closely controlled, hence, equations describing the conservation of energy were not necessary in order to obtain an isothermal solution.

The following relatively standard assumptions for solving these equations were employed:

- Two equation K-ε turbulence model
- Diffusivity computed from basic kinetic molecular theory
- Density of mixture calculated by the volume-mixing law
- Standard wall function – no slip, smooth, and no diffusion of species into the wall
- Body force weight scheme for pressure-volume coupling
- First-order upwinding scheme for turbulence, momentum, and species
- Convergence criterion = normalized sum of residuals of all scalars $\leq 1.0 \times 10^{-6}$.

Grid independence was confirmed by comparing the velocity values predicted at the source for a model with 120,000 cells with the velocities at the corresponding locations for a model with 295,000 cells. The difference was 0.173 %.

Five boundary conditions were provided: supply inlets, right boundary, fans, exhaust openings, and source. The average measured velocity from each of the two supply inlets in

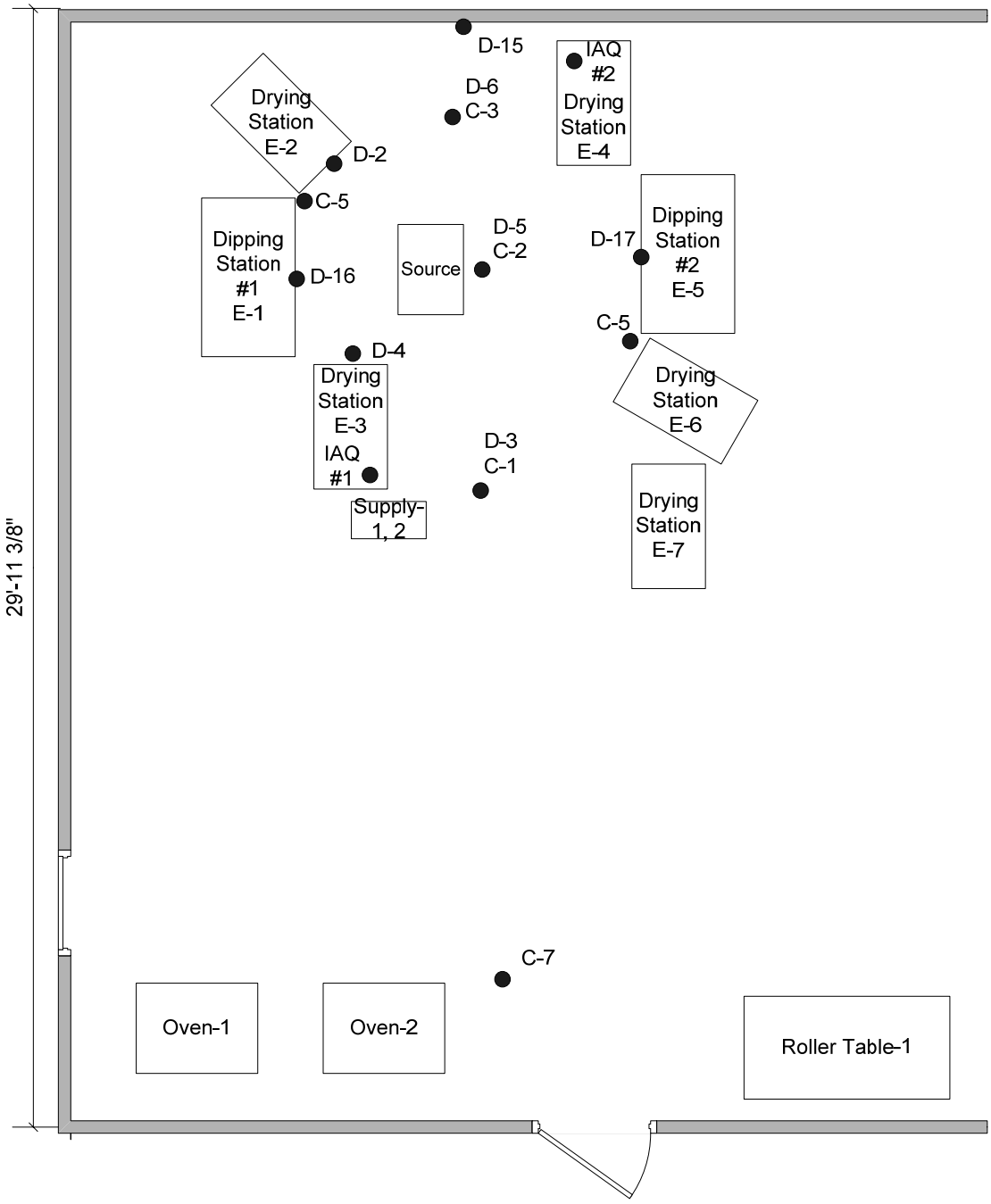

Figure 8.2. Silver ink work area showing the locations of diffusive samplers (D), charcoal tubes samplers (C) and the indoor air quality monitor (IAQ).

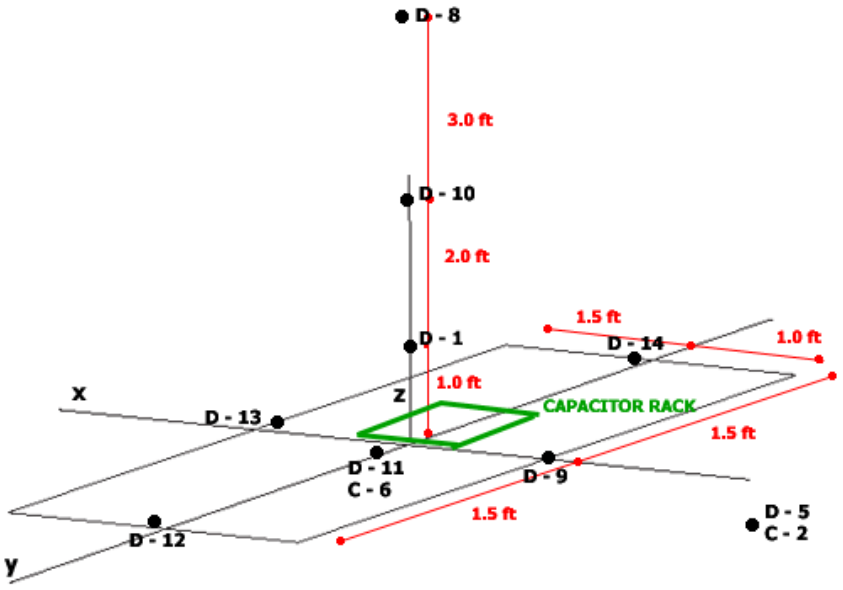

Figure 8.3. Silver Ink Cart with capacitor source area outlined and Diffusive Samplers (D) and Charcoal Tube (C) locations.

the solution space (2.595 and 2.216 m/s) were used as velocity boundary conditions, assuming that flow was normal to the face of the inlet. Assuming incompressible, viscous flow, the right boundary velocity was calculated from the sum of the supply flow rate to the right of the boundary minus the air loss from the workroom to adjacent spaces or ambient air (2.209 m^3/s). Because the jets from the supply inlets flowed parallel to the right boundary, the velocity of air crossing into the silver ink station was likely to be relatively uniform. The boundary condition was set to the effective flow rate divided by the area of the right boundary (0.055 m/s) – a low velocity when compared with the velocities measured in the work area near the source (0.13 to 0.43 m/s). See Figure 8.4.

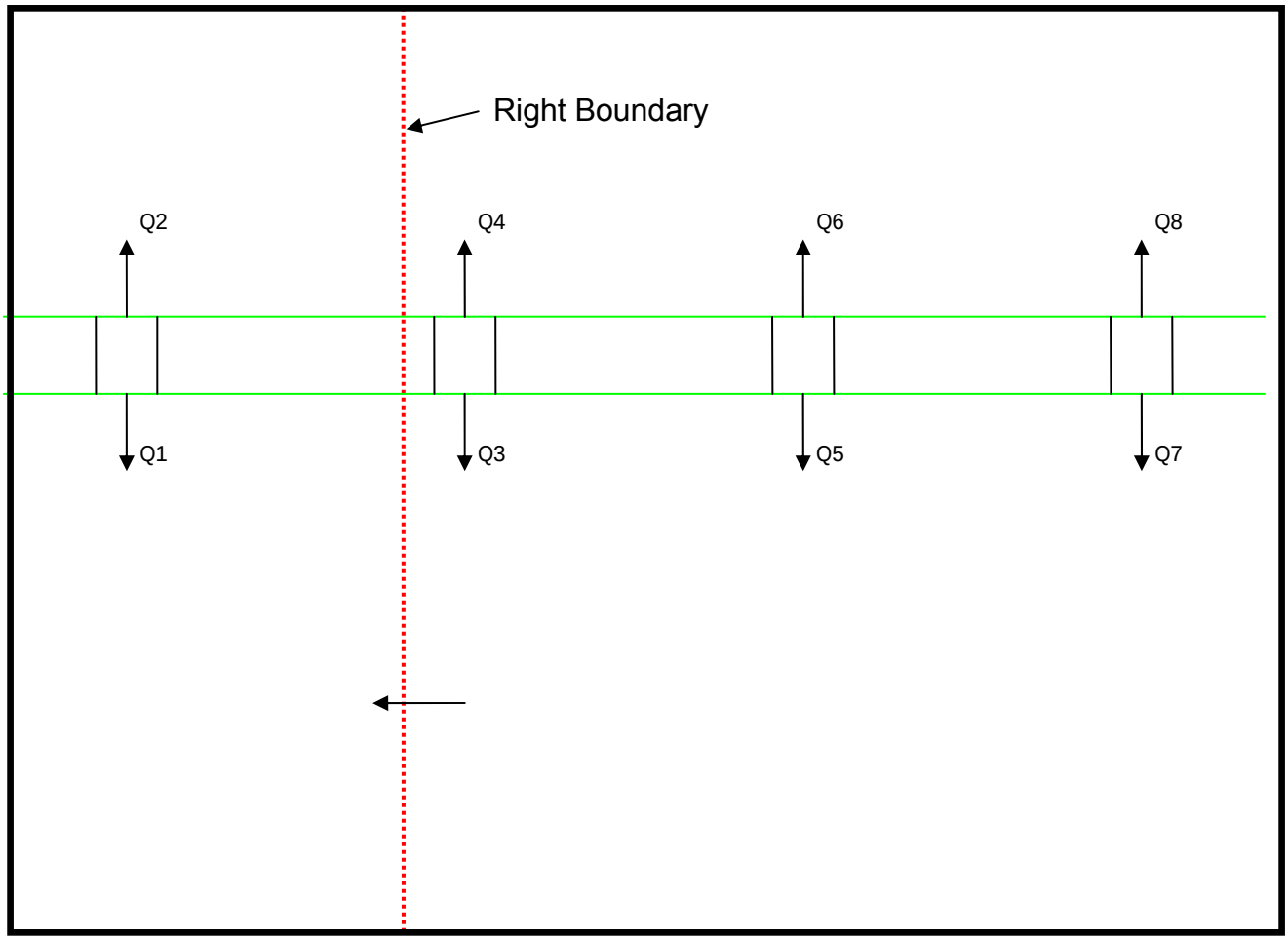

Figure 8.4. The Right Boundary

The two fans operating in the silver ink area were treated as momentum sources. One fan was on the right side facing south while the other fan was facing northeast. The axial velocity was set equal to 2.12 m/s, which was based on average measured velocity.

The boundary conditions of the oven and lab hood exhaust outlets were based upon the solution of the simultaneous equations described above.

The source boundary condition was the most challenging to estimate. The approach used here was described in a paper by Feigley, et al. presented at the 2006 American Industrial Hygiene Association Conference (Paper 150). The two-zone model was modified for obtaining the average emission rates for each of the three days. The model was modified because a large amount of data was collected near the source and we wanted to take maximum advantage of this information. The model is based upon the IAA mass balance in the near-field zone and assumes that the near-field and the far-field are independently well mixed. The traditional formulation of the two-zone model is as follows:

$$C_N = \frac{G}{Q} + \frac{G}{\beta} \qquad \text{Eq. 8.1}$$

$$C_F = \frac{G}{Q} \qquad \text{Eq. 8.2}$$

where β is the flow rate of air from the far-field into the near-field, Q is the flow rate of dilution air into the far-field, G is the emission rate, and C_N and C_F are the near-field and far-field concentrations.

Substituting CF for G/Q in the first equation yields and then solving for G:

$$C_N = C_F + \frac{G}{\beta} \qquad \text{Eq. 8.3}$$

$$G = \beta(C_N - C_F) \qquad \text{Eq. 8.4}$$

Finally, βC_F represents the rate at which IAA is carried into the near-field zone from the far-field zone. Rather that using points that are far away from the source to estimate C_F, we used the measured concentration at point D-5, which was directly upwind of the source. Thus, this yields a much more accurate estimate of the rate at which IAA is blown into the near-field.

Results. The initial simulations were dedicated to demonstration of the grid independence of the CFD model. For all three days, the room domain was discretized into 120,584 cells. Grid independence was established by changing the grid sizes and comparing results. The simulations for all three days were performed with a finer mesh, a total of 295,350 cells. The velocity and IAA concentrations were nearly identical, with a less than 1% difference throughout.

Using the two-zone model, a β of 0.093 m^3/s was calculated from the average velocity measured at the source, multiplied by the cross-sectional area of the hemispherically shaped near-field with a radius of 0.457 m. G was estimated to be 4.14, 11.3, and 4.66 mg/s. These values may be divided by the number of batches of capacitors made during each sampling period (10, 24, and 14) to give the IAA emission factors for this process – 0.41. 0.47, and 0.33 mg/s/batch.

CFD simulation was performed using the estimated emissions for each day as the rate of emission of pure IAA vapors. The results were quite different from the observed values: the CFD estimates were generally much lower than the measured concentrations. Graphical results showed rather low concentrations through most of the simulation space, but high concentrations in a zone at the floor level near the staging cart. A closer examination of the area around the source revealed very high concentrations just above the source, on the downstream side of the cart top, along the downstream side of the cart, and just below it,

near the floor. Apparently, the IAA vapors were not mixing vertically with the air blowing across the cart. Instead they were carried along the upper surface of the cart and off the edge, falling down to the floor.

The source boundary in this simulation had been placed at the surface of the cart with the emission of pure IAA evenly distributed across the source boundary. Because pure IAA vapor is nearly five times as dense as air (MW=130), it tends to seek the lowest altitude until it is substantially diluted. Also, because the cart surface suppresses turbulent mixing, the poor mixing of IAA with air in the preliminary simulation was not surprising. However, it was unrealistic.

To be released to workroom air, the IAA vapors must slowly diffuse through a layer of drying capacitor coating. The capacitors, hanging from the drying rack, were surrounded by flowing air. Thus, the contaminant at the point of emission should be a dilute mixture of IAA in air. This mixture would be much less apt to hug the surface of the cart and to remain a coherent stream when it reaches the edge of cart. Without very detailed data regarding the velocity of air through the drying racks, the exact concentration at emission could not be determined theoretically. Fortunately, an array of diffusive samplers was located directly in the near-field. Thus, based upon the maximum measured near-field concentrations for each of the three days (50, 75 and 55 ppm) and the corresponding estimated G values (given above), the flow rate through the source boundary was calculated (0.16, 0.028, and 0.018 m^3/s).

Results. Particular attention was paid to the region near the source, where the highest concentrations were found. The air speeds were only measured at the sampling locations in the near field. The CFD estimated speeds at these locations agree well with observations as shown in Figure 8.5. The mean absolute difference between CFD and measured air speeds was 1.8%. They also were compared using a two-tailed paired t-test. These differences were not found to be statically significant (p = 0.10).

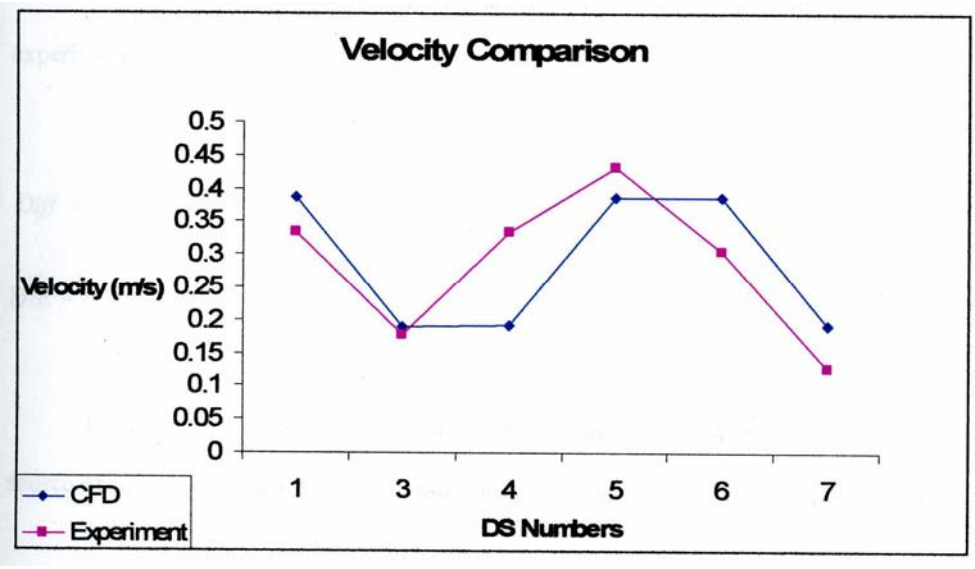

Figure 8.5. Comparison of CFD and measured air speeds at near-field sampling locations.

The workroom IAA concentration results from CFD simulations at three elevations for all three days are shown in Figures 8.6 through 8.14. The middle plane figures display the concentrations closest to the workers' breathing zones. As anticipated, the highest values occur very near to the staging table, the principal source of IAA vapor. However, the locations of the highest concentrations in the bottom and top planes were not intuitively obvious. They were a function of the air velocity patterns which transport IAA vapors. The CFD concentration estimates in the near-field were compared with the measured concentrations. Figures 8.15 through 8.17 demonstrate that CFD predicted the pattern of those concentrations relatively well, even though the predictions for some individual locations are in have substantial errors

Comparison between CFC concentration estimates and observations were made at the six locations in the source near-field using a two-tailed, paired t-test. The CFD concentrations at these points were not significantly different from the measured values ($p= 0.92$).

Thus, careful consideration of boundary conditions greatly improved agreement with measured values.

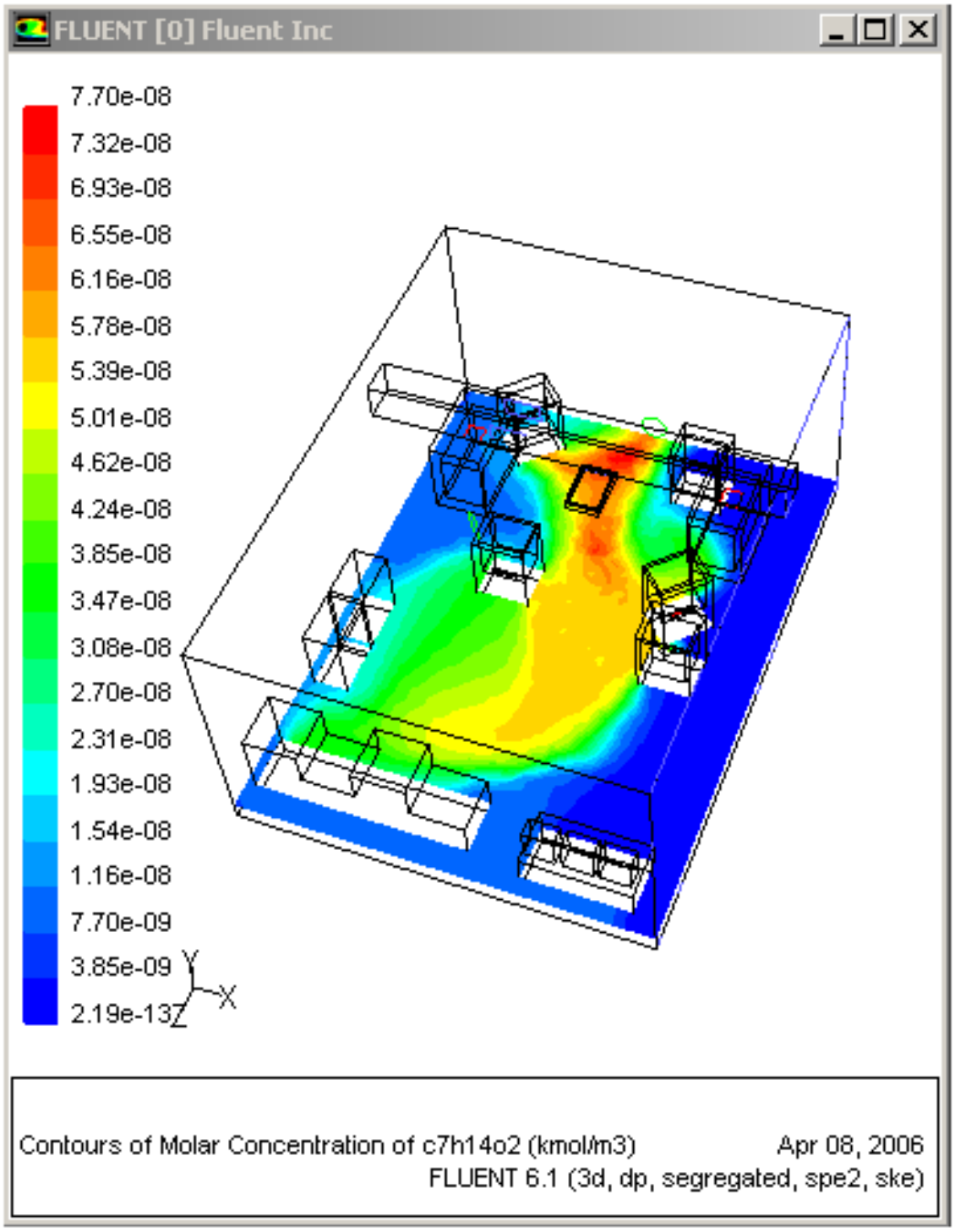

Figure 8.6. The Contour of Molar IAA Concentration at Bottom Plane in Day 1.

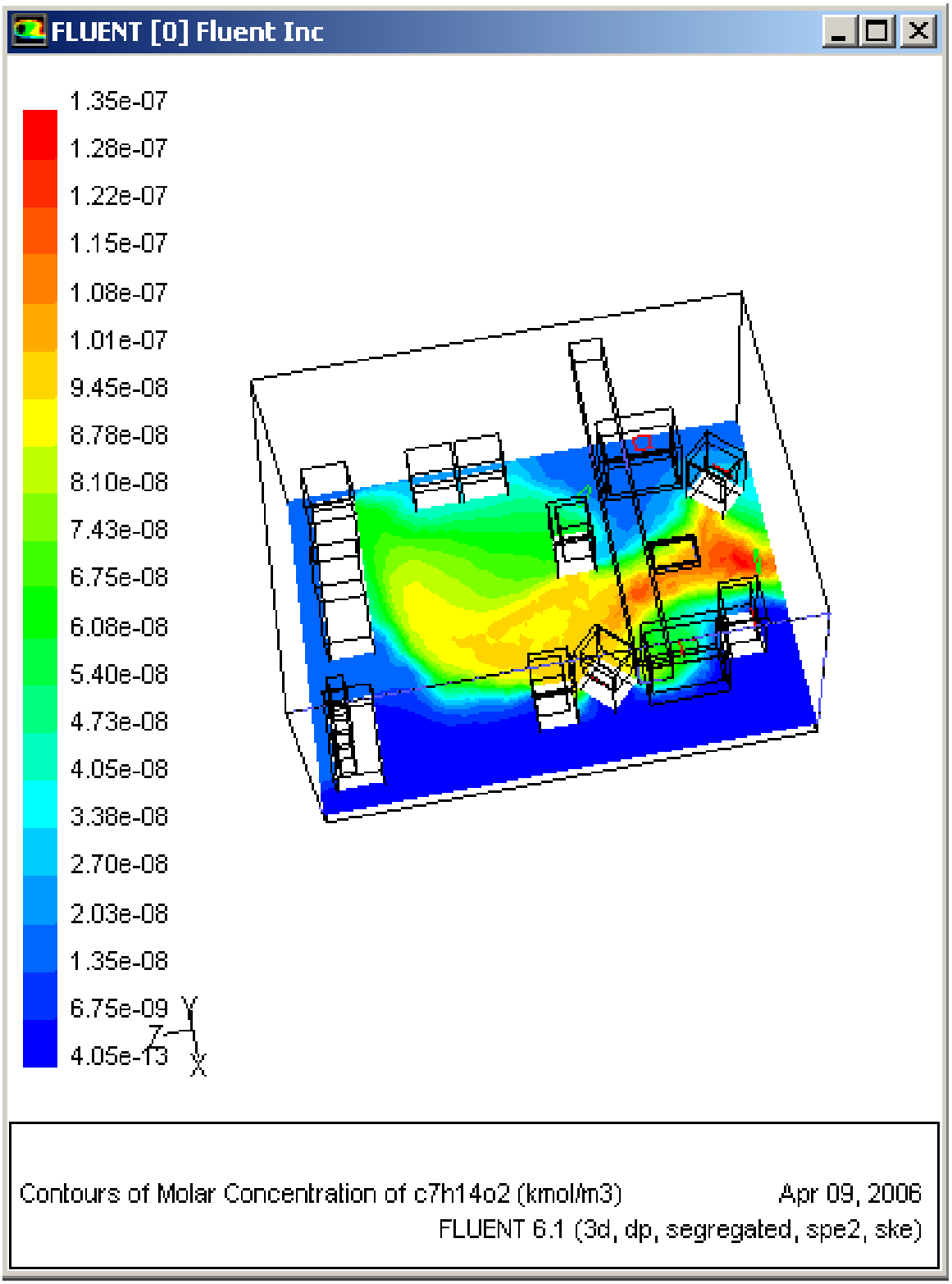

Figure 8.7. The Contour of Molar IAA Concentration at Bottom Plane in Day 2.

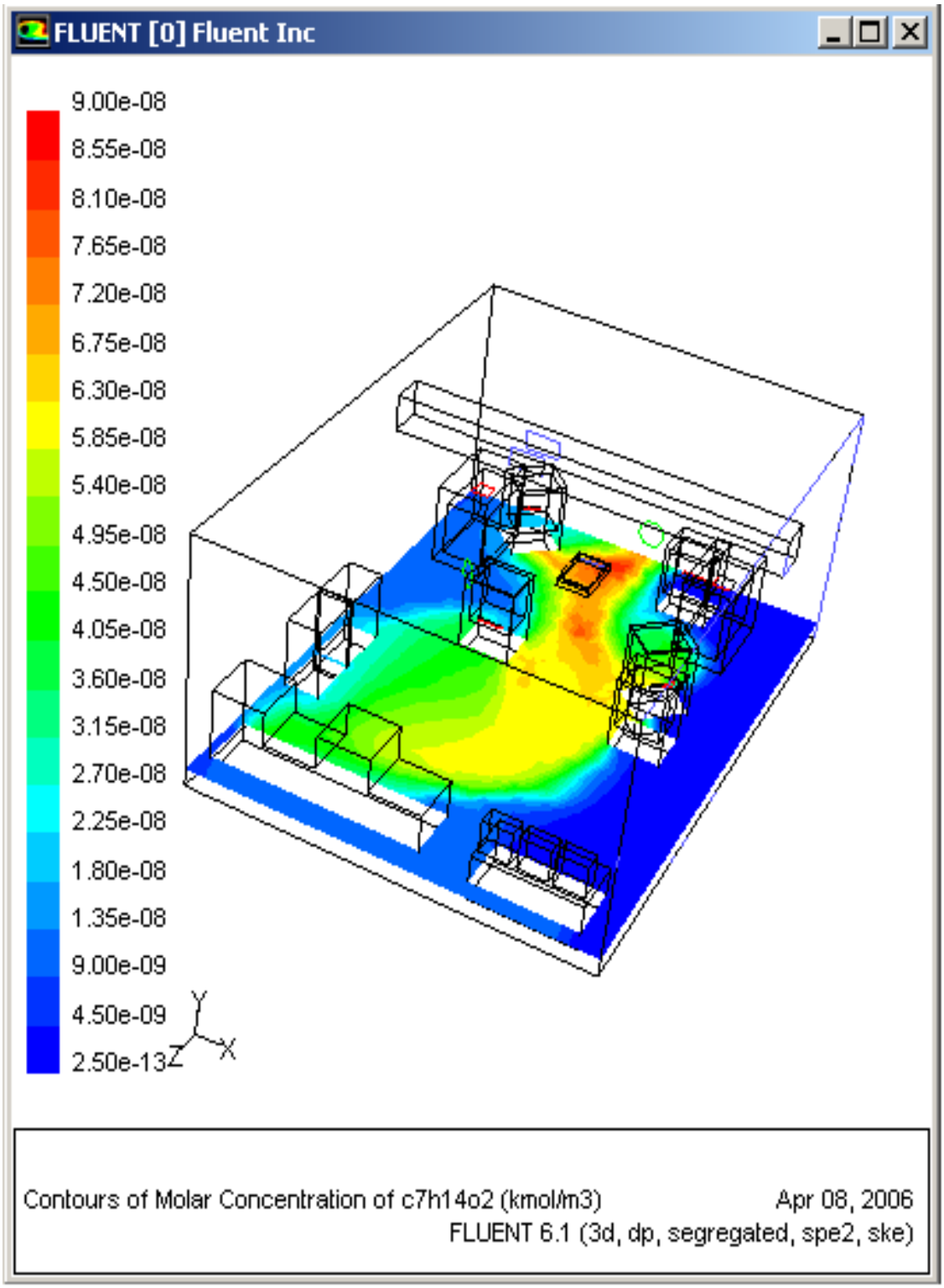

Figure 8.8. The Contour of Molar IAA Concentration at Bottom Plane in Day 3.

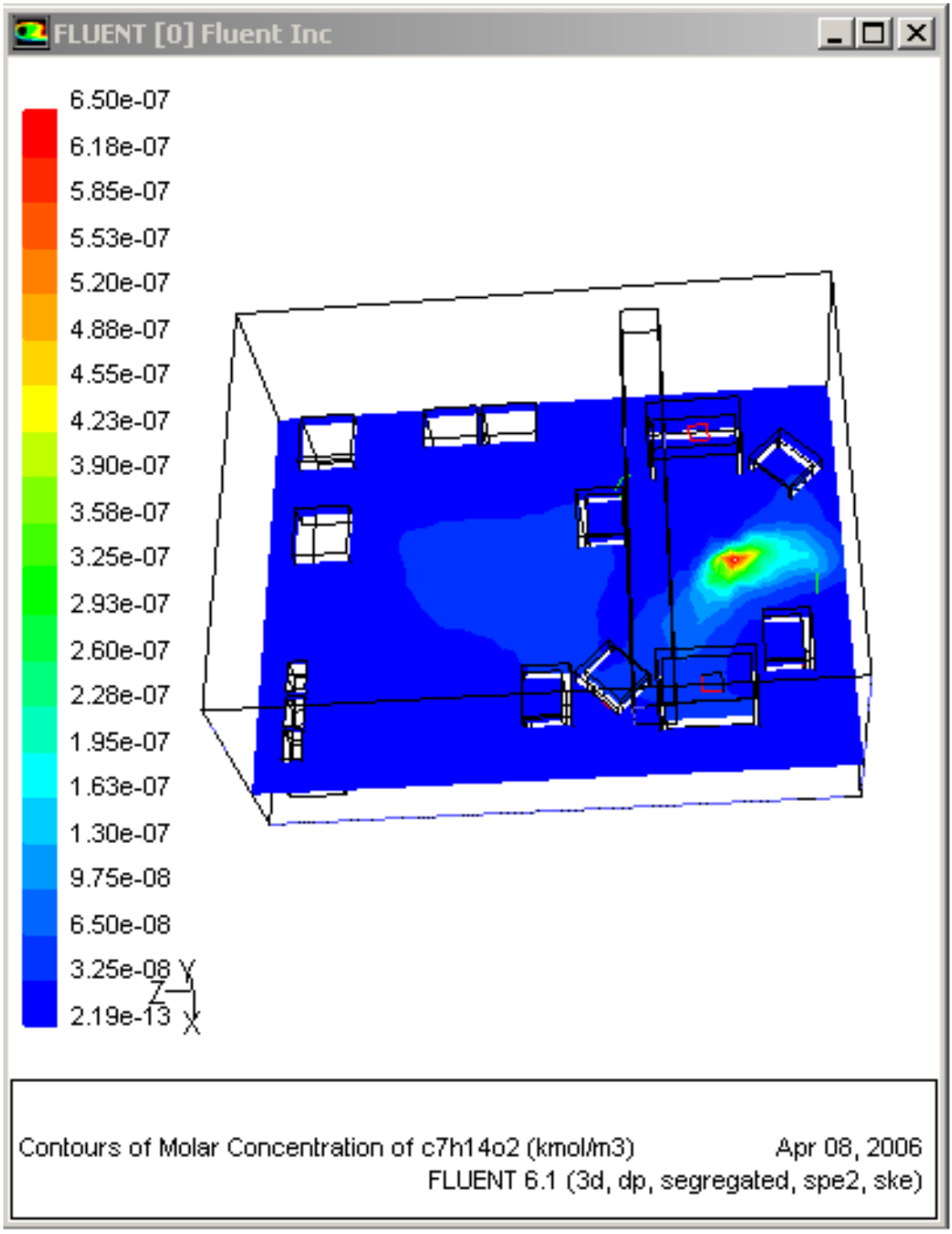

Figure 8.9. The Contour of Molar IAA Concentration at Middle Plane in Day 1.

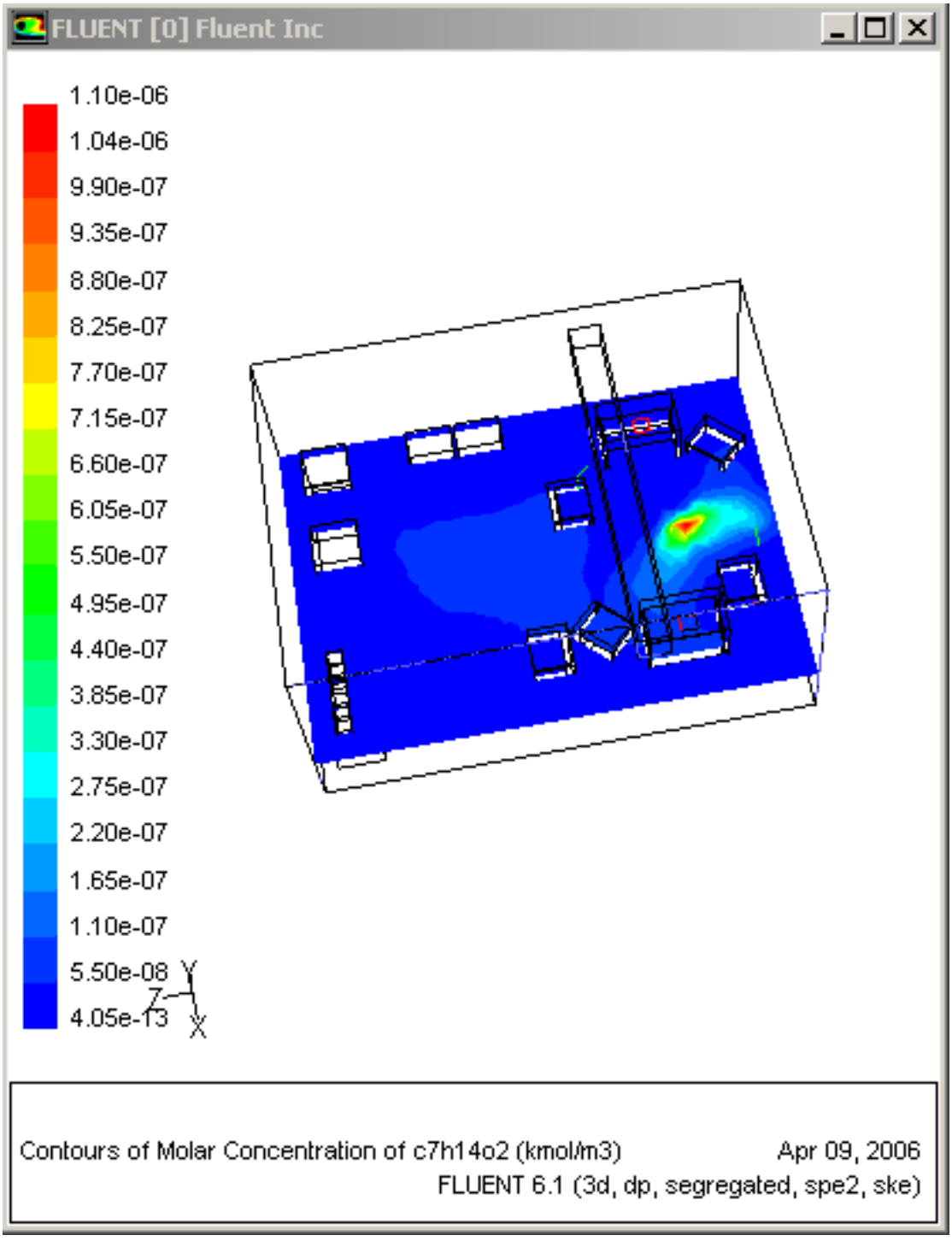

Figure 8.10. The Contour of Molar IAA Concentration at Middle Plane in Day 2.

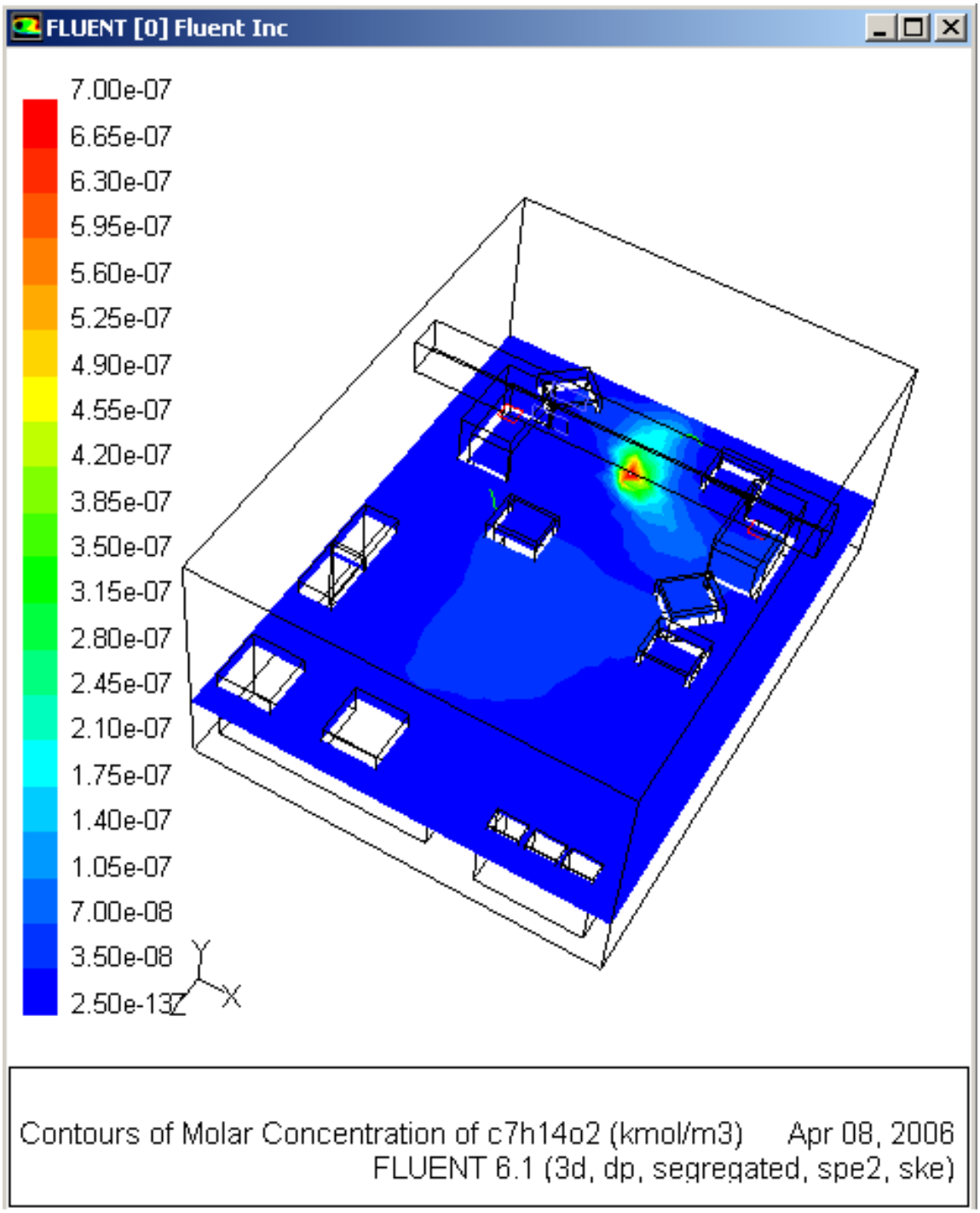

Figure 8.11. The Contour of Molar IAA Concentration at Middle Plane in Day 3.

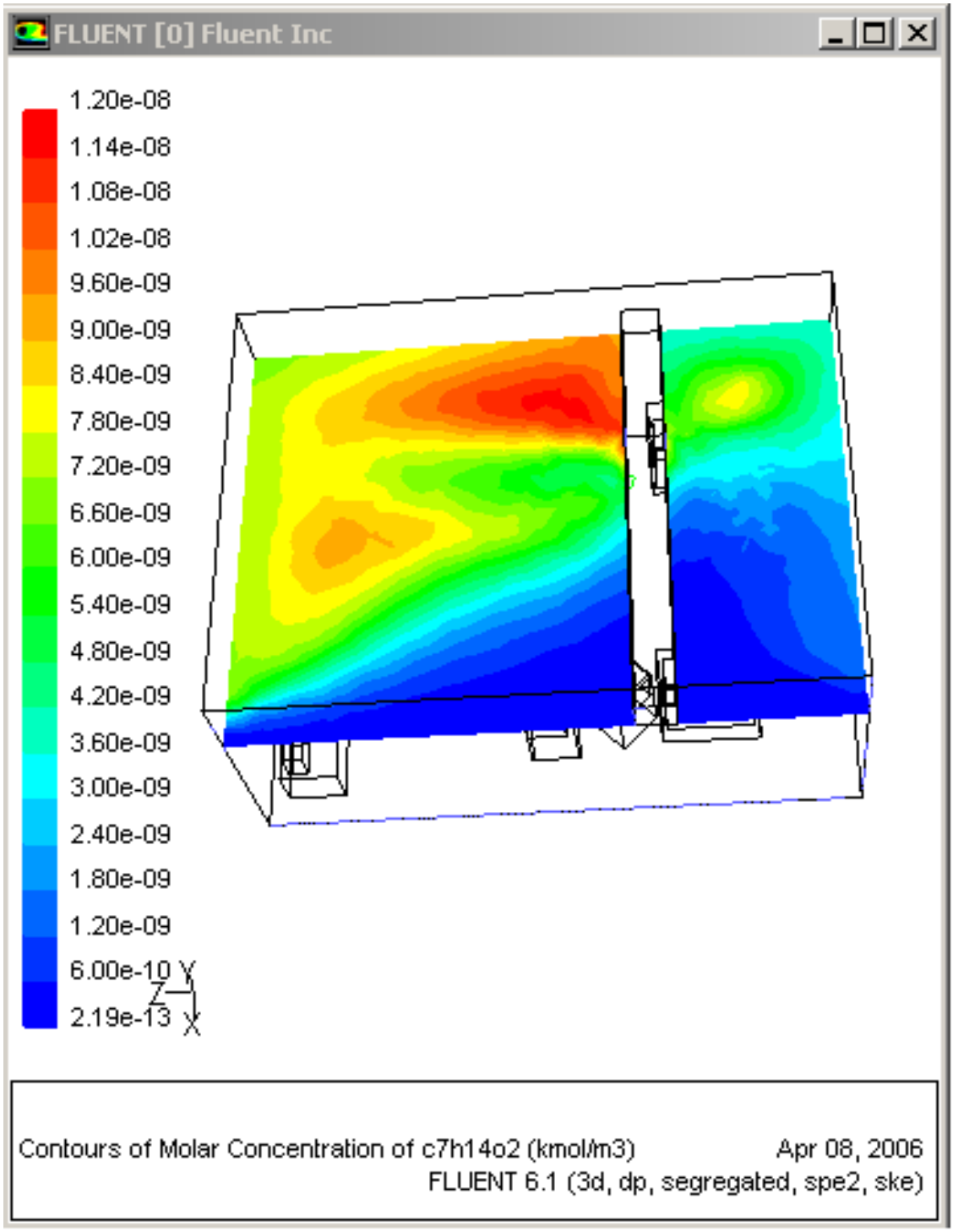

Figure 8.12. The Contour of Molar IAA Concentration at Top Plane in Day 1.

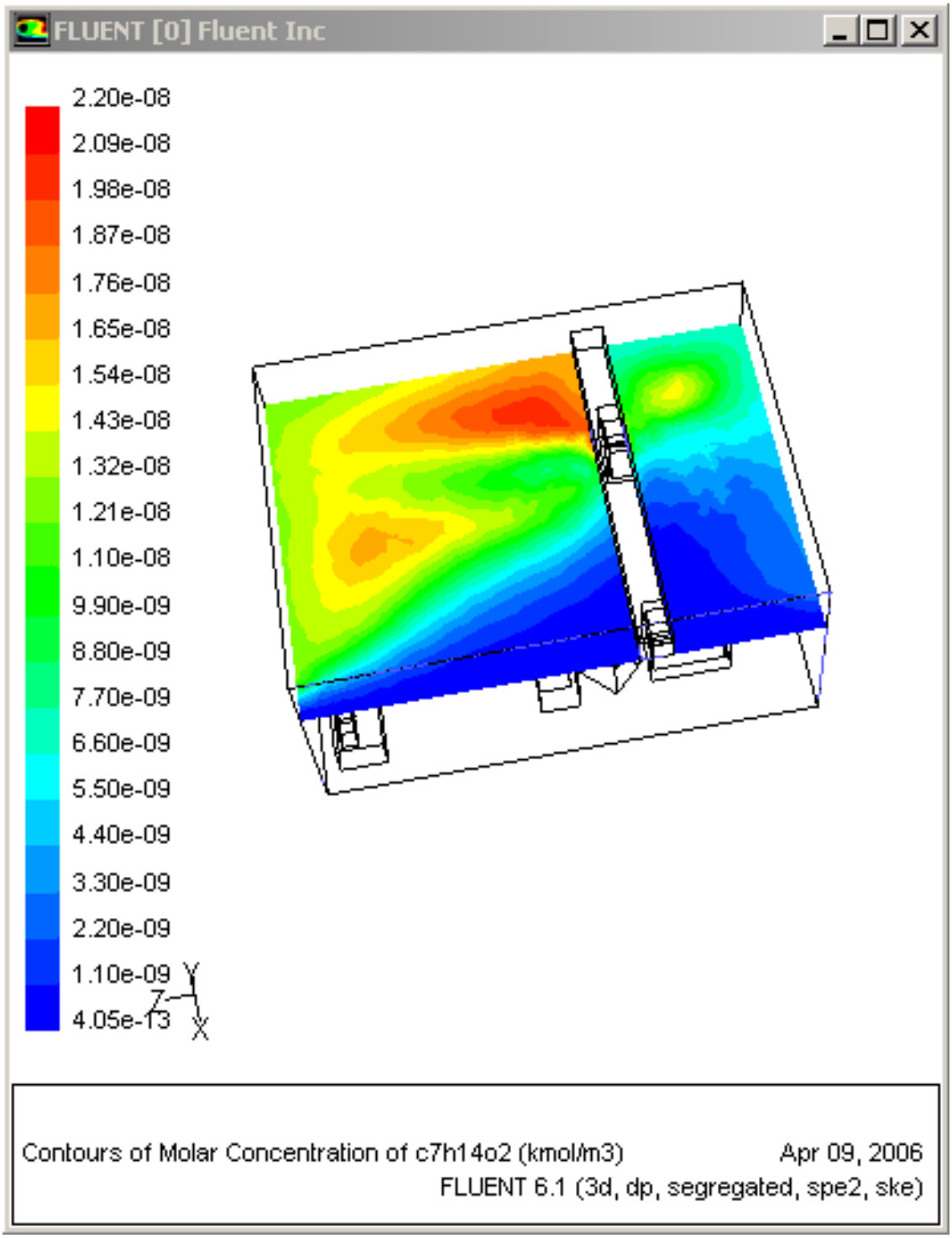

Figure 8.13. The Contour of Molar IAA Concentration at Top Plane in Day 2.

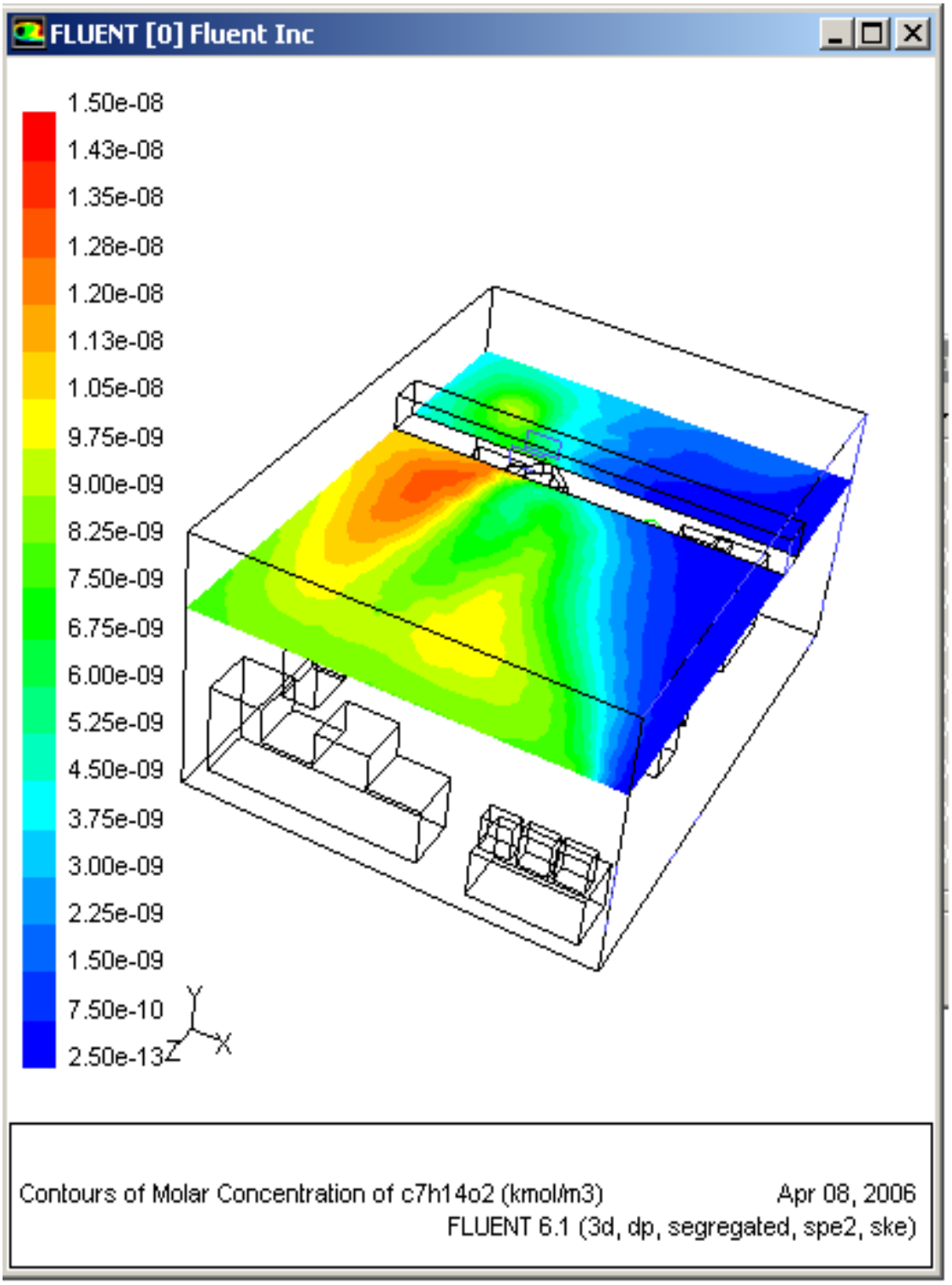

Figure 8.14. The Contour Of Molar IAA Concentration at Top Plane in Day 3.

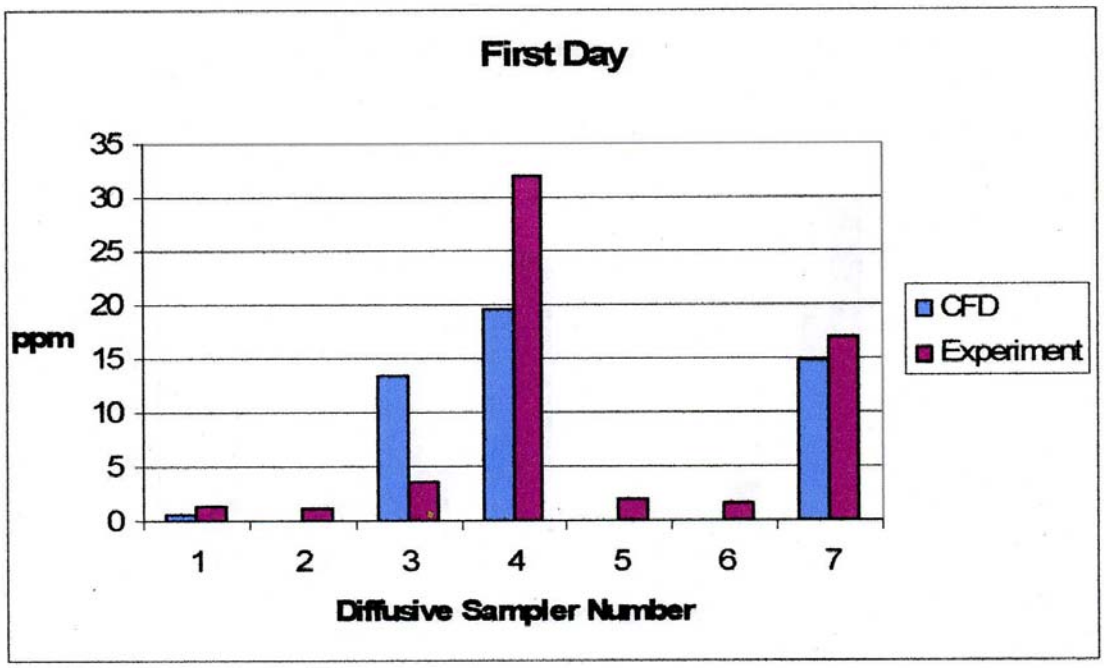

Figure 8.15. IAA concentration values at source on first day.

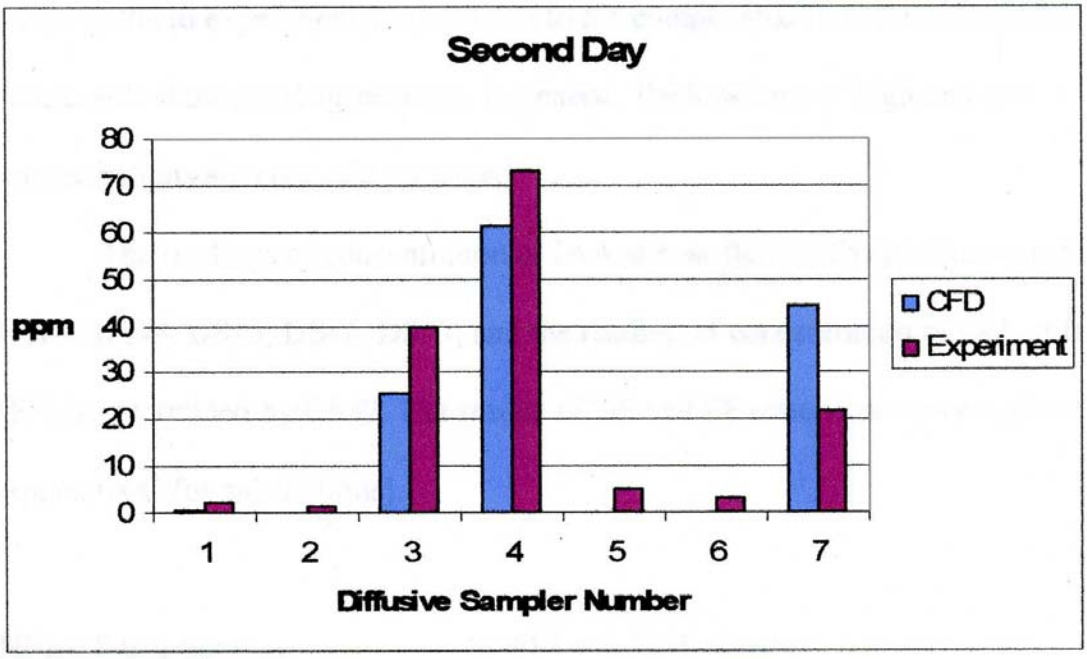

Figure 8.16. IAA concentration values at source on second day.

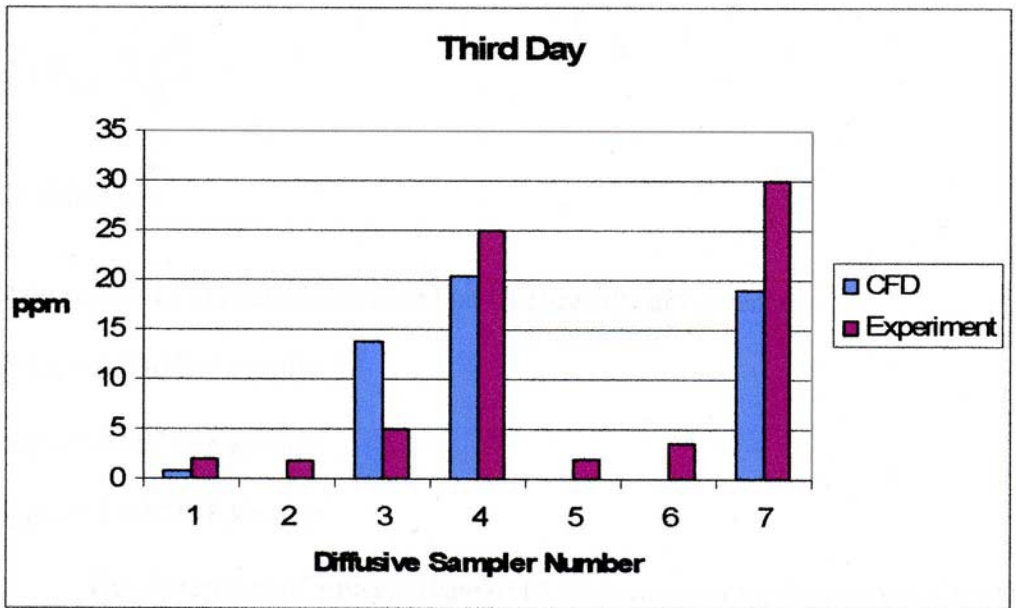

Figure 8.17. IAA concentration values at source on third day.

Conclusions. The objective of this portion of our research was to explore the use of CFD for simulating contaminant concentration within an industrial workroom that could then be employed for exposure assessment.

The use of a modified two-zone mixed model was shown to be valuable for characterizing the source boundary conditions. Although the estimated IAA emission rate for the second day was over twice that of the first and third days, the good agreement of the emission factors (emission rate divided by the number of capacitor batches processed during sampling) for all three days lends credibility to these rates.

For the initial simulation attempts, the predicted concentrations near the source did not agree with the measured concentrations, and the spatial trends near the source were not realistic. Recognizing that the initial source boundary conditions assuming pure IAA vapor was incorrect, an approach was developed to estimate the concentration and flow rate from the source. When this new boundary condition was used, the CFD simulations performed well in predicting the spatial trends of air speed near the source and the concentration distribution within the room.

Near the source, no statistically significant differences between CFD and measured values of air speed or IAA concentration were observed. Nevertheless, large differences between CFD concentration estimates and measure values were observed at some individual points. While CFD performance was greatly improved by refining the treatment of source boundary conditions, other boundary conditions depended upon simplifying assumptions. For example, isothermal conditions were assumed, but, despite temperature control, most workrooms have temperature gradients. As shown by our experimental work (Lee, 2006a), such gradients can

affect the distribution of airborne contaminants. Also, the flow of air from the right boundary was assumed to be uniform; however, even though the mean air speed through this side of the control volume was low, it may not have been completely uniform and might have been affected by temperature differences. Also, sufficient information was not available to improve our treatment of turbulence and wall effects.

The maximum measured value in the near field for each day was used to establish the concentration at and the flow rate through the source boundary, in order to compensate for the lack of sufficiently detailed information to allow theoretical estimation.

In conclusion, CFD is a promising research tool for exploring the impact of various physical factors that influence the distribution of contaminant species in a workroom, including supply inlets, exhaust outlets, source characteristics, and operating conditions. CFD software that could be used by practitioners in occupational hygiene and indoor air quality should be developed. It is equally important that further research be done to develop and validate methods for easily acquiring boundary condition information. This is essential for improved predictive capability and use of CFD for a wider range of applications.

9. REFERENCES

ACGIH. 2004. *Industrial Ventilation - a Manual of Recommended Practice.* 25 Ed. Amer. Conf. of Gov. Industrial Hygienists. Cincinnati, OH p. 2-4.

AIHA Exposure Assessment Committee. 2000. User's Guide to A Strategy for Assessing and Managing Occupational Exposures. 2nd ed. eds. TW Armstrong and BD Silverstein. Amer. Ind. Hyg. Assoc., Fairfax, VA.

Tamanna S., M. Ahmed, J. Khan, E. Lee, C. Feigley. 2003. "A User-Friendly Software for Indoor Air Exposure Assessment." American Industrial Hygiene Conference and Exhibition. Dallas, TX (May 10-15, 2003)

Aitken RJ, Baldwin PEJ, Beaumont GC, et al. 1999. Aerosol inhalability in low air movement environments. *Journal of Aerosol Science.* 30(5):613-626, June.

American Industrial Hygiene Association. 2000. *Mathematical models for estimating occupational exposure to chemicals.* CB Keil, ed. AIHA Press. Fairfax, VA.

Axley JW. 2001. Surface-drag flow relations for zonal modeling. *Building and Environment* 36:843-850.

Baldwin PJ, and AD Maynard. 1998. A survey of wind speeds in indoor workplaces. *Ann. Occup. Hyg.* 42(5):303–313.

Bennett JS, CE Feigley, and J Khan. 2003. Comparison of Emission Models with Computational Fluid Dynamic Simulation and a Proposed Improved Model. *Amer. Industrial Hygiene Assoc. J.* 64:739-54.

Bennett J S 1998. Exposure, Emission, and Control: Evaluation of the Completely-Mixed Mass Balance Model Using Computational Fluid Dynamics Doctoral Dissertation. University of South Carolina.

Bennett JS, Feigley CE, Khan J, and Hosni MH. 2000. Comparision of mathematical models for exposure assessment with computational fluid dynamic simulation. *Appl. Occup. Environ. Hyg*. 15: 131-144.

Bishop, EC, W Popendorf, D Hanson, and J Prausnitz, 1982: Predicting Relative Vapor Ratios for Organic Solvent Mixtures. *Amer. Ind. Hyg. Assoc. J.*, 43(9):656-661.

Bjorn, E, and PV Nielsen: 2002. Dispersal of exhaled air and personal exposure in displacement ventilated rooms. *Indoor Air 12*:147–164.

Bjorn, E, M Mattsson, M Sandberg, and PV Nielsen. 1997. Displacement ventilation-Effects of movement and exhalation. In *Proceedings of Healthy Buildings '97, 5th International Conference on Healthy Buildings*, *Volume 2*, 27 Sept.–2 Oct. 1997, Bethesda, Md., pp. 163– 168.

Brief RS 1960. Simple way to determine air contaminants. *Air Engineering*. 2:39-40.

Brohus H, KD Balling, D Jeppesen. 2006. Influence of movements on contaminant transport in an operating room. *Indoor Air*. 16:356-372.

Burstyn I, and H Kromhut. 2002. Trends in inhalation exposure to hydrocarbons among commercial painters in The Netherlands. *Scandinavian Journal of Work Environment and Health*. 28(6):429-438, December.

Busbin D, CE Feigley, DW Underhill, and D Salzberg. 2006. A Second Look at the Palmes' Diffusive Sampler. *J. Air and Waste Management Assoc.* 56:1431-1439.

Carslaw HS and JC Jaeger. 1959. *Conduction of Heat in Solids*. Oxford University Press. London, UK. pp. 255-281.

Checkoway H. 1986. Methods of Treatment of Exposure Data in Occupational Epidemiology. *Medic. Lavaro*. 77:48-73.

Cheong KWD, E Djunaedy, TK Poh, KW Tham, SC Sekhar, NH Wong. and MB Ullah. 2003. Measurements and computations of contaminant's distribution in an office environment. Building and Environment; 38:135-145.

Cherrie JW, and GW Hughson. 2005. The validity of the EASE expert system for inhalation exposures. Annals of Occup Hyg, 49(2): 125-134.

Cherrie JW. 1999a. The effect of room size and general ventilation on the relationship between near and far-field concentrations. *Appl. Occ.and Env. Hyg*., 14(8): 539 – 546.

Cherrie JW, and T Schneider. 1999b. Validation of a new method for structured subjective assessment of past concentrations. Ann. Occup. Hyg. 43 (4): 235 – 245.

Cherrie JW, T Schneider, S Spankie, and M Quinn. 1996. A new method for structured, subjective assessments of past concentrations. *Occupational Hygiene*, Vol.3: 75 – 83.

Conroy LM, RA Wadden, PA Scheff, JE Franke, and CB Keil. 1995. Workplace emission factors for hexavalent chromium plating. *Appl. Occup. Environ. Hyg*. 10:620-627.

Creely KS, J Tickner, AJ Soutar, GW Hughson, DE Pryde, ND Warren, R Rae, C Money, A Phillips, JW Cherrie. 2005. Evaluation and Further Development of EASE Model 2.0. *Ann. Occup. Hyg*. 49:135-145.

Do TH. 2008. Modeling and numerical simulation of airborne contaminant distribution in an actual workroom. Master of Science thesis. Department of Mechanical Engineering, University of South Carolina.

Dunnett SJ. 1994. A numerical investigation into the flow field around a worker positioned by an exhaust opening. *Ann. Occup. Hyg*. 38:663-686.

Eastman Kodak Company. 1983. *Ergonomic Design for People at Work*, Vol. 1. New York: Van Nostrand Reinhold, p. 26.

Emmerich SJ and T McDowell. 2005. *Initial Evaluation of Displacement Ventilation and Dedicated Outdoor Air Systems in Commercial Buildings*. NISTIR 72244. National Institute of Standards and Technology. Gaithersburg, MD.

Emmerich SJ. 1997. Use of Computational Fluid Dynamics to Analyze Indoor Air Quality Issues. Report No. NISTIR 5997. National Institute for Standards and Technology. Gaithersberg, MD.

Feigley CE, JS Bennett, J Khan, and E Lee. 2002a. Performance of deterministic workplace exposure assessment models for various contaminant source, air inlet, and exhaust locations. *AIHA Journal*. 63:402-412.

Feigley CE, JS Bennett, E Lee, and J Khan. 2002b. Improving the use of mixing factors for dilution ventilation design. *Appl. Occup. Environ. Hyg*. 17:333-343.

Feigley CE, FM Ehmke, TH Goodson and JR Brown. 1981. Experimental determination of volatile evolution rates from coated surfaces. *Amer. Indust. Hygiene Assoc. J.*, 42:365.

Feigley, C, N Schnaufer, T Do, E Lee, M Ventrakaman, J Khan, and R Haggerty. 2006. Estimating Emission Factors in a Capacitor Factory Using a Modified Two-Zone Model. Paper # 150. American Industrial Hygiene Conference. Chicago, IL (May 17, 2006).

Fluent 4.4 User's Guide volume 3, second edition, Fluent Incorporated.

Flynn MR, and WK Shelton. 1990. Factors affecting the design of local exhaust ventilation for control of contaminants from hand-held sources. *Appl. Occup. Environ. Hyg*. 5:501-509.

Franke JE, and RA Wadden. 1989. Some observations of eddy diffusivities in industrial settings. Paper # 307, Amer. Indust. Hygiene Conf. and Exhibition. St. Louis, MO.

Hanna, SR and PJ Drivas. 1987. *Guidelines for Use of Vapor Cloud Dispersion Models.* American Institute for Chemical Engineers, New York.

Hawkins AN.; Hosni, M.H.; Jones, B.W. 1995. Comparison of Room Air Motion in a Full Size Test Room Using Different Diffusers and Operating Conditions. *ASHRAE* Trans, vol. 101, pt. 2. pp. 81–100.

Heinsohn RJ. 1991. *Industrial Ventilation Engineering Principles*. John Wiley and Sons, NY. a. pp. 264-271; b. p179-181.

Hemeon WCL. 1963. *Plant and Process Ventilation*. 2nd Ed, Industrial Press Inc. NY., pp. 235-245.

Hofmann W. 1996. Modeling techniques for inhaled particle deposition: the state of the art. *J. of Aerosol Medicine - Depostion, Clearance and Effects in the Lung*. 9:369-388.

Hosni MH, K Tsai, and AN Hawkins. 1996. Numerical predictions of room air motion. Proceedings of Fluid Engineering Division Conference, ASME Vol.2, 745-750.

Hummel AA, Braun KO, and Fehrenbacher MC. 1996. Evaporation of a liquid in a flowing airstream. *American Industrial Hygiene Association Journal* 57:519-529.

Hyun S, and C Kleinstreuer. 2001. Numerical simulation of mixed convection heat and mass transfer in a human inhalation test chamber. *Int. J. Heat Mass Transfer 44*:247–2260.

Jayjock MA. 2003. "Modeling inhalation exposure." in *The Occupational Environment: Its Evaluation, Control, and Management.* SR DiNardi. Ed. Amer. Indust. Hyg. Assoc. Fairfax, VA.

Johnson AE, B Fletcher, and CJ Saunders. 1996. Air movement around a worker in a low-speed flow field. Annals of Occupational Hygiene. 40:57-64.

Johnston KL, ML Phillips, NA Phillips, et al. 2005. Evaluation of an artificial intelligence program for estimating occupational exposures. Annals of Occupational Hygiene, 49(2): 147-153.

Keil CB, M Nicas. 2003. Predicting room vapor concentrations due to spills of organic solvents. *AIHA Journal* 64:445-454.

Keil C, D Krupinski, and M Chamachkine. 1997. Eddy diffusivity measurements for exposure modeling. Paper #182. Amer. Indust. Hygiene Conf. and Exhibition, Dallas, TX. May 22, 1997.

Keil, CB. 2000. A tiered approach to deterministic models for indoor air exposures. Amer. Indus. Hygiene Assoc. J. 15(1):145-151.

Khan, JA, CE Feigley, E Lee, MR Ahmed, and S Tamana. 2006. Effects of inlet and exhaust locations and emitted gas density on indoor air contaminant concentrations. *Buildings and Environment*. 41:851-863.

Kim T and MR Flynn. 1991. Modeling a worker's exposure from a hand-held source in a uniform freestream. *Amer. Indust. Hygiene Assoc. J.* 52:458-463.

Kromhout H, E Tielemans, L Preller, and D Heederik. 1996. Estimates of individual dose from current exposure measurements. *Occup. Hyg*. 3:23-39.

Lee E, CE Feigley, J Khan, JR Hussey. 2007. The effect of worker's location, orientation, and activity on exposure. *Journal of Occupational and Environmental Hygiene*. 4:572-582.

Lee, E, CE Feigley, J Khan, and S Tamanna. 2005. The Effect of an Occupant's Presence in a Room on Pollutant Dispersion. Paper II-2603. *Proceedings: Indoor Air 2005*. Beijing, China (September 5, 2005)

Lee E. and CE Feigley. 2002. An Investigation of Air Inlet Velocity in Simulating the Dispersion of Indoor Contaminants via Computational Fluid Dynamics. *Annals of Occupational Hygiene*. 46:701-712.

Lee E, CE Feigley, JA Khan, and JR Hussey. 2006. The effect of temperature differences on the distribution of an airborne contaminant in an experimental room. *Annals of Occupational Hygiene.* 50:527-537 http://annhyg.oxfordjournals.org/papbyrecent.dtl

Lee E, JA Khan, CE Feigley, MR Ahmed, and JR Hussey. 2006. An investigation of air inlet types in mixing ventilation. In press. *Building and Environment*, Available online January.

Lee E. 1999. Validation of computational fluid dynamics for simulating experimental contaminant dispersion. Masters thesis. University of South Carolina, Columbia, SC.

Lennert A, F Nielsen, and NO Breun. 1997. Evaluation of evaporation and concentration distribution models – A test chamber study. *Ann Occup Hyg*. Dec; 41(6):625-41.

Lidwell, OL and JE Lovelock. 1946. Some methods for measuring ventilation. *Journal of Hygiene* (Cambridge). 44:326-332.

Luoma M, and SA Batterman. 2000. Autocorrelation and Variability of Indoor Air Quality Measurements. *Am. Ind. Hyg. Assoc. J.;* 61 658-668.

Mattsson M, and M Sandberg. 1994. Displacement ventilation-influence of physical activity. In *Proceedings of ROOMVENT '94, 4th International Conference on Air Distribution in Rooms*, Kracow, Poland, Volume 2, pp. 77–92.

Mattsson M, and M Sandberg. 1996. Velocity field created by moving objects in rooms. In *Proceedings of ROOMVENT '96, 5th International Conference on Air Distribution in Rooms, Volume 1*, Yokohama, Japan, July 17–19, S. Murakami (ed.). pp. 547–554.

Mattsson M, E Bjorn, M Sandberg and PV Nielsen. 1997. Simulating people moving in displacement ventilated rooms. In: Wood, J.E., Grimsrud, D. T. and Boschi, N. (eds) proc. Healthy buildings '97, 5th International Conference on Healthy Buildings, Bethesda, MD, USA, 27 September – 2 October, Vol.1, 495-500.

Mulhausen JR and J Damiano. 1998. *A Strategy of Assessing and Managing Occupational Exposures.* 2nd ed. AIHA Press. Fairfax, VA.

National Research Council. 1991. *Human Exposure Assessment for Airborne Pollutants: Advances and Opportunities.* National Academy Press. Washington, DC.

Nicas M. 1996. Estimating exposure intensity in an imperfectly mixed room. *Amer. Indust. Hygiene Assoc. J.* 57:542-550.

Nielsen F, E Olsen, and Fredenslund. 1995. Prediction of isothermal evaporation rates of pure volatile organic compounds in occupational environments – a theoretical approach based on laminar boundary line theory *Annals of Occupational Hygiene* 39(4): 497-511.

Park C and RP Garrison. 1990. Multicellular model for contaminant dispersion and ventilation effectiveness with application for oxygen deficiency in a confined space. Am. Ind. Hyg. Assoc. J. 51:70-78.

Ramachandran G. 2001. Retrospective exposure assessment using Bayesian methods. *Annals of Occupational Hygiene*. 45:651-667.

Ramachandran G, S Bannerjee, and JH Vincent. 2003. Expert judgment and occupational hygiene: Application to aerosol speciation in the nickel primary production industry. *Annals of Occupational Hygiene*. 47:461-475.

Rappaport SM and LL Kupper. 2008. *Quantitative Exposure Assessment*. Stephen Rappaport, El Cerrito, CA.

Rappaport, SM. 1991. Exposure assessment strategies. in *Exposure Assessment for Epidemiology and Hazard Control*. SM Rappaport and TJ Smith, eds. Lewis Publishers. Chelsea, MI.

Ren Z, and Stewart J. 2005. Prediction of personal exposure to contaminant sources in industrial buildings using a sub-zonal model. *Environmental Modeling and Software*. 20:623-638.

Riley EC. 1968. Estimation of Atmospheric Concentration of Volatile Compounds from Surface Coatings by Means of Laboratory Model. *Amer. Ind. Hyg. Assoc. J*. 29:450-455.

Roach SA. 1991. Alternative Ways of Monitoring Occupational Exposure. Chapter 1. in *Exposure Assessment for Epidemiology and Hazard Control*. SM Rappaport and TJ Smith, Eds. Lewis Publishers, Chelsea, MI.

Scheff PA, RL Friedman, JE Franke, LM Conroy, and RA Wadden. 1992. Source activity modeling of freon emissions from open-top vapor degreasers. *Appl. Occup. Environ. Hygiene*. 7:127-134.

Semple SE, LA Proud, SN Tannahill, ME Tindall, and J.W Cherrie. 2001. A Training exercise in subjectively estimating inhalation exposures. Scand J Work Environ Health. 27(6): 395 – 401.

Sinden FW. 1978. Multi-chamber theory of air infiltration. *Building and Environment*. 13:21-28.

Stewart PA, RF Herrick, CE Feigley, DF Utterback, R Hornung, H Mahar, R Hayes, DE Douthit, and A Blair. 1992. Exposure Assessment for Embalmers in a Case-Control Study: An Experimental Design. Applied Occupational and Environmental Hygiene 7:532-540.

Stewart PA, and M Dosemeci. 1994. A bibliography for occupational exposure assessment for epidemiological studies. *Amer. Indust. Hygiene Assoc. J*. 55:1178-1187.

Tamanna S, M Ahmed, J Khan, E Lee, and C Feigley. A User-Friendly Software for Indoor Air Exposure Assessment. American Industrial Hygiene Conference and Exhibition. Dallas, TX (May 10-15, 2003). Refereed with published abstract.

Tamanna S. 2004. A simplified approach to estimating work room contaminant concentration distribution. Masters thesis. University of South Carolina, Columbia, SC.

Tielemans E, LL Kupper, H Kromhout, D Heederick, and R Houba. 1998. *Ann. Occup. Hyg*. 42:115-119.

Topp C, PV Nielsen and L Davidson. 2000. Room airflows with low Reynolds number effects. Air Distribution in Rooms (Roomvent 2000); Vol. 1, 541-546.

Wadden RA, JL Hawkins, PA Scheff, and JE Franke. 1991.Characterization of emission factors related to source activity for trichloroethylene degreasing and chrome plating processes. *Am. Ind. Hyg. Assoc. J*. 52:349-356.

Wadden RA, PA Scheff, and JE Franke. 1989. Emission factors for trichloroethylene vapor degreasers. *Amer. Indust. Hygiene Assoc. J*. 50:496-500.

Welling I, IM Andersson, G Rosen, et al. 2000. Contaminant dispersion in the vicinity of a worker in a uniform velocity field. *Ann. Occup. Hyg.44(3)*:219–225.

Wurtz E, J-M Nataf, and F Winkelmann. 1999. Two- and three-dimensional natual and mixed convection simulation using modular zonal models in buildings. *Int. J. of Heat and Mass Trans.* 42:923-940.

Xing HJ., A Hatton, and HB Awbi. 2000. “The air quality at the breathing zone with displacement ventilation.” Air Distribution in Rooms (Roomvent 2000). 1: 113-118.

Xue, H. and C Shu. 1999. Mixing characteristics in a ventilated room with non-isothermal ceiling air supply. Building and Environment 34:245-251.

PUBLICATIONS AND PRESENTATIONS RESULTING FROM GRANT

Peer-reviewed Papers

The following peer-reviewed articles resulted from this research project. Several additional articles, not included below, are in review or in preparation. Annotations are provided relating papers to specific aims.

Articles	Aims
Lee E. and CE Feigley. An Investigation of Air Inlet Velocity in Simulating the Dispersion of Indoor Contaminants via Computational Fluid Dynamics. *Annals of Occupational Hygiene*. 46:701-712 (2002).	1,2
Bennett JS, CE Feigley, and J Khan. Comparison of Emission Models with Computational Fluid Dynamic Simulation and a Proposed Improved Model. *Amer. Industrial Hygiene Assoc. J. 64:739-54* (2003)	3
Lee E, CE Feigley, J Khan, and S Tamanna, The Effect of an Occupant's Presence in a Room on Pollutant Dispersion. Paper II-2603. *Proceedings: Indoor Air 2005*. Beijing, China (September 5, 2005)	1, 2
Lee E, CE Feigley, JA Khan, and JR Hussey. The effect of temperature differences on the distribution of an airborne contaminant in an experimental room. *Annals of Occupational Hygiene.* 50:527-537 http://annhyg.oxfordjournals.org/papbyrecent.dtl (2006).	1,2
Khan JA, CE Feigley, E Lee, MR Ahmed, and S Tamana. Effects of inlet and exhaust locations and emitted gas density on indoor air contaminant concentrations. *Buildings and Environment*. 41:851-863 (2006).	1, 2
Lee E, JA Khan, CE Feigley, MR Ahmed, and JR Hussey. 2007. An investigation of air inlet types in mixing ventilation. *Building and Environment* 42:1089-1098.	1, 2
Lee E, JA Khan, CE Feigley, MR Ahmed, and JR Hussey. The effect of worker's location, orientation, and activity on exposure. *J. Occup. Environ. Hyg.* 4:572-582 (2007).	3, 4

Presentations/Symposia/Roundtables (with reviewed abstracts)

Presentation	Aim
Feigley CE, J Khan, JS Bennett, and E Lee. CFD Computations to Show the Effects of Air Inlet and Exhaust Locations Relative to Contaminant Source on the Concentration Profile of a Room. The 37th Annual Technical Meeting of The Society of Engineering Science. Session TC-8 – Fluids. Columbia, SC (October 24, 2000). Refereed with Published Abstract. Submitted.	3, 4

Lee E, and C Feigley. Air Inlet Velocity Profile: An Important Factor in Computational Fluid Dynamic Simulation of Indoor Contaminant Dispersion. American Industrial Conference and Exhibition, Session PS-601, New Orleans, LA (June 4, 2001). Refereed with published abstract.	3, 4
Lee E, and C Feigley. Effect of Worker Location, Orientation and Activity on Exposure. American Industrial Conference and Exhibition, Session PS-605, New Orleans, LA (June 4, 2001). Refereed.	1, 2
Lee E, C Feigley, and J Khan. Performance of Exposure Models in Experimental Room for Various Thermal Conditions, Airflows and Worker Locations. Paper No. 216. American Industrial Hygiene Conference and Exhibition. San Diego, CA (June 5, 2002). Refereed with published abstract.	3
Lee E, CE Feigley, R Semeniuc, and J Khan. Estimating Adequate Duration of Short-term Samples in an Experimental Room. Paper No. 10313. International Society for Exposure Analysis/International Society for Environmental Epidemiology. Vancouver, Canada (August 14, 2002). Refereed with published abstract.	1, 2
Lee E, C Feigley, J Hussey, J Khan, M Ahmed. Short-term sampling time requirements in rooms. American Industrial Hygiene Conference and Exhibition, Dallas, TX (May 10-15, 2003). Refereed with published abstract.	1, 2
Ahmed M, S Tamanna, ELee, C Feigley, J.Khan. Effect of Inlet and Exhaust Locations and Density of Contaminant Gas on Indoor Air Contaminant Concentration. American Industrial Hygiene Conference and Exhibition, Dallas, TX (May 10-15, 2003). Refereed with published abstract.	1, 2
Tamanna S, M Ahmed, J Khan, E. Lee, C Feigley. A User-Friendly Software for Indoor Air Exposure Assessment. American Industrial Hygiene Conference and Exhibition. Dallas, TX (May 10-15, 2003). Refereed with published abstract.	3
Feigley CE, J Khan, E Lee, M Ahmed, S Tamana, RO Semeniuc, and JJ Jenkins. Investigating Principles of Workroom Exposure. National Occupational Reasearch Agenda Symposium - 2003. Arlington, VA. (June 24, 2003). Refereed with published abstract.	1, 2, 3
Tamanna S, M. Ahmed, E Lee, C Feigley, J Khan. Assessment of Concentration and Velocity Field Using Coarse Grid. Am. Indust. Hygiene Conference. Atlanta, GA. (May 8-12, 2004). Refereed with published abstract.	3
Ahmed M, S Tamanna, E Lee, C Feigley, J Khan. Effect of Furniture Presence on Optimum Relative Location of Inlet and Exhaust and on Indoor Air Contaminant Concentration. Am. Indust. Hygiene Conference. Atlanta, GA. (May 8-12, 2004). Refereed with published abstract.	1, 2

Lee E, C Feigley, K Lakshman, J.Khan, M Ahmed, S Tamanna The Effect of Temperature Differences in a Room on Contaminant Dispersion. Am. Indust. Hygiene Conference. Atlanta, GA. (May 8-12, 2004). Refereed with published abstract.	1, 2
Lee E, C Feigley, J Khan, and S Tamanna. The Investigation of the Impact of Worker Locations, Orientation, and Activity on Exposure. Paper #74. American Industrial Hygiene Conference. Anaheim, CA (May 24, 2005).	1, 2
Lee E, C Feigley, J Khan, and S Tamanna. The Effect of a Worker's Presence in a Room on Contaminant Dispersion. Paper #80. American Industrial Hygiene Conference. Anaheim, CA (May 24, 2005).	1, 2
Lee E, CE Feigley, J Khan, and S Tamanna, The Effect of an Occupant's Presence in a Room on Pollutant Dispersion. Abstract #2603. Indoor Air 2005. Beijing, China (September 5, 2005).	1, 2
Feigley C. Models, Monitoring, and CFD: Putting CFD in Perspective. Vent 2006. Roundtable D2. Challenges of Applying Computational Fluid Dynamics to Ventilated Spaces. Chicago, IL (May 16, 2006)	3
Feigley, C, N Schnaufer, T Do, E Lee, M Ventrakaman, J Khan, and R Haggerty. Estimating Emission Factors in a Capacitor Factory Using a Modified Two-Zone Model. Paper # 150. American Industrial Hygiene Conference. Chicago, IL (May 17, 2006)	3, 4
Feigley C, T Do, N Schnaufer, E Lee, M Ventrakaman, J Khan, and R Haggerty. The Importance of Boundary Conditions in CFD Simulation of a Workroom. Accepted for presentation. American Industrial Hygiene Conference. Minneapolis, MN (June 5, 2008)	3, 4

Inclusion of Gender and Minority Study Subjects

Not Applicable

Inclusion of Children

Not Applicable

Materials Available to Other Researchers

Tracer gas concentration data at 144 monitoring locations inside the experimental room is available from this project. These data were taken in triplicate experiments for factorial experiments at two levels of dilution flow rate, two types of inlet diffusers (wall jet and ceiling diffuser), and six levels of difference between the temperatures of the simulated exterior wall and the supply air. Smaller datasets are available which explore the effects of worker presence, location, orientation, and activity.